2010-08-18

Integrated Affinity Column Capillary Electrophoresis Microdevices for Biomarker Analysis

Weichun Yang
Brigham Young University - Provo

Integrated Affinity Column/Capillary Electrophoresis Microdevices for Biomarker Analysis

Weichun Yang

A dissertation submitted to the faculty of
Brigham Young University
in partial fulfillment of the requirements for the degree of

Doctor of Philosophy

Adam T. Woolley, Chair
Daniel E. Austin
Steven W. Graves
Aaron Hawkins
Milton L. Lee

Department of Chemistry and Biochemistry

Brigham Young University

December 2010

ABSTRACT

Integrated Affinity Column/Capillary Electrophoresis

Microdevices for Biomarker Analysis

Weichun Yang

Department of Chemistry and Biochemistry

Doctor of Philosophy

In this dissertation, microfluidic systems that integrate antibody-based sample preparation methods with electrophoretic separation are developed to analyze multiple biomarkers in a point-of-care setting. To form an affinity column, both monolith materials and wall-coated channels were explored.

I successfully demonstrated that monolith columns can be prepared in microfluidic devices via photopolymerization. The selectivity of monolith columns was improved by immobilizing antibodies on the surface. These affinity columns can selectively enrich target analytes and reduce the signal of contaminant proteins up to 25,000 fold after immunoaffinity extraction. These results clearly demonstrate that microchip affinity monoliths can selectively concentrate and purify target analytes through specific antibody-antigen interactions.

These monolith columns operated well for simple systems such as buffered solution, but suffered from clogging with real biological samples such as human serum. Therefore, I developed new affinity columns using a wall coating protocol. To form the affinity columns, a thin film of a reactive polymer was UV polymerized in a microchannel. Antibodies were attached by reaction between the polymer epoxy groups and antibody amine groups. All steps, including loading, washing, and elution for affinity extraction, as well as capillary electrophoresis analysis, were achieved simply via applying voltages to reservoirs on the microdevice. By adding reservoirs containing alpha-fetoprotein (AFP) standard into the same device, a quantitative method, either standard addition or calibration curve, can also be performed on-chip. These polymer microdevices have been applied in determining AFP levels in spiked serum samples, and the results are comparable with the values measured using a commercial enzyme linked immunosorbent assay kit.

These microchips have also been adapted for detection of multiple biomarkers by immobilizing different antibodies on the affinity column. Four kinds of antibodies were

attached to microchip columns, and the amounts of immobilized antibodies were characterized. The fluorescence signals of all four protein antigens were in the same range after rinsing, indicating that the derivatization reaction had little bias toward any of the four antibodies. With spiked human blood serum samples, four proteins in the ng/mL range were simultaneously quantified using both calibration curves and standard addition. In general, the calibration curve and standard addition results were close to the known spiked concentrations. These results indicate that my integrated microdevices can selectively retain and analyze targeted compounds in clinical samples. Moreover, my platform is generalizable and applicable for the simultaneous quantification of multiple biomarkers in complex matrices.

Keywords: microfluidic systems, biomarkers, capillary electrophoresis, affinity extraction

ACKNOWLEDGEMENTS

First and foremost, I would like to sincerely thank Dr. Adam T. Woolley for his mentoring, understanding, countless hours, patience, and most importantly, his scientific guidance during my graduate studies at Brigham Young University. Working with Dr. Woolley has been one of the greatest experiences in my life. His mentorship provided a profound experience consistent with my long-term career goals. I will always be grateful to him for what I learned by working in his laboratory. I also want to thank my graduate committee members, Dr. Austin, Dr. Graves, Dr. Hawkins, and Dr. Lee for their valuable ideas and suggestions. I thank the many people who have directly contributed to this work: Dr. Xiuhua Sun, Dr. Ming Yu, Dr. Hsiang-Yu Wang, and Dr. Tao Pan. I also want to thank my lab mates and other friends in the Department of Chemistry and Biochemistry for useful discussions and collaborative efforts. Finally, I want to express my love and appreciation for my family members, Shanshan Luo, Changgen Yang, Changxia Jiao, Yuyao Luo and Huilian Yang. Their love and devotion, and especially patience, are invaluable in all of my endeavors.

Brigham Young University

SIGNATURE PAGE

of a dissertation submitted by

Weichun Yang

The dissertation of Weichun Yang is acceptable in its final form including (1) its format, citations, and bibliographical style are consistent and acceptable and fulfill university and department style requirements; (2) its illustrative materials including figures, tables, and charts are in place; and (3) the final manuscript is satisfactory and ready for submission.

Date	Adam T. Woolley, Ph.D., Chair
Date	Daniel E. Austin, Ph.D.
Date	Steven W. Graves, Ph.D.
Date	Aaron Hawkins, Ph.D.
Date	Milton L. Lee, Ph.D.
Date	Matthew R. Linford, Ph.D. Graduate Coordinator
Date	Thomas W. Sederberg, Ph. D. Associate Dean, College of Physical and Mathematical Sciences

TABLE OF CONTENTS

LIST OF TABLES

LIST OF FIGURES

1. INTRODUCTION*

1.1 CANCER BIOMARKERS

1.1.1 Facts about cancer screening

Cancer (malignant neoplasms) is a group of many diseases where cells are abnormal and divide without control. These tumor cells also can invade neighboring tissues and spread to the whole body.[1] Overall, cancer was not only the second most common cause of death in the US (~23% of all deaths in 2006),[2] but also has significant financial impact. The National Institutes of Health (NIH) estimated that direct and indirect costs associated with cancer were about $157 billion in 2001.[3] More importantly, many patients are diagnosed too late to be cured, as most cancer treatments are more effective at early stages. For instance, the 5-year relative survival rate for all patients with colorectal cancer is only 64%, but it can be improved to 90% if tumors are detected at an early, localized stage.[4] In one study, researchers found that removal of polyps could reduce the incidence of colorectal cancer by 76 to 90 percent.[5] Early cancer detection can also provide other significant advantages that directly impact the quality of a person's life. For breast cancer, many women have the option of breast-conserving surgery rather than removal of the entire breast if diagnosed early.[6] Due to early stage diagnosis and other advances in cancer treatment, cancer death rates began decreasing in the early 1990s. For instance, the death rate from cancer decreased ~8.0% from 2001 to 2005 (**Figure 1.1**). Consequently, there are tremendous opportunities to further improve the survival rate of patients by better cancer screening and treatment methods.

* Sections 1.2 to 1.3 in this chapter are adapted with permission from *Journal of the Association for Laboratory Automation*, 2010, 15(3), 198-209. Copyright 2010 Elsevier

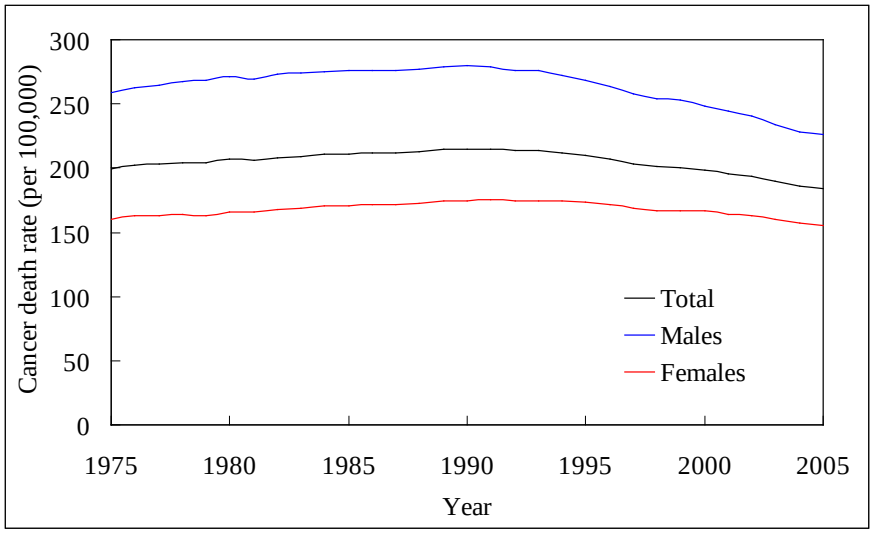

Figure 1.1. Cancer death rates in the United States from 1975-2005. Source: American Cancer Society. Cancer Statistics 2009 Presentation. http://www.cancer.org/docroot/PRO/content/PRO_1_1_Cancer_Statistics_2009_presentation.asp (Accessed date: 4/12/2010)

Currently, morphological examination of tumor biopsies is one of the most widely used methods to diagnose cancer. However, this process is time-consuming, uncomfortable and expensive. For instance, bone marrow biopsy requires an anesthetic to numb the area, and a long needle is inserted into the marrow to aspirate cells for study.[7] Therefore, noninvasive screening tests such as ultrasound, roentgenography, magnetic resonance imaging (MRI), computed tomography (CT), and biomarker analysis are more attractive for early diagnosis and screening. Using CT scanning, the internal structure of an object in a human body can be regenerated from multiple X-ray projections. CT can detect minute angle differences in tissue, but its contrast for soft-tissue is rather poor.[8] Therefore, MRI, which has higher soft-tissue contrast, is a commonly used alternative to CT. In addition, since MRI is based on the distribution of hydrogen atoms, and unlike CT, MRI is safe for children and pregnant women.[6] Using imaging techniques such as CT and MRI for large-scale cancer screening is still a continuing controversal topic due to non-reliable data and inaccuracy.[9, 10] Indeed, Beinfeld et al.[11] calculated the cost-effectiveness of whole-

body CT screening, and concluded that on average a person will only get 6 more days of life expectancy at a cost of $2500. Compared with CT and MRI, ultrasound is a cheaper technique with comparable spatial and contrast resolution. However, ultrasound images are collected manually and their quality is directly related to the operator's experience. Because the acoustic properties of bone and air are different from soft tissues, bone and air bring shadows into ultrasound images. Thus, tissues with bone and air interfaces such as lung tissue cannot be scanned well by ultrasound.[6]

1.1.2 Biomarkers in cancer screening

On the other hand, biomarkers are a rapidly developing area in cancer research. There are more than 160,000 articles with the "cancer biomarker" keyword in a Pubmed database search. A cancer marker can be a molecule either produced by tumor cells, or a specific chemical produced by the human body in response to tumor cells.[12] These substances can be found in the blood, urine, and tissues. Different tumor markers are found in different types of cancer, and levels of the same tumor marker can be different depending on the type of cancer.[13] The major benefits of using these molecularly based biomarkers are the potential to: (1) assess the likelihood that cancer will develop in high-risk groups, (2) diagnose cancer at an early stage, (3) evaluate therapy treatment, and (4) guide new drug discovery.[14]

The validity of cancer biomarker tests is generally evaluated by two parameters: sensitivity and specificity (**Table 1.1**).[15] Sensitivity refers to the percentage of true-positive test results (A, individuals with cancer whose biomarker level is above T, the action threshold) in all patients with cancer (M). Specificity refers to the percentage of

true-negative results (D, individuals without cancer whose biomarker level is below T) in all patients without cancer (N). Obviously, the values of both parameters are highly dependent on the value set for T. If T is lower, A will be larger, which results in a higher sensitivity number; however, D will be smaller which means it lowers the specificity. Either way, an accurate determination of biomarker concentration will be essential for biomarker discovery and application.

Table 1.1 Definition of sensitivity and specificity for biomarker screening tests.

Test result	With cancer	Without cancer
Above action threshold (> T, positive)	True positive (A)	False positive (C)
Below action threshold (< T, negative)	False negative (B)	True negative (D)
	Total patients with cancer (M=A+B)	Total individuals without cancer (N=C+D)
	Sensitivity=A/M × 100%	Specificity=D/N × 100%

To date, some markers such as prostate specific antigen (PSA) have been approved by the US Food and Drug Administration for early detection of cancer.[16] Another example is thyro-calcitonin which has sufficient sensitivity and specificity for thyroid cancer diagnosis.[17] The American Society of Clinical Oncology (ASCO) first published clinical practice guidelines for the use of tumor markers in breast and colorectal cancer in 1996.[18] In a recent update, the tumor markers considered (**Table 1.2**) were expanded from 7 to 13 categories.[19] However, ASCO believes most of the new markers (4 out of 6) are not sufficiently reliable and definitive for clinical usage. In addition, some old markers such as p53 are still inadequately characterized for application in disease management. Based on these guidelines, 6 categories of

Table 1.2 ASCO updated clinical practice guidelines for use of tumor markers in breast cancer (*adapted with permission from ref. 19).*

Specific marker	Use	New markers since the 2000 guideline	Change from the 2000 guideline
CA 15.3 and CA 27.29	monitoring patients with metastatic disease during active therapy	No	No
CEA	monitoring patients with metastatic disease during active therapy	No	No
ERs and PgRs	predictive factors for endocrine therapy	No	Yes
DNA flow cytometry	data are insufficient to recommend use for prognosis	No	No
HER2	prognosis, guiding use of taxane chemotherapy, and determining sensitivity to endocrine therapy are not recommended	No	Yes
p53	data are insufficient to recommend use for management of patients	No	No
uPA and PAI-1	prognosis, evaluating risk of recurrence	Yes	Yes
Cathepsin D	data are insufficient to recommend use for management of patients	No	No
Cyclin E	data are insufficient to recommend use for management of patients	Yes	Yes
Proteomic analysis	data are insufficient to recommend use for management of patients	Yes	Yes
Multiparameter gene expression	predict the risk of recurrence in patients treated with tamoxifen	Yes	Yes
Bone marrow micrometastases	data are insufficient to recommend use for management of patients	Yes	Yes
Circulating tumor cell assays	application still under investigation	Yes	Yes

Abbreviations: CA, carbohydrate antigen; CEA, carcinoembryonic antigen; ER, estrogen receptor; PgR, progesterone receptor; HER, human epidermal growth factor receptor; uPA, urokinase plasminogen activator; PAI-1, plasminogen activator inhibitor 1; CMF, cyclophosphamide, methotrexate, and fluorouracil.

biomarkers are recommended for clinical use, and only uPA and PAI-1 is recommended for prognosis. Because the sensitivity and specificity of biomarkers are highly dependent on the accurate measurement of biomarker levels in human fluids, a fast, sensitive, and cost-effective method for biomarker analysis is highly desirable for a clinical setting.

1.1.3 Current cancer biomarker analysis methods

Currently, most biomarkers are detected via immunoassays such as enzyme linked immunosorbent assay (ELISA).[20] This method was invented in the 1960s, and has been heavily used in bioanalysis ever since.[21] There are many different ways of designing ELISAs, but in general, they involve at least one antigen-antibody pair and an enzyme which generates a detectable signal.[22] **Table 1.3** and **Figure 1.2** summarize commonly used ELISAs and their schemes. Immobilization of the antigen of interest can be achieved by direct adsorption to the assay plate or indirectly via an immobilized antibody. The antigen is then detected either indirectly (labeled secondary antibody, **Figure 1.2a**) or directly (labeled primary antibody, **Figure 1.2b, c**). A competitive ELISA is commonly used when the antigen is small and has only one antibody binding site. Antigen from sample and the immobilized antigen compete for binding to the labeled antibody. A decrease in signal indicates the presence of the antigen in the sample (**Figure 1.2d**) when compared to assay wells with labeled antibody alone (**Figure 1.2e**). One variation of this method is to use labeled antigen instead of the antibody.[23]

Among these protocols, asymmetrical ELISA methodologies are widely applied in commercial immunoassays since monoclonal antibodies are expensive. A commonly

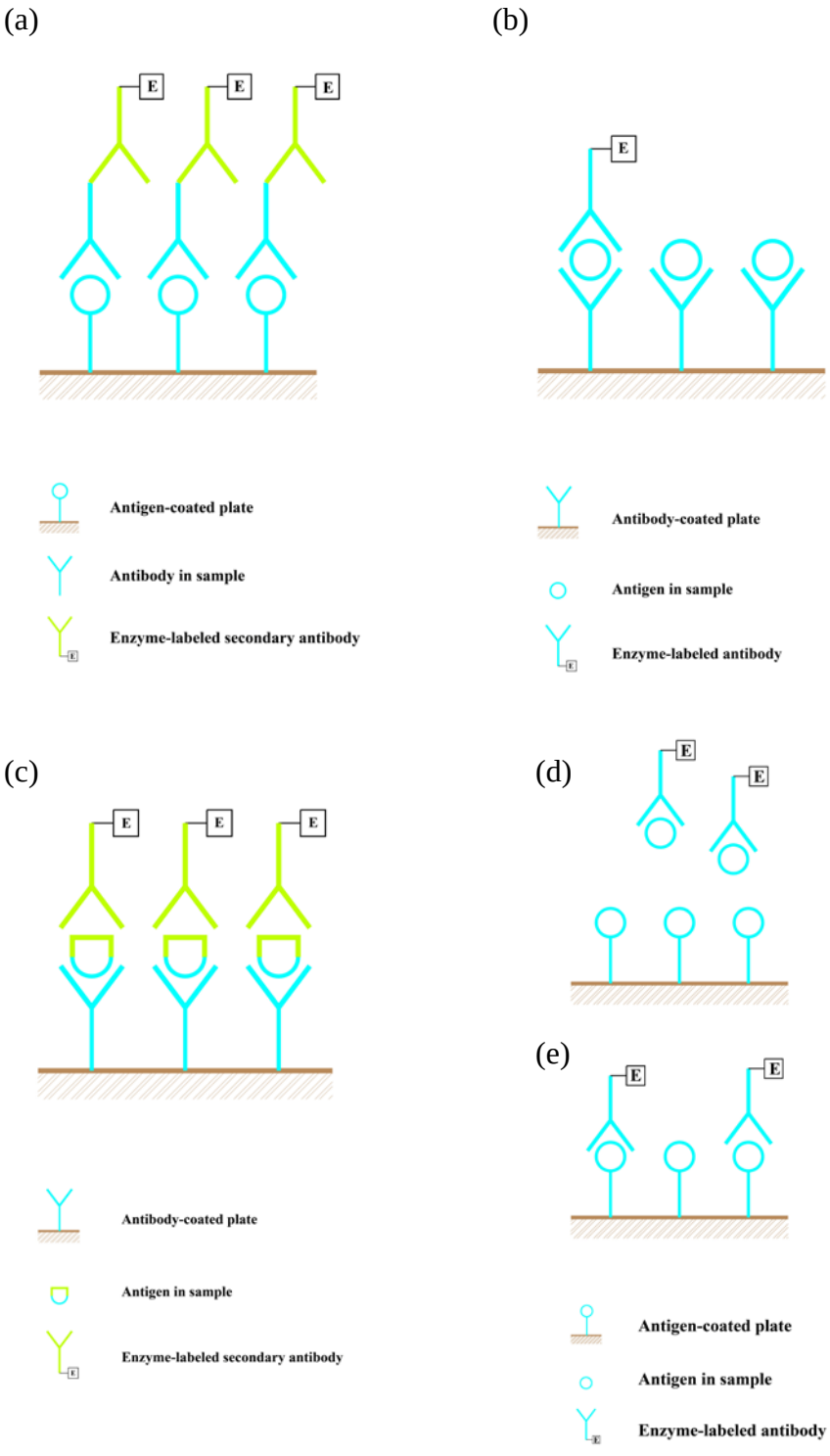

Figure 1.2. Schematic diagram of commonly used ELISAs. (a) Antigen-coated ELISA plate. (b) Symmetrical, and (c) asymmetrical two-site ELISA. Competitive ELISA for antigen analysis using labeled antibody, (d) antigen is present in the sample and (e) no antigen is in the sample.

Table 1.3 Commonly used ELISAs.

			Detected species	Scheme
Non-competitive	Antigen-coated		Antibody or antigen	Figure 1.2a
	Antibody-coated	Symmetrical	Antigen	Figure 1.2b
		Asymmetrical	Antigen	Figure 1.2c
Competitive	Antigen-coated	Labeled antibody	Antigen	Figure 1.2d, e
		Labeled antibody	Antibody	
	Antibody-coated	Labeled antigen	Antigen	
		Labeled antigen	Antibody	

Table 1.4. Commercially available immunoassays for determination of alpha fetoprotein (AFP) concentration.

Kit manufacturer	Panomics	Anogen	United Biotech	Pishtaz Teb
Kit catalog #	BC1009	EL10049	CM-105	PT-AFP-96
ELISA format	Figure 1.2c	Figure 1.2b	Figure 1.2c	Figure 1.2c
Immobilized capture	Goat anti-AFP	Monoclonal anti-human AFP	Monoclonal anti-AFP	Monoclonal anti-AFP
Dynamic range (ng/ml)	2.0-350	2.0-400	1.2-240	1.0-200
Conjugate	Monoclonal anti-AFP-HRP	Monoclonal anti-AFP-HRP	Anti-AFP-HRP	Mouse monoclonal anti-AFP-HRP
Substrate	TMB	TMB	TMB	TMB

Abbreviations: HRP: horseradish peroxidase; TMB, tetramethylbenzemidine.

used combination is a monoclonal antibody as capture reagent and a polyclonal antibody for detection. For alpha fetoprotein (AFP, a liver cancer biomarker) assays, although the procedures and substrates are similar, different antibodies are used to react with AFP in samples, resulting in different dynamic ranges and limits of detection (**Table 1.4**). Consequently, it can be problematic to directly compare the clinical data when different assays are used for quantifying biomarkers.[24] In addition, labor-intensive rinsing steps are involved in these assays (at least 5 washing steps), and the total analysis time is about 2 hours. ELISA can simultaneously analyze ~100 samples in a clinical setting; however, this approach is more expensive (counting the number of reference standards and reagents for each test) and less time effective for a single or a few samples.

Thus, to develop a biomarker analysis system in a point-of-care (POC) setting, analytical-grade diagnostic tools will need to be translated from conventional laboratory facilities to "bedside" settings.[25] As a consequence, many new biosensors have been developed to offer low cost, high speed and high throughput. For example,

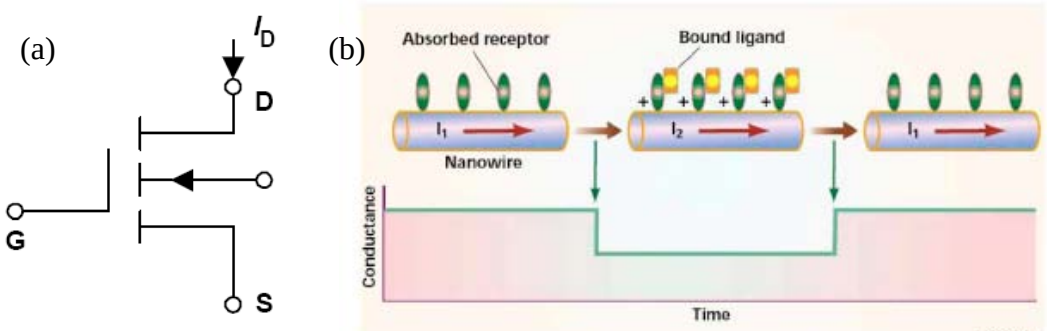

Figure 1.3. (a) Schematic of a typical MOSFET (D, drain; G, gate; I_D, drain current; S, source). (b) An example of nanowire biosensing. Introduction of anti-biotin decreased the conductance of a biotin labeled NW, and NW conductance returned to its original value after washing with buffer (reproduced with permission from ref. 30).

96-well plates can be transferred from the molded polymer to paper format.[26] These paper microzone plates require small volumes of sample (~5 μL) and are cost-effective (about 5 cents for each plate).[27, 28] New detector systems such as semiconducting nanowires (NWs) configured as field-effect transistors (FETs) have also been applied to detect proteins or cells in solution.[29] The setup of these NW-FETs is similar to conventional metal oxide semiconductor field effect transistors (MOSFETs, **Figure 1.3a**): the NW serves as the wire connecting source and drain, and the ions in the buffer solution serve as the gate. Once ions (such as biomarkers) in bulk solution (such as serum) bind to the sensor surface, the gate potential changes which in turn changes the channel current (**Figure 1.3b**).[30] Such devices can also be applied for T-cell detection by preparing deprotonated silanol groups on the NW. If a T-cell is present in the solution, it brings extra H^+ ions near the NW and increases protonation of the NW surface, which decreases I_D.[31] These NW devices can directly detect macromolecules without labeling, and the detection limit can be as low as 100 fM.[32] However, the fabrication of these NWs is rather complicated, and significant device-to-device variation was found even within the same batch.[33] More importantly, the Debye length (λ_D) is critical and must be carefully controlled in NW-FET devices. A concentrated buffer solution (λ_D < 0.7 nm) effectively screens most of a protein's charge, resulting in baseline signal in a biotin-streptavidin system.[34] Therefore, for these surface-bound ligand NW systems, measurements must be performed in a low salt (<1.5 mM) buffer solution. To overcome this shortcoming, Stern et al.[35] recently developed an ELISA to detect interleukin-2 in physiologically buffered solution. Instead of using colorimetric methods as in traditional ELISA, changes in the local pH value were used to monitor protein concentrations. However, a relatively complex setup was needed for these nano-ELISA assays.

Although these emerging technologies hold promise, an abnormal level of a single biomarker alone is not generally sufficient to diagnose cancer.[17] For example, many men with PSA levels less than the 4.0 ng/mL action threshold had prostate cancer detected by biopsy (i.e., false-negatives).[36] Furthermore, PSA levels above 4 ng/mL are associated with other conditions such as prostatitis, reducing the specificity (i.e., false-positives).[37] To overcome these shortcomings, using a group of markers would enable more sensitive and accurate cancer screening with higher throughput.[38] There are two common approaches to multiplex testing. One is series testing, where various tests are performed one after the other. In general, the biomarker test is combined with another methodology such as ultrasound, to improve sensitivity and specificity. The other multiplex method is parallel testing, where all tests are performed at the same time. Parallel testing is more commonly used in multi-biomarker analysis. For instance, Ward et al.[39] found that the sensitivity of ovarian cancer diagnosis had increased from 18% using CA125 alone to 64 % using human milk-fat globulin II as a second marker and placental alkaline phosphatase as a third assay. Similarly, Yang et al.[40] evaluated 12 biomarkers for gastrointestinal cancer diagnosis, and a combination of five markers significantly improved the diagnostic rate to ~40% relative to the ~27% rate achieved with just carcinoembryonic antigen (CEA). Thus, a biosensor with readily accessible, portable, rapid, and multimarker assays would be ideal as a POC platform.

1.2 MINIATURIZATION IN BIOCHEMICAL ANALYSIS

1.2.1 Advantages of microfabricated devices

Since the early 1990s, there has been strong interest in the miniaturization of chemical analysis systems,[41] which provides new capabilities for chemistry, biology, and medicine. These systems have the potential to influence broad areas, from biological analysis to optics technology, because of their many advantages.[42] For instance, microfluidic devices offer low sample and reagent consumption (which is critical for trace samples like biomarkers),[43] small dead volume,[44] high analysis speed (separation in minutes or less),[45] high throughput (up to 384 samples),[46] and valveless flow control (which enables integration of several functions).[47] More importantly, for diffusion-limited mixing processes like ELISAs, the diffusion time can be significantly reduced in miniaturized devices, because the diffusion time decreases to 1/100th if the diffusion distance is 10-fold less.[48] Consequently, a 2-hour assay in a traditional 96-well plate (~1 cm diameter per well) could be accomplished in less than 1 second in a 100-μm microchannel. These advantages of microfabricated devices have been exploited widely in biological analysis, and reviews cover areas such as protein separation,[49] cell analysis,[50] genomics,[51] and biomarker assays.[25, 52]

1.2.2 Microchip capillary electrophoresis

In 1981, Jorgenson et al.[53] successfully transferred zone electrophoresis into the open-tubular capillary format. A very high voltage can be applied in this technique, called capillary electrophoresis (CE). The number of theoretical plates (N) in CE is only proportional to the separation voltage (V, **Eq. 1.1**) if band broadening is limited to diffusion:

$$N = \frac{\mu_e V}{2D} \qquad \textbf{(Eq. 1.1)}$$

where μ_e is the electrophoretic mobility in the separation medium and D is the diffusion coefficient of the analyte. With high voltages such as 30 kV, theoretical plates near one million can be achieved.[54]

Once the voltage is applied to a buffer solution in a capillary or microchannel, electrophoretic movement is not always the only driving force in the system. The inner wall of the capillary acquires a charge in most cases. This is due to either ionization of the wall (such as with fused silica) or adsorption of ions from the buffer solution onto the wall (such as with Teflon). Both of these effects result in the formation of a double layer of ions near the surface and a potential difference known as the zeta potential.[55] When a voltage is applied along this capillary, the outside of the double layer (the mobile layer) is attracted to the electrode, and it drags the bulk buffer solution with it. Such movement is called electroosmotic flow (EOF).[56] Because EOF has a relatively flat profile compared with laminar flow, the molecules move in narrow bands, giving a high separation efficiency in CE. When considering EOF, μ_e in **Eq. 1.1** should be replaced with the sum of electrophoretic and electroosmotic mobility (μ_{EOF}):

$$N = \frac{(\mu_e + \mu_{EOF})V}{2D} \qquad \textbf{(Eq. 1.2)}$$

And the migration time (t_m) can be given by:

$$t_m = \frac{L^2}{(\mu_e + \mu_{EOF}) \times V} \qquad \textbf{(Eq. 1.3)}$$

where L is the separation length. The theoretical resolution of two components (A and B) in CE can be given by:

$$R_s = 0.177(\mu_A - \mu_B)\left[\frac{V}{(\overline{\mu} + \mu_{EOF})D}\right] \qquad \textbf{(Eq. 1.4)}$$

where R_s is the resolution, μ_A and μ_B are the electrophoretic mobilities of the two components, and $\bar{\mu}$ is their average mobility. From **Eq. 1.4**, the best resolution will be attained when $\bar{\mu}+\mu_{EOF}$ is very close to zero. The EOF can be changed via the applied voltage, pH of the solution (changing zeta potential), temperature, organic solvent addition, and surface modification.

From **Eq. 1.3**, with voltages of ~1 kV and separation lengths of ~1 cm, the migration time can be a few seconds. Importantly, because N is independent of the column length, miniaturized separation channels will not reduce separation efficiency, provided the same overall voltage is applied. In contrast, shorter column lengths in chromatography will result in a smaller number of theoretical plates, meaning reduced separation efficiency. Consequently, microchip CE offers shorter analysis times compared with traditional chromatography instruments. In addition, sample processing such as preconcentration and purification can also be carried out in a single device with potential automation. Moreover, because of the small dimensions of microfabricated channels, Joule heat dissipation is more effective, and higher voltage can be applied to improve separation efficiency. Thus, microchip CE has been widely used in biological sample separation.[41]

1.2.3 Device materials

Initially, because of well-developed semiconductor technologies, many devices were fabricated in silicon in the early stages of microfluidics. For instance, Terry et al.[57] micromachined a gas chromatography (GC) system in a silicon wafer in the late 1970s. However, because silicon cannot withstand high potentials and it is very difficult to use conventional optical detection methods with it, other materials have

been explored in microfluidic applications. Due to its established fabrication methods and characterized surface properties, glass was the dominant substrate material for microdevices in the 1990s.[58-60] However, the process of glass fabrication generally involves HF etching and high bonding temperatures (>600˚C), which slow down the whole process and are not desirable for mass production. On the other hand, polymers offer a wide range of available materials to choose from based on desired properties. For instance, polydimethylsiloxane (PDMS) is gas permeable (cells can grow inside a device) and easy to bond to itself and glass (simple fabrication).[61] Poly(cyclic olefin copolymer) (COC) is chemically resistant to many organic solvents, which is suitable for chromatography in microdevices.[62] A review summarized commonly used polymers in microfluidic systems, including their material properties, fabrication methods, and device applications.[63] In addition to the more common thermal annealing technique (where the polymer interface is heated to near its glass transition temperature causing the polymer chains to interdiffuse on the surface of the two substrates), solvent can also be used to bond polymeric devices.[64] The solvent dissolves the surface of the polymeric material, and facilitates polymer chain interdiffusion at the interface.[65] In general, solvent bonding offers stronger enclosure (withstands higher internal pressure than thermal bonding) and a fast bonding process.[64]

1.2.4 Limitations of miniaturized devices

To date, many microfluidic designs have been made, but they are generally tested with low complexity samples. For actual biological specimens, which are mixtures with wide analyte concentration ranges, it remains a challenge to directly separate even tens of compounds on microdevices. The small microchip platform size usually

results in a short separation length, limiting the resolving power and peak capacity, which are critical for separating complex mixtures.[66] For a chromatographic or electrophoretic system, the maximum number of separated elements (i.e., peak capacity) can be calculated by:

$$n=L/w \quad \textbf{(Eq. 1.5)}$$

where L is the separation length and w is the mean value of the zone width.[67] Because separation lengths in microdevices are generally at the cm scale, the peak capacity is rather low compared with conventional instruments. For instance, the peak capacity of a PDMS microchip for micellar electrokinetic chromatography (MEKC) was only ~12 for protein separation.[68] Importantly, to completely isolate a 20-component mixture with 95% probability, the peak capacity should be ~800.[69] Clearly, resolving power and peak capacity in microfluidic systems could be improved. In addition, tiny sample volumes (usually in the microliter range)[70] are placed on microdevices, and often nanoliter or smaller volumes are injected. Furthermore, microchips generally have a short optical detection path,[71] such that the detection limit is another aspect of microfluidic devices that could be improved.

1.2.5 Integrating multiple functions in miniaturized devices

Fortunately, these separation and detection limitations can be overcome by integrating multiple functions and components at the chip scale. Methods for microfluidic device fabrication are generally based on photolithographic techniques, which make complex designs possible.[72] Moreover, fabrication techniques have been developed to transfer these complex designs into low-cost materials like plastics.[73, 74] By integrating sample preparation processes into a single microdevice, trace samples can be preconcentrated

before analysis. Multi-dimensional separations on-chip can significantly improve the sample capacity. Importantly, because the samples in many integrated microdevices are manipulated by voltages, these microfluidic systems can be readily automated. Compared with traditional methods, automated sample analysis can be more economical, requiring less human intervention, and enabling increased sample throughput.[75] Consequently, these advantages make integrated microdevices especially attractive for automating the characterization of complex mixtures.

1.3 ON-CHIP SAMPLE PREPARATION

1.3.1 Dynamic preconcentration techniques

Sample concentration techniques in CE, such as sweeping and stacking, have been proven effective for pharmaceutical species,[76] herbicides,[77] steroids,[78] and peptides.[79] The principle of stacking is based on the conductivity difference between sample and buffer zone. Briefly, a sample solution with a low conductivity is introduced into a capillary filled with buffer solution with a high conductivity. After applying a voltage on the capillary, the local electric field in the sample zone is higher than the buffer zone since the electric current in the capillary is constant. Therefore, the analytes in the sample zone move faster than in the buffer zone, which results in concentrating the analytes at the boundary. Generally, stacking can easily provide over l00-fold enhancement of the ionic analytes.[80] These methods have also been applied in microfluidic formats. For instance, Jung et al.[81] developed a porous-polymer plug in a microchannel to create a high conductivity buffer zone and enriched fluorescent analytes 1000-fold using field-amplified sample stacking. The same group developed CE microchips coupled with isotachophoresis (ITP), which could enrich Alexa Fluor 488 nearly two million fold,[82] and under optimized conditions the detection limit of

Alexa Fluor 488 was ~100 aM.[83] For ITP preconcentration, a sample is loaded between a fast leading electrolyte and a slow terminating electrolyte. After applying a voltage and reaching equilibrium, since the current through the entire column is the same, the electric field is smaller for faster bands and larger for slower bands. Consequently, each sample component is migrating in a band at the same electrophoretic mobility. The boundary between bands is sharp and discrete.[56] However, it is important but difficult to find suitable leading and terminating electrolytes for ITP. A review on stacking and sweeping in microchip systems was recently published.[84] These traditional dynamic techniques have been easily transferred from CE systems to microchip CE systems, while providing effective enrichment. For instance, Bercovici et al.[85] developed a method for identification of unlabeled analytes using indirect fluorescence-based detection and ITP on commercially available microfluidic borosilicate chips. Such systems can also be applied for chemical toxin detection in tap water without sample preparation steps.[86]

One interesting area within dynamic preconcentration techniques is equilibrium gradient focusing, including electric field gradient focusing (EFGF) and temperature gradient focusing.[84] Equilibrium gradient focusing is attractive for isolating and concentrating trace proteins. In EFGF, an equilibrium band is formed for each protein when the electrophoretic velocity is equal in magnitude, but opposite in direction to the hydrodynamic counterflow. EFGF was developed by Koegler and Ivory[87] using a tapered glass cylinder to generate the electric field gradient. Humble et al.[88] successfully transferred EFGF into capillary format, and 10,000-fold preconcentration was achieved for green fluorescent protein (GFP). Kelly et al.[89] used a phase-changing sacrificial layer to protect a microchannel during formation of a designed

conductive polymer which generated an electric field gradient in a microdevice. Liu et al.[90] applied a different approach to divide the separation channel from the electric field generating component. A buffer ion-permeable membrane was integrated into the microdevice to divide the separation and field channels, and GFP was concentrated up to 4,000-fold using this device. To reduce non-specific adsorption, EFGF devices can be completely fabricated from a poly(ethylene glycol) based polymer,[91] and the performance can be further improved by replacing the Tris buffer in the hydrogel with KCl-phosphate buffer.[92]

1.3.2 Solid phase extraction

Solid phase extraction (SPE) is a widely used method for sample preparation. It can be fully automated with commercial systems like SPE-DEX (Horizon Technology), OSP2 (Merck), and MicroLab SPE (Hamilton).[93] In SPE, sample is retained on a solid medium, allowing the matrix to be rinsed away and the retained material to be eluted for analysis.[94] The promise of sample enrichment and cleanup by SPE has led researchers to apply this approach in microdevices. A SPE column has been fabricated by coating microchip walls with silanes, and 80-fold preconcentration of coumarin C460 was observed;[95] however, due to the limited surface area, the loading capacity of this approach was relatively low.

1.3.2.1 Packed bead columns

Because silica beads are commercially available and their properties are well characterized, microchip SPE columns made by packed beads are attractive. However, it is necessary to localize these particles in targeted regions of microchips using physical barriers. For example, a sol-gel structure was fabricated to retain silica beads,

and this system was tested in on-chip DNA purification.[96] In an alternate format, a two-weir design which constructed a cavity to trap beads was explored.[97] Two photomasks were used in device fabrication, one to pattern the tops of the weirs for etching, and the other to pattern the channels for etching to a different depth. In this manner, a 1-μm gap was formed to prevent beads from passing out from the SPE bed.[98] Zhong et al.[99] developed a two-side etching and alignment protocol to construct weirs in a different manner. A top plate containing weirs and a bottom plate having the connection channels were aligned, and a 4-μm gap was created by sealing the plates together. Instead of a microfabricated weir structure, a physical barrier can be prepared on-chip with a photopolymerized frit.[100] In a different approach, beads can be packed through a tapered geometry by the keystone effect.[101] The channel which contained the beads tapered from a 70-μm to a 16-μm width. When beads flowed through the channel, the density of the particles increased in the taper, such that they aggregated without a physical barrier.

1.3.2.2 Monolith columns

Packed-bead columns have disadvantages in terms of packing procedures and frit fabrication, which complicate microdevice preparation. On the other hand, monoliths are an attractive alternative to packed particles because of low back pressure and high surface area.[102] Thermally polymerized monolith materials have been successfully applied as SPE columns.[103] In 2001, Yu et al.[104] photopolymerized a monolith column in a microfluidic system and performed SPE. Enrichment of peptides and proteins up to 1000 fold was achieved on this column. More importantly, due to low back pressure, the linear flow rate in these monoliths could reach 10 μL/min, which far exceeded flow in packed microchip columns.

Monolith columns have also been applied for DNA enrichment in complex mixtures like blood. However, nonspecific binding hindered elution of nucleic acids and decreased sample loading capacity due to competitive adsorption; the presence of proteins lowered the monolith extraction efficiency from ~80% to <40%.[105] Therefore, Wen et al.[106] developed a two-stage microchip SPE system. Before monolith column extraction, a C18 reversed-phase column was used to remove proteins in the sample. Although the procedure was more complex, whole blood DNA extraction capabilities were significantly improved. For a 10-μL whole blood sample, ~70% of the protein was removed by the C18 column, which then afforded more interaction between DNA and the monolithic material. This two-stage system enriched DNA ~20 fold in the reversed-phase portion, and the overall DNA extraction efficiency was ~70%.

1.3.2.3 Affinity columns

In the previous applications, SPE enriched analytes based on general interactions like hydrophobic absorption. To improve the selectivity, affinity elements can be immobilized on the column. In general, the immobilization of an antibody to a solid support is obtained via one of four main functional groups of the antibody molecule (**Figure 1.4**):[107] ε-amino groups of lysine,[108] carbohydrate residues in the Fc region of the antibody,[109] carboxyl residues[110] and sulfhydryl groups[111] of the reduced antibodies. The formation of a covalent bond between the antibody and the column can enhance the stability compared with direct adsorption methods,[112] which is critical for flow-through systems or high pressure systems. In some cases, antibodies can also be immobilized via another antibody, which is specific to the Fc portion of the first antibody.[113]

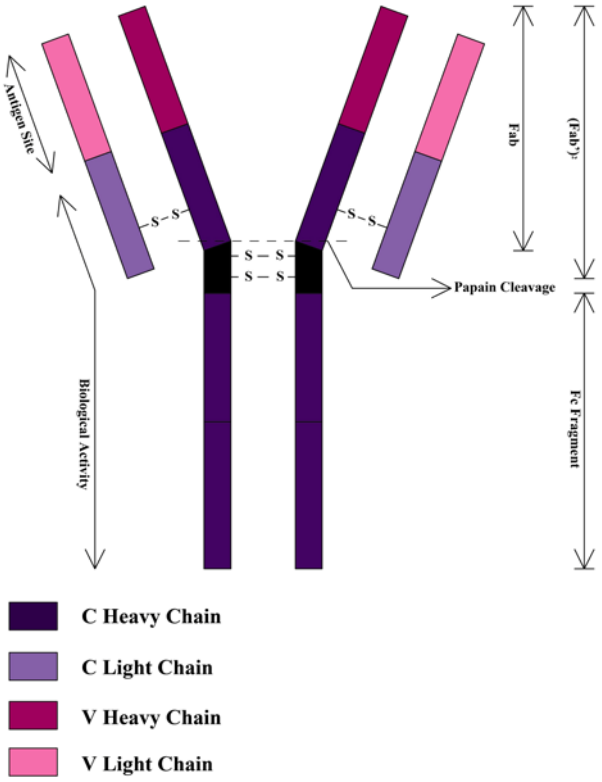

Figure 1.4. Antibody structure. (*adapted with permission from ref. 107*)

Antibody immobilization has been applied successfully in a microfluidic format. For instance, rabbit immunoglobulin G was concentrated and detected at the 50 nM level.[114] However, this approach is only effective in capturing target analytes in simple buffer solutions instead of complex matrixes like tissue or blood. Phillips and Wellner[115, 116] have utilized immunoaffinity CE to measure biomarkers and neuropeptides in human biopsies. The analytes were captured by a replaceable immunoaffinity disk having attached antibodies. After removing non-target materials, the captured analyte was labeled in situ, released, and then separated by microchip CE. The system was semi-automated, and the separation step was completed within 5 min.

Surface modification can be achieved on monolithic materials as well. For instance, glycoproteins were retained on a monolith with immobilized pisum sativum agglutinin, and then eluted in several fractions due to different affinities.[117] Recently, He et al.[118] prepared a streptavidin acrylamide gel to immobilize biotinylated antibodies. The blotting membrane effectively reduced antibody consumption to ~1 μg and could detect as little as 0.05 pg of protein. This approach has recently been

extended into a 2-D system,[119] where the entire process for immunoblotting, including separation, sample transfer, and antibody-based blotting, was performed in less than 2 min.

Non-electrically driven immunoassays can also be performed in microchip devices. For instance, Kong et al.[120] formed elastomeric microvalves in 3-layer microchips to control flow, although the valves were actuated by a vacuum pump and a compressor. Using this system, clenbuterol was determined in pig urine samples in 30 min. Fan et al.[121] designed a PDMS-on-glass microsystem to perform protein assays on blood samples. Plasma was separated from whole blood on chip, and selected proteins were detected by antigen-antibody interaction. Stern et al.[122] developed an affinity extraction chamber coupled with a label-free nanosensor to detect PSA and CA15.3 in human blood. In this study, a two-stage approach with a valve was applied to isolate the detector from the complex environment of whole blood.

1.3.3 Membrane filtration

Another common method for sample preconcentration and cleanup is membrane filtration, which utilizes the size difference between analytes and buffer ions. Larger molecules cannot pass through a porous layer in a semipermeable hollow fiber,[123] membrane,[124] or joint,[125] while smaller species are allowed to transit. In one design, a porous membrane was sandwiched between two PDMS pieces to create a three-dimensional microfluidic channel structure.[126] This system achieved 300-fold concentration of fluorescein in around 40 min. The fluorescein was concentrated outside a 10-nm pore membrane with openings larger than the molecular size of fluorescein, because the negatively charged diffuse layer on the interior of the

membrane repelled anions. Song et al.[127] used a laser to pattern a nanoporous membrane at the junction of a cross channel. This device could concentrate proteins over 100–fold in 2 min, and the degree of concentration was limited only by analyte solubility. Similarly, an anionic polyacrylamide gel preconcentrator was laser photopolymerized in one arm of a cross channel in a PMMA microdevice.[128] The negatively charged sulfonate groups in the gel repelled negatively charged proteins, enabling concentrating of proteins up to 100,000-fold. Foote et al.[124] used a silicate membrane deposited between two adjacent microchannels, and a ~600-fold signal increase for proteins was achieved. Kim and Han[129] developed a simple protocol to fabricate a nanoporous membrane in microdevices. They used razor blades to form a gap in the microchannels in a PDMS substrate; Nafion 117 was then filled into the gap and a portion of the microchannels via capillary forces. In this protocol, preconcentration was achieved in large channels with dimensions up to 1 mm.

Semi-permeable membranes can also be integrated with other microchip functionalities. Herr et al.[130] fabricated a size-exclusion membrane at the injection junction of a microdevice, allowing antibody enrichment at the membrane surface. Sample loaded on the membrane was captured via antigen-antibody interaction, and enriched species were eluted into a separation channel for electrophoretic immunoassay. This system measured a biomarker for periodontal disease in saliva in <10 min with comparable results to ELISA. A similar design has been developed into a portable diagnostic format for rapid detection of biological toxins.[131] A membrane can also be used for SPE. Lion et al.[132] integrated a poly(vinylidene difluoride) membrane to desalt and concentrate samples before analyzing with mass spectrometry. Kim and Gale[133] sandwiched an aluminum oxide membrane between PDMS pieces;

when a blood sample passed through the membrane, DNA was selectively enriched and then eluted with buffer. The extraction time was <10 min while the recovery was ~40 ng of DNA per microliter of blood. A membrane has also been applied to enrich nonvolatile analytes by evaporation to reduce the amount of liquid phase.[134] The membrane was located at the interface between a gas and liquid channel; sample was introduced into the liquid channel, and water was evaporated into the gas channel through which nitrogen flowed.

In addition to the size exclusion mechanism, ion concentration polarization[135] can also be used to enrich biological samples. By applying a DC voltage on a cation-selective membrane, cations can enter the nanochannel under the voltage, while anions are driven away from the nanochannel. Consequently, the local ion concentration on the anodic side of the membrane decreases and forms an ion depletion zone. This depletion thickens the Debye layer and causes it to overlap in a nanofluidic channel. Electrical double layer overlap gives the nanochannels a preference for cation transfer and speeds up the concentration polarization. Hence, an extended space charge layer is formed near the membrane, and negatively charged analytes such as proteins can be continuously trapped and collected. The process can be maintained for several hours, resulting in million-fold enrichment.[136] This technique can be used for affinity,[137] enzyme,[138] and cellular kinase activity assays.[139] Because both antibody (or enzyme) and antigen (or substrate) are trapped in a small region, the reaction time is significantly shorter while sensitivity is improved. For instance, a kinase assay took less than 10 min, and the sample volume was as low as 5 cells in the cellular assay.[139]

1.4 DISSERTATION OVERVIEW

In my dissertation, I describe efforts to develop new approaches to quantify several biomarkers in human serum using integrated microfluidic devices. Microfluidic technologies have been applied extensively in rapid sample analysis. Some current challenges for standard microfluidic systems are relatively high detection limits, and reduced resolving power and peak capacity compared to conventional approaches. The integration of multiple functions and components onto a single platform can overcome these separation and detection limitations of microfluidics. I show that on-chip sample preparation, including cleanup and preconcentration, can serve to speed up and automate processes in integrated microfluidic systems. This chapter has provided a brief overview of integrated multi-process microfluidic systems for biological sample analysis. My work in the following chapters focuses on monolith columns, affinity columns and membrane filtration described in Section 1.3.

In Chapter 2, I present the design, fabrication and evaluation of monolith materials for off-chip solid phase extraction. Monoliths were prepared in microfabricated channels *in situ* by UV photopolymerization. This chapter serves as a proof of concept for SPE in microfluidic devices. These devices were used to enrich fluorescently labeled amino acids 20-fold and purify them from a mixture containing a contaminant protein. However, the off-chip extraction done in Chapter 2 slows the overall analysis speed and efficiency. Therefore, affinity column extraction and microchip CE have been integrated into one platform in Chapter 3. Sample loading, rinsing, elution, and separation were performed in an automated manner on a single chip by controlling potentials applied to appropriate reservoirs. FITC-tagged proteins were purified from

other contaminant species by an anti-FITC column and then separated by rapid microchip CE.

All samples tested on monolith columns in Chapters 2 and 3 were in simple buffer solutions, but for complex mixtures such as human serum, the monolith column can be easily clogged. In addition, acidic buffer was used to interrupt the antigen-antibody interaction and elute target components off the column, which significantly decreased the fluorescence signal. To address these issues in Chapter 3 I integrated additional functions, including online titration of acidic eluent and on-chip quantitation into these microdevices. Furthermore, affinity columns were fabricated via a wall-coated thin film of reactive polymer instead of monolith to alleviate column clogging with real samples. These systems can quantify AFP at ~1 ng/mL levels in ~10 μL of human serum in a few tens of minutes. AFP concentrations measured in these microdevices using both calibration curve and standard addition methods compared favorably with those determined using a commercial ELISA kit.

In Chapter 4, I demonstrate the quantitation of four cancer biomarkers in human serum using my integrated microdevices. After coating a thin film of reactive polymer in a microchannel, four antibodies were covalently immobilized to it. The retained protein amounts were consistent from chip to chip, demonstrating reproducibility. Furthermore, the signals from four fluorescently labeled proteins captured on-column were in the same range after rinsing, indicating the column has little bias toward any of the four antibodies or their antigens. These affinity columns have been integrated with capillary electrophoresis separation, enabling simultaneous quantification of four protein biomarkers in human blood serum in the low ng/mL range using either a

calibration curve or standard addition. These results could be easily adapted for detection of other biomarkers by simply immobilizing different antibodies in the affinity column. This system could also be expanded to detect ~30 biomarkers by immobilizing additional different antibodies on the affinity column, in conjunction with longer separation channels and spectral multiplexing to improve peak capacity.

Finally, in Chapter 5, I give general conclusions regarding my work and consider future directions for the field.

1.5 REFERENCES

1. Ward, D. E., *The cancer handbook : a guide for the nonspecialist*. Ohio State University Press: Columbus, 1995.
2. Heron, M.; Hoyert, D. L.; Murphy, S. L.; Xu, J.; Kochanek, K. D.; Tejada-Vera, B., Deaths: final data for 2006. *Natl Vital Stat Rep* **2009,** 57, (14), 1-134.
3. Bellenir, K., *Cancer sourcebook*. fourth ed.; Omnigraphics: Detroit, 2003.
4. American Cancer Society, Cancer Facts and Figures 2009. http://*www.cancer.org/downloads/STT/500809web.pdf (Access date: 3/23/2010*)
5. Winawer, S. J.; Zauber, A. G.; Ho, M. N.; O'Brien, M. J.; Gottlieb, L. S.; Sternberg, S. S.; Waye, J. D.; Schapiro, M.; Bond, J. H.; Panish, J. F.; et al., Prevention of colorectal cancer by colonoscopic polypectomy. The National Polyp Study Workgroup. *N Engl J Med* **1993,** 329, (27), 1977-1981.
6. Alison, M., *The cancer handbook*. Nature publishing group: New York, 2002; Vol. 2.
7. Bain, B. J., Bone marrow biopsy morbidity: review of 2003. *J Clin Pathol* **2005,** 58, (4), 406-408.
8. D'Amico, A. V.; Loeffler, J. S.; Harris, J. R., *Image-guided diagnosis and treatment of cancer* Humana Press Totowa, 2003.
9. Schoder, H.; Gonen, M., Screening for cancer with PET and PET/CT: potential and limitations. *J Nucl Med* **2007,** 48 Suppl 1, 4S-18S.
10. Smith, R. A.; Cokkinides, V.; Brawley, O. W., Cancer screening in the United States, 2009: a review of current American Cancer Society guidelines and issues in cancer screening. *CA Cancer J Clin* **2009,** 59, (1), 27-41.
11. Beinfeld, M. T.; Wittenberg, E.; Gazelle, G. S., Cost-effectiveness of whole-body CT screening. *Radiology* **2005,** 234, (2), 415-422.
12. Nass, S. J.; Moses, H. L., *Cancer biomarkers the promises and challenges of improving detection and treatment*. National Academies Press: Washington, D.C., 2007.
13. Ludwig, J. A.; Weinstein, J. N., Biomarkers in cancer staging, prognosis and treatment selection. *Nat Rev Cancer* **2005,** 5, (11), 845-856.
14. Dalton, W. S.; Friend, S. H., Cancer biomarkers--an invitation to the table. *Science* **2006,** 312, (5777), 1165-1168.
15. Miller, A. B., *Screening for cancer*. Academic Press: Orlando, 1985.
16. The U S Food and Drug Administration, Code of Federal Regulations: 21 CFR 866.6010, Immunology and Microbiology Devices, 1997.
17. Sinise, G. A., *Tumor markers research perspectives*. Nova Science Publishers: New York, 2007.
18. Bast, R. C.; Bates, S.; Bredt, A. B.; Desch, C. E.; Fritsche, H.; Fues, L.; Hayes, D. F.; Kemeny, N. E.; Kragen, M.; Jessup, J.; Locker, G. Y.; Macdonald, J. S.; Mennel, R. G.; Norton, L.; Ravdin, P.; Smith, T. J.; Taube, S.; Winn, R. J., Clinical practice guidelines for the use of tumor markers in breast and colorectal cancer. *J Clin Oncol* **1996,** 14, (10), 2843-2877.
19. Harris, L.; Fritsche, H.; Mennel, R.; Norton, L.; Ravdin, P.; Taube, S.; Somerfield, M. R.; Hayes, D. F.; Bast, R. C., Jr., American Society of Clinical Oncology 2007 update of recommendations for the use of tumor markers in breast cancer. *J Clin Oncol* **2007,** 25, (33), 5287-5312.
20. Bronchud, M. H.; Foote, M.; Giaccone, G.; Olopade, O.; Workman, P., *Principles of molecular oncology*. 2nd ed.; Humana Press: Totowa, N.J., 2004.

21. Lequin, R. M., Enzyme immunoassay (EIA)/enzyme-linked immunosorbent assay (ELISA). *Clin Chem* **2005,** 51, (12), 2415-2418.
22. Wreghitt, T. G.; Morgan-Capner, P., *ELISA in the clinical microbiology laboratory*. Public Health Laboratory Service London, 1990.
23. Kemeny, D. M., *A Practical guide to ELISA*. Pergamon Press New York, 1991.
24. Bowsher, R. R.; Sailstad, J. M., Insights in the application of research-grade diagnostic kits for biomarker assessments in support of clinical drug development: bioanalysis of circulating concentrations of soluble receptor activator of nuclear factor kappaB ligand. *J Pharm Biomed Anal* **2008,** 48, (5), 1282-1289.
25. Hou, C.; Herr, A. E., Clinically relevant advances in on-chip affinity-based electrophoresis and electrochromatography. *Electrophoresis* **2008,** 29, (16), 3306-3319.
26. Martinez, A. W.; Phillips, S. T.; Carrilho, E.; Thomas, S. W., 3rd; Sindi, H.; Whitesides, G. M., Simple telemedicine for developing regions: camera phones and paper-based microfluidic devices for real-time, off-site diagnosis. *Anal Chem* **2008,** 80, (10), 3699-3707.
27. Carrilho, E.; Phillips, S. T.; Vella, S. J.; Martinez, A. W.; Whitesides, G. M., Paper microzone plates. *Anal Chem* **2009,** 81, (15), 5990-5998.
28. Martinez, A. W.; Phillips, S. T.; Whitesides, G. M.; Carrilho, E., Diagnostics for the developing world: microfluidic paper-based analytical devices. *Anal Chem* **2010,** 82, (1), 3-10.
29. Stern, E.; Vacic, A.; Reed, M. A., Semiconducting Nanowire Field-Effect Transistor Biomolecular Sensors. *IEEE Trans Electr Dev* **2008,** 55, (11), 3119-3130.
30. Klemic, J. F.; Stern, E.; Reed, M. A., Hotwiring biosensors. *Nature Biotechnol* **2001,** 19, (10), 924-925.
31. Stern, E.; Steenblock, E. R.; Reed, M. A.; Fahmy, T. M., Label-free Electronic Detection of the Antigen-Specific T-Cell Immune Response. *Nano Letters* **2008,** 8, (10), 3310-3314.
32. Stern, E.; Klemic, J. F.; Routenberg, D. A.; Wyrembak, P. N.; Turner-Evans, D. B.; Hamilton, A. D.; LaVan, D. A.; Fahmy, T. M.; Reed, M. A., Label-free immunodetection with CMOS-compatible semiconducting nanowires. *Nature* **2007,** 445, (7127), 519-522.
33. Stern, E.; Cheng, G.; Cimpoiasu, E.; Klie, R.; Guthrie, S.; Klemic, J.; Kretzschmar, I.; Steinlauf, E.; Turner-Evans, D.; Broomfield, E.; Hyland, J.; Koudelka, R.; Boone, T.; Young, M.; Sanders, A.; Munden, R.; Lee, T.; Routenberg, D.; Reed, M. A., Electrical characterization of single GaN nanowires. *Nanotechnol* **2005,** 16, (12), 2941-2953.
34. Stern, E.; Wagner, R.; Sigworth, F. J.; Breaker, R.; Fahmy, T. M.; Reed, M. A., Importance of the debye screening length on nanowire field effect transistor sensors. *Nano Letters* **2007,** 7, (11), 3405-3409.
35. Stern, E.; Vacic, A.; Li, C.; Ishikawa, F. N.; Zhou, C.; Reed, M. A.; Fahmy, T. M., A nanoelectronic enzyme-linked immunosorbent assay for detection of proteins in physiological solutions. *Small* **2010,** 6, (2), 232-238.
36. Thompson, I. M.; Pauler, D. K.; Goodman, P. J.; Tangen, C. M.; Lucia, M. S.; Parnes, H. L.; Minasian, L. M.; Ford, L. G.; Lippman, S. M.; Crawford, E. D.; Crowley, J. J.; Coltman, C. A., Jr., Prevalence of prostate cancer among men with a prostate-specific antigen level < or =4.0 ng per milliliter. *N Engl J Med* **2004,** 350, (22), 2239-2246.

37. Makarov, D. V.; Loeb, S.; Getzenberg, R. H.; Partin, A. W., Biomarkers for prostate cancer. *Annu Rev Med* **2009,** 60, 139-151.
38. Sunami, E.; Shinozaki, M.; Higano, C. S.; Wollman, R.; Dorff, T. B.; Tucker, S. J.; Martinez, S. R.; Singer, F. R.; Hoon, D. S. B., Multimarker circulating DNA assay for assessing blood of prostate cancer patients. *Clin Chem* **2009,** 55, (3), 559-567.
39. Ward, B. G.; Cruickshank, D. J.; Tucker, D. F.; Love, S., Independent Expression in Serum of 3 Tumor-Associated Antigens - Ca-125, Placental Alkaline-Phosphatase and Hmfg2 in Ovarian-Carcinoma. *Br J Obstet Gynaecol* **1987,** 94, (7), 696-698.
40. Yang, X.-Q.; Yan, L.; Chen, C.; Hou, J.-X.; Li, Y., Application of C12 Multi-Tumor Marker Protein Chip in the Diagnosis of Gastrointestinal Cancer: Results of 329 Surgical Patients and Suggestions for Improvement. *Hepatogastroenterology* **2009,** 56, (94-95), 1388-1394.
41. Dolnik, V.; Liu, S., Applications of capillary electrophoresis on microchip. *J Sep Sci* **2005,** 28, (15), 1994-2009.
42. Whitesides, G. M., The origins and the future of microfluidics. *Nature* **2006,** 442, (7101), 368-373.
43. Auroux, P. A.; Iossifidis, D.; Reyes, D. R.; Manz, A., Micro total analysis systems. 2. Analytical standard operations and applications. *Anal Chem* **2002,** 74, (12), 2637-2652.
44. Fuentes, H. V.; Woolley, A. T., Electrically actuated, pressure-driven liquid chromatography separations in microfabricated devices. *Lab Chip* **2007,** 7, (11), 1524-1531.
45. Liu, P.; Mathies, R. A., Integrated microfluidic systems for high-performance genetic analysis. *Trends Biotechnol* **2009,** 27, (10), 572-581.
46. Emrich, C. A.; Tian, H.; Medintz, I. L.; Mathies, R. A., Microfabricated 384-lane capillary array electrophoresis bioanalyzer for ultrahigh-throughput genetic analysis. *Anal Chem* **2002,** 74, (19), 5076-5083.
47. Huynh, B. H.; Fogarty, B. A.; Martin, R. S.; Lunte, S. M., On-line coupling of microdialysis sampling with microchip-based capillary electrophoresis. *Anal Chem* **2004,** 76, (21), 6440-6447.
48. Janasek, D.; Franzke, J.; Manz, A., Scaling and the design of miniaturized chemical-analysis systems. *Nature* **2006,** 442, (7101), 374-380.
49. Peng, Y.; Pallandre, A.; Tran, N. T.; Taverna, M., Recent innovations in protein separation on microchips by electrophoretic methods. *Electrophoresis* **2008,** 29, (1), 157-178.
50. El-Ali, J.; Sorger, P. K.; Jensen, K. F., Cells on chips. *Nature* **2006,** 442, (7101), 403-411.
51. Ali, I.; Aboul-Enein, H. Y.; Gupta, V. K., Microchip-Based Nano Chromatography and Nano Capillary Electrophoresis in Genomics and Proteomics. *Chromatographia* **2009,** 69, S13-S22.
52. Marko-Varga, G. A.; Nilsson, J.; Laurell, T., New directions of miniaturization within the biomarker research area. *Electrophoresis* **2004,** 25, (21-22), 3479-3491.
53. Jorgenson, J. W.; Lukacs, K. D., Zone Electrophoresis in Open-Tubular Glass-Capillaries. *Anal Chem* **1981,** 53, (8), 1298-1302.
54. Shakalisava, Y.; Regan, F., Determination of montelukast sodium by capillary electrophoresis. *J. Sep. Sci.* **2008**, 31, (6-7), 1137-1143.

55. Van Theemsche, A.; Deconinck, J.; Van den Bossche, B.; Bortels, L., Numerical solution of a multi-ion one-potential model for electroosmotic flow in two-dimensional rectangular microchannels. *Anal Chem* **2002,** 74, (19), 4919-4926.
56. Skoog, D. A.; Holler, F. J.; Crouch, S. R., *Principles of Instrumental Analysis* 6th ed.; Thomson/Brooks Cole: Belmont, CA, 2007.
57. Terry, S. C.; Jerman, J. H.; Angell, J. B., A Gas Chromatographic Analyzer Fabricated in a Silicon Wafer. *IEEE Trans Electr Dev* **1979,** ED26, 1880-1886.
58. Lin, C. H.; Lee, G. B.; Lin, Y. H.; Chang, G. L., A fast prototyping process for fabrication of microfluidic systems on soda-lime glass. *J Micromech Microeng* **2001,** 11, (6), 726-732.
59. Harrison, D. J.; Fluri, K.; Seiler, K.; Fan, Z. H.; Effenhauser, C. S.; Manz, A., Micromachining a Miniaturized Capillary Electrophoresis-Based Chemical-Analysis System on a Chip. *Science* **1993,** 261, (5123), 895-897.
60. Woolley, A. T.; Mathies, R. A., Ultra-High-Speed DNA Fragment Separations Using Microfabricated Capillary Array Electrophoresis Chips. *Proc Nat Acad Sci U S A* **1994,** 91, (24), 11348-11352.
61. Sia, S. K.; Whitesides, G. M., Microfluidic devices fabricated in poly(dimethylsiloxane) for biological studies. *Electrophoresis* **2003,** 24, (21), 3563-3576.
62. Gustafsson, O.; Mogensen, K. B.; Kutter, J. P., Underivatized cyclic olefin copolymer as substrate material and stationary phase for capillary and microchip electrochromatography. *Electrophoresis* **2008,** 29, (15), 3145-3152.
63. Becker, H.; Locascio, L. E., Polymer microfluidic devices. *Talanta* **2002,** 56, (2), 267-287.
64. Kelly, R. T.; Pan, T.; Woolley, A. T., Phase-Changing Sacrificial Materials for Solvent Bonding of High-Performance Polymeric Capillary Electrophoresis Microchips. *Anal. Chem.* **2005,** 77, (11), 3536-3541.
65. Shah, J. J.; Geist, J.; Locascio, L. E.; Gaitan, M.; Rao, M. V.; Vreeland, W. N., Capillarity induced solvent-actuated bonding of polymeric microfluidic devices. *Anal Chem* **2006,** 78, (10), 3348-3353.
66. Bharadwaj, R.; Santiago, J. G.; Mohammadi, B., Design and optimization of on-chip capillary electrophoresis. *Electrophoresis* **2002,** 23, (16), 2729-2744.
67. Rocklin, R. D.; Ramsey, R. S.; Ramsey, J. M., A microfabricated fluidic device for performing two-dimensional liquid-phase separations. *Anal Chem* **2000,** 72, (21), 5244-5249.
68. Roman, G. T.; Carroll, S.; McDaniel, K.; Culbertson, C. T., Micellar electrokinetic chromatography of fluorescently labeled proteins on poly(dimethylsiloxane)-based microchips. *Electrophoresis* **2006,** 27, (14), 2933-2939.
69. Ramsey, J. D.; Jacobson, S. C.; Culbertson, C. T.; Ramsey, J. M., High-efficiency, two-dimensional separations of protein digests on microfluidic devices. *Anal Chem* **2003,** 75, (15), 3758-3764.
70. Roddy, E. S.; Xu, H.; Ewing, A. G., Sample introduction techniques for microfabricated separation devices. *Electrophoresis* **2004,** 25, (2), 229-242.
71. Yi, C.; Zhang, Q.; Li, C. W.; Yang, J.; Zhao, J.; Yang, M., Optical and electrochemical detection techniques for cell-based microfluidic systems. *Anal Bioanal Chem* **2006,** 384, (6), 1259-1268.
72. Reyes, D. R.; Iossifidis, D.; Auroux, P. A.; Manz, A., Micro total analysis systems. 1. Introduction, theory, and technology. *Anal Chem* **2002,** 74, (12), 2623-2636.

73. Soper, S. A.; Ford, S. M.; Qi, S.; McCarley, R. L.; Kelly, K.; Murphy, M. C., Polymeric microelectromechanical systems. *Anal Chem* **2000,** 72, (19), 642A-651A.
74. Kelly, R. T.; Woolley, A. T., Thermal bonding of polymeric capillary electrophoresis microdevices in water. *Anal Chem* **2003,** 75, (8), 1941-1945.
75. Hille, J. M.; Freed, A. L.; Watzig, H., Possibilities to improve automation, speed and precision of proteome analysis: a comparison of two-dimensional electrophoresis and alternatives. *Electrophoresis* **2001,** 22, (19), 4035-4052.
76. Zhao, Y.; McLaughlin, K.; Lunte, C. E., On-column sample preconcentration using sample matrix switching and field amplification for increased sensitivity of capillary electrophoretic analysis of physiological samples. *Anal Chem* **1998,** 70, (21), 4578-4585.
77. Carabias-Martinez, R.; Rodriguez-Gonzalo, E.; Revilla-Ruiz, P.; Dominguez-Alvarez, J., Solid-phase extraction and sample stacking-micellar electrokinetic capillary chromatography for the determination of multiresidues of herbicides and metabolites. *J Chromatogr A* **2003,** 990, (1-2), 291-302.
78. Kim, J. B.; Otsuka, K.; Terabe, S., On-line sample concentration in micellar electrokinetic chromatography with cationic micelles in a coated capillary. *J Chromatogr A* **2001,** 912, (2), 343-252.
79. Siri, N.; Riolet, P.; Bayle, C.; Couderc, F., Automated large-volume sample stacking procedure to detect labeled peptides at picomolar concentration using capillary electrophoresis and laser-induced fluorescence detection. *J Chromatogr B* **2003,** 793, (1), 151-157.
80. Burgi, D. S.; Chien, R. L., Application and limits of sample stacking in capillary electrophoresis. *Methods Mol Biol* **1996,** 52, (1), 211-226.
81. Jung, B.; Bharadwaj, R.; Santiago, J. G., Thousandfold signal increase using field-amplified sample stacking for on-chip electrophoresis. *Electrophoresis* **2003,** 24, (19-20), 3476-3483.
82. Jung, B.; Bharadwaj, R.; Santiago, J. G., On-chip millionfold sample stacking using transient isotachophoresis. *Anal Chem* **2006,** 78, (7), 2319-2327.
83. Jung, B.; Zhu, Y.; Santiago, J. G., Detection of 100 aM fluorophores using a high-sensitivity on-chip CE system and transient isotachophoresis. *Anal Chem* **2007,** 79, (1), 345-349.
84. Sueyoshi, K.; Kitagawa, F.; Otsuka, K., Recent progress of online sample preconcentration techniques in microchip electrophoresis. *J Sep Sci* **2008,** 31, (14), 2650-2666.
85. Bercovici, M.; Kaigala, G. V.; Santiago, J. G., Method for analyte identification using isotachophoresis and a fluorescent carrier ampholyte assay. *Anal Chem* **2010,** 82, (5), 2134-2138.
86. Bercovici, M.; Kaigala, G. V.; Backhouse, C. J.; Santiago, J. G., Fluorescent carrier ampholytes assay for portable, label-free detection of chemical toxins in tap water. *Anal Chem* **2010,** 82, (5), 1858-1866.
87. Koegler, W. S.; Ivory, C. F., Focusing proteins in an electric field gradient. *J Chromatogr A* **1996,** 726, (1-2), 229-236.
88. Humble, P. H.; Kelly, R. T.; Woolley, A. T.; Tolley, H. D.; Lee, M. L., Electric field gradient focusing of proteins based on shaped ionically conductive acrylic polymer. *Anal Chem* **2004,** 76, (19), 5641-5648.
89. Kelly, R. T.; Li, Y.; Woolley, A. T., Phase-changing sacrificial materials for interfacing microfluidics with ion-permeable membranes to create on-chip preconcentrators and electric field gradient focusing microchips. *Anal Chem* **2006,** 78, (8), 2565-2570.

90. Liu, J.; Sun, X.; Farnsworth, P. B.; Lee, M. L., Fabrication of conductive membrane in a polymeric electric field gradient focusing microdevice. *Anal Chem* **2006,** 78, (13), 4654-4662.
91. Sun, X.; Farnsworth, P. B.; Woolley, A. T.; Tolley, H. D.; Warnick, K. F.; Lee, M. L., Poly(ethylene glycol)-functionalized devices for electric field gradient focusing. *Anal Chem* **2008,** 80, (2), 451-460.
92. Sun, X.; Farnsworth, P. B.; Tolley, H. D.; Warnick, K. F.; Woolley, A. T.; Lee, M. L., Performance optimization in electric field gradient focusing. *J Chromatogr A* **2009,** 1216, (1), 159-164.
93. Hennion, M. C., Solid-phase extraction: method development, sorbents, and coupling with liquid chromatography. *J Chromatogr A* **1999,** 856, (1-2), 3-54.
94. Berrueta, L. A.; Gallo, B.; Vicente, F., A Review of Solid-Phase Extraction - Basic Principles and New Developments. *Chromatographia* **1995,** 40, (7-8), 474-483.
95. Kutter, J. P.; Jacobson, S. C.; Ramsey, J. M., Solid phase extraction on microfluidic devices. *Journal of Microcolumn Separations* **2000,** 12, (2), 93-97.
96. Wolfe, K. A.; Breadmore, M. C.; Ferrance, J. P.; Power, M. E.; Conroy, J. F.; Norris, P. M.; Landers, J. P., Toward a microchip-based solid-phase extraction method for isolation of nucleic acids. *Electrophoresis* **2002,** 23, (5), 727-733.
97. Oleschuk, R. D.; Shultz-Lockyear, L. L.; Ning, Y.; Harrison, D. J., Trapping of bead-based reagents within microfluidic systems: on-chip solid-phase extraction and electrochromatography. *Anal Chem* **2000,** 72, (3), 585-590.
98. Jemere, A. B.; Oleschuk, R. D.; Ouchen, F.; Fajuyigbe, F.; Harrison, D. J., An integrated solid-phase extraction system for sub-picomolar detection. *Electrophoresis* **2002,** 23, (20), 3537-3544.
99. Zhong, R.; Liu, D.; Yu, L.; Ye, N.; Dai, Z.; Qin, J.; Lin, B., Fabrication of two-weir structure-based packed columns for on-chip solid-phase extraction of DNA. *Electrophoresis* **2007,** 28, (16), 2920-2926.
100. Ramsey, J. D.; Collins, G. E., Integrated microfluidic device for solid-phase extraction coupled to micellar electrokinetic chromatography separation. *Anal Chem* **2005,** 77, (20), 6664-6670.
101. Ceriotti, L.; de, R.; Verpoorte, E., An integrated fritless column for on-chip capillary electrochromatography with conventional stationary phases. *Anal Chem* **2002,** 74, (3), 639-647.
102. Svec, F., Less common applications of monoliths: I. Microscale protein mapping with proteolytic enzymes immobilized on monolithic supports. *Electrophoresis* **2006,** 27, (5-6), 947-961.
103. Xie, S. F.; Svec, F.; Frechet, J. M. J., Porous polymer monoliths: Preparation of sorbent materials with high-surface areas and controlled surface chemistry for high-throughput, online, solid-phase extraction of polar organic compounds. *Chem Mat* **1998,** 10, (12), 4072-4078.
104. Yu, C.; Davey, M. H.; Svec, F.; Frechet, J. M., Monolithic porous polymer for on-chip solid-phase extraction and preconcentration prepared by photoinitiated in situ polymerization within a microfluidic device. *Anal Chem* **2001,** 73, (21), 5088-5096.
105. Wen, J.; Guillo, C.; Ferrance, J. P.; Landers, J. P., DNA extraction using a tetramethyl orthosilicate-grafted photopolymerized monolithic solid phase. *Anal Chem* **2006,** 78, (5), 1673-1681.
106. Wen, J.; Guillo, C.; Ferrance, J. P.; Landers, J. P., Microfluidic-based DNA purification in a two-stage, dual-phase microchip containing a reversed-phase and a photopolymerized monolith. *Anal Chem* **2007,** 79, (16), 6135-6142.

107. Noll, F.; Lutsch, G.; Bielka, H., Structure of IgG and IgY molecules in ribosome-antibody complexes as studied by electron microscopy. *Immunol Lett* **1982,** 4, (3), 117-123.
108. Ebner, A.; Wildling, L.; Kamruzzahan, A. S.; Rankl, C.; Wruss, J.; Hahn, C. D.; Holzl, M.; Zhu, R.; Kienberger, F.; Blaas, D.; Hinterdorfer, P.; Gruber, H. J., A new, simple method for linking of antibodies to atomic force microscopy tips. *Bioconjug Chem* **2007,** 18, (4), 1176-1184.
109. Lin, P. C.; Chen, S. H.; Wang, K. Y.; Chen, M. L.; Adak, A. K.; Hwu, J. R.; Chen, Y. J.; Lin, C. C., Fabrication of oriented antibody-conjugated magnetic nanoprobes and their immunoaffinity application. *Anal Chem* **2009,** 81, (21), 8774-8782.
110. Cass, T.; Ligler, F. S., *Immobilized biomolecules in analysis : a practical approach*. Oxford University Press: Oxford, 1998.
111. Cho, I. H.; Paek, E. H.; Lee, H.; Kang, J. Y.; Kim, T. S.; Paek, S. H., Site-directed biotinylation of antibodies for controlled immobilization on solid surfaces. *Anal Biochem* **2007,** 365, (1), 14-23.
112. Qian, W.; Yao, D.; Yu, F.; Xu, B.; Zhou, R.; Bao, X.; Lu, Z., Immobilization of antibodies on ultraflat polystyrene surfaces. *Clin Chem* **2000,** 46, (9), 1456-1463.
113. Gunaratna, P. C.; Wilson, G. S., Optimization of multienzyme flow reactors for determination of acetylcholine. *Anal Chem* **1990,** 62, (4), 402-407.
114. Dodge, A.; Fluri, K.; Verpoorte, E.; de Rooij, N. F., Electrokinetically driven microfluidic chips with surface-modified chambers for heterogeneous immunoassays. *Anal Chem* **2001,** 73, (14), 3400-3409.
115. Phillips, T. M.; Wellner, E. F., Analysis of inflammatory biomarkers from tissue biopsies by chip-based immunoaffinity CE. *Electrophoresis* **2007,** 28, (17), 3041-3048.
116. Phillips, T. M.; Wellner, E. F., Chip-based immunoaffinity CE: application to the measurement of brain-derived neurotrophic factor in skin biopsies. *Electrophoresis* **2009,** 30, (13), 2307-2312.
117. Mao, X.; Luo, Y.; Dai, Z.; Wang, K.; Du, Y.; Lin, B., Integrated lectin affinity microfluidic chip for glycoform separation. *Anal Chem* **2004,** 76, (23), 6941-6947.
118. He, M.; Herr, A. E., Microfluidic polyacrylamide gel electrophoresis with in situ immunoblotting for native protein analysis. *Anal Chem* **2009,** 81, (19), 8177-8184.
119. He, M.; Herr, A. E., Polyacrylamide gel photopatterning enables automated protein immunoblotting in a two-dimensional microdevice. *J Am Chem Soc* **2010,** 132, (8), 2512-2513.
120. Kong, J.; Jiang, L.; Su, X.; Qin, J.; Du, Y.; Lin, B., Integrated microfluidic immunoassay for the rapid determination of clenbuterol. *Lab Chip* **2009,** 9, (11), 1541-1547.
121. Fan, R.; Vermesh, O.; Srivastava, A.; Yen, B. K.; Qin, L.; Ahmad, H.; Kwong, G. A.; Liu, C. C.; Gould, J.; Hood, L.; Heath, J. R., Integrated barcode chips for rapid, multiplexed analysis of proteins in microliter quantities of blood. *Nat Biotechnol* **2008,** 26, (12), 1373-1378.
122. Stern, E.; Vacic, A.; Rajan, N. K.; Criscione, J. M.; Park, J.; Ilic, B. R.; Mooney, D. J.; Reed, M. A.; Fahmy, T. M., Label-free biomarker detection from whole blood. *Nat Nanotechnol* **2010,** 5, (2), 138-142.
123. Wu, X.-Z.; Hosaka, A.; Hobo, T., An On-Line Electrophoretic Concentration Method for Capillary Electrophoresis of Proteins. *Anal Chem* **1998,** 70, (10), 2081 - 2084.

124. Foote, R. S.; Khandurina, J.; Jacobson, S. C.; Ramsey, J. M., Preconcentration of proteins on microfluidic devices using porous silica membranes. *Anal Chem* **2005,** 77, (1), 57-63.
125. Wei, W.; Yeung, E. S., On-line concentration of proteins and peptides in capillary zone electrophoresis with an etched porous joint. *Anal Chem* **2002,** 74, (15), 3899-3905.
126. Zhang, Y.; Timperman, A. T., Integration of nanocapillary arrays into microfluidic devices for use as analyte concentrators. *Analyst* **2003,** 128, (6), 537-542.
127. Song, S.; Singh, A. K.; Kirby, B. J., Electrophoretic concentration of proteins at laser-patterned nanoporous membranes in microchips. *Anal Chem* **2004,** 76, (15), 4589-4592.
128. Yamamoto, S.; Hirakawa, S.; Suzuki, S., In situ fabrication of ionic polyacrylamide-based preconcentrator on a simple poly(methyl methacrylate) microfluidic chip for capillary electrophoresis of anionic compounds. *Anal Chem* **2008,** 80, (21), 8224-8230.
129. Kim, S. J.; Han, J., Self-sealed vertical polymeric nanoporous-junctions for high-throughput nanofluidic applications. *Anal Chem* **2008,** 80, (9), 3507-3511.
130. Herr, A. E.; Hatch, A. V.; Throckmorton, D. J.; Tran, H. M.; Brennan, J. S.; Giannobile, W. V.; Singh, A. K., Microfluidic immunoassays as rapid saliva-based clinical diagnostics. *Proc Natl Acad Sci U S A* **2007,** 104, (13), 5268-5273.
131. Meagher, R. J.; Hatch, A. V.; Renzi, R. F.; Singh, A. K., An integrated microfluidic platform for sensitive and rapid detection of biological toxins. *Lab Chip* **2008,** 8, (12), 2046-2053.
132. Lion, N.; Gellon, J. O.; Jensen, H.; Girault, H. H., On-chip protein sample desalting and preparation for direct coupling with electrospray ionization mass spectrometry. *J Chromatogr A* **2003,** 1003, (1-2), 11-19.
133. Kim, J.; Gale, B. K., Quantitative and qualitative analysis of a microfluidic DNA extraction system using a nanoporous AlO(x) membrane. *Lab Chip* **2008,** 8, (9), 1516-1523.
134. Timmer, B. H.; van Delft, K. M.; Olthuis, W.; Bergveld, P.; van den Berg, A., Micro-evaporation electrolyte concentrator. *Sensors Actuat B* **2003,** 91, (1-3), 342-346.
135. Kim, S. J.; Wang, Y. C.; Lee, J. H.; Jang, H.; Han, J., Concentration polarization and nonlinear electrokinetic flow near a nanofluidic channel. *Phys Rev Lett* **2007,** 99, (4), 044501.
136. Wang, Y. C.; Stevens, A. L.; Han, J., Million-fold preconcentration of proteins and peptides by nanofluidic filter. *Anal Chem* **2005,** 77, (14), 4293-4299.
137. Wang, Y. C.; Han, J., Pre-binding dynamic range and sensitivity enhancement for immuno-sensors using nanofluidic preconcentrator. *Lab Chip* **2008,** 8, (3), 392-394.
138. Lee, J. H.; Song, Y. A.; Tannenbaum, S. R.; Han, J., Increase of reaction rate and sensitivity of low-abundance enzyme assay using micro/nanofluidic preconcentration chip. *Anal Chem* **2008,** 80, (9), 3198-3204.
139. Lee, J. H.; Cosgrove, B. D.; Lauffenburger, D. A.; Han, J., Microfluidic concentration-enhanced cellular kinase activity assay. *J Am Chem Soc* **2009,** 131, (30), 10340-10341.

2. AFFINITY MONOLITH PRECONCENTRATORS FOR POLYMER MICROCHIP CAPILLARY ELECTROPHORESIS*

2.1 INTRODUCTION

Clinical assays, biological analysis, and pharmaceutical effectiveness studies increasingly require the monitoring of multiple analytes in complex mixtures. For instance, to detect cancer and other diseases at early stages, biomarker detection in bodily fluids is used widely.[1] However, these species often have low abundances and are in complex matrices.[2] Consequently, it is an ongoing challenge to detect trace analytes in real samples.

Since the early 1990s, there has been strong interest in the miniaturization of chemical analysis systems.[3] Such instrumentation offers small volume analysis, fast separation, and the potential to combine multiple processes in a single device. Despite successful applications in areas such as biomarker assays,[4] a major challenge with microfluidic devices is the detection limit, because small sample volumes (in the microliter range) can be loaded on chip,[5] and the optical path for detection is short (typically <100 μm).[6] In addition, the separation length in microdevices limits the resolving power, which is critical for analyzing complex mixtures.[7] As a consequence, sample preconcentration and pretreatment will play an important role in the determination of trace analytes in biological specimens using miniaturized devices.

* This chapter is reproduced with permission from *Electrophoresis*, 2008, 29, 3429-3435. Copyright 2008 Wiley-VCH Verlag GmbH & Co.

Traditional sample concentration techniques in capillary electrophoresis (CE)[8] such as sweeping and stacking have been shown for molecules like pharmaceutical species[9] and peptides[10]. Moreover, the stacking technique has been integrated into microdevices.[11] However, in stacking, the conductivity of the sample matrix must be lower than the running buffer,[12, 13] constraining experimental conditions. Other online concentration methods have also been reported that utilize the size difference between analytes and buffer ions. These techniques take advantage of the inability of larger molecules to pass through a porous layer in a semipermeable hollow fiber,[14] membrane[15] or joint,[16] while smaller ions are allowed to transit. However, complex device fabrication and detection instrumentation are needed for these systems.

Solid phase extraction (SPE) is a widely used method for sample preparation, in which a targeted analyte is retained on a column to separate it from the matrix and is then eluted for analysis.[17] The promise of enriching samples by SPE has led researchers to apply this approach in microdevices. In one study, microchip walls were coated with silanes to form an SPE column, and 80-fold preconcentration was observed;[18] however, due to the limited surface area, the loading capacity of this approach was relatively low. To address loading, silica bead[19] and polymer monolith[20, 21] SPE columns have also been integrated into microdevices. Silica bead columns have disadvantages in terms of packing and frit fabrication, which complicate microdevice preparation. On the other hand, monoliths are an attractive alternative to packed particles because of low back pressure and relative ease of column formation.[22]

However, SPE in as-formed monoliths typically has low selectivity. In addition, nonspecific binding sites hinder elution of desired analytes and decrease sample loading capacity due to competitive adsorption. One way to overcome these shortcomings is to introduce a precolumn to remove most interferences from the matrix. Landers' group[23] recently demonstrated a packed octadecyl bead precolumn coupled with monolith extraction on chip, which increased the loading capacity around 100-fold for DNA analysis. An alternative approach to improve selectivity is to immobilize enzymes or antibodies on a monolith. In fact, solid-phase supports have been used for the attachment of enzymes since the 1970s.[24] A recent review summarizes the application of monoliths as supports for attaching protease enzymes in protein mapping.[22] These studies indicate a promising future for monolithic materials as pretreatment columns for biological samples.

Here I demonstrate a technique for *in situ* preparation of sample pretreatment monoliths in microfluidic devices. These monoliths are integrated readily into microdevices and used as SPE columns for sample preconcentration and pretreatment. I demonstrate the preconcentration of amino acids on monoliths to show the general nature of this approach. To enhance extraction selectivity, I immobilized antibodies on monoliths and blocked nonspecific adsorption sites. I have used these affinity monoliths to enrich fluorescently labeled amino acids 20-fold and purify them from a mixture containing a contaminant protein. My results build a foundation for future fabrication of fully integrated sample preparation and separation microdevices for fast, sensitive, and inexpensive protein analysis.

2.2 MATERIALS AND METHODS

2.2.1 Reagents and materials

All amino acids except Trp were obtained from ICN Biomedicals (Aurora, OH). Lysozyme (95% protein), hydroxypropyl cellulose (HPC, average MW 100,000), Trp (99%), glycidyl methacrylate (GMA, 97%), ethylene dimethacrylate (EDMA, 98%), 2,2-dimethoxy-2-phenylacetophenone (DMPA, 99%), and 1-dodecanol (98%) were purchased from Sigma-Aldrich (Milwaukee, WI). PBS-EDTA coupling buffer (pH 7.2), sulfo-SMCC, and 2-mercaptoethylamine (MEA) were from Pierce (Rockford, IL). FITC was from Molecular Probes (Eugene, OR). Ethylenediamine (EDA) and Tris (electrophoresis grade) were from Fisher (Fair Lawn, NJ). Cyclohexanol (100%) was from J.T. Baker (Phillipsburg, NJ). Anti-FITC was from Biomeda (Foster City, CA). Green fluorescent protein (GFP, 1.0 mg/mL) was from BD Biosciences (San Jose, CA). Sodium azide was from Merck (Darmstadt, Germany). All solutions were prepared with deionized water (18.3 MΩ-cm) purified by a Barnstead EASYpure UV/UF system (Dubuque, IA). Poly(methyl methacrylate) (PMMA, Acrylite FF, 3-mm thick) was from Cyro Industries (Rockaway, NJ) and was cut to 1.8×5.0 cm^2 by a CO_2 laser cutter (C200, Universal Laser Systems, Scottsdale, AZ) before use.

2.2.2 Device fabrication

Two kinds of microdevices were utilized in this study (**Figure 2.1**): extractor and separation chips. The fabrication protocol was adapted from previous work in Dr. Woolley's lab to transfer the pattern from photomasks to polymeric devices.[25] A ~0.5 μm thickness of silicon dioxide was grown on a 4-inch silicon <100> wafer by flowing a humidified oxygen stream at 1110 °C for 90 min. The oxidized wafer was then spin-coated with a thin film (~1 μm) of Shipley 812 photoresist, and prebaked on

a hot plate at 110 °C for 60 s to remove residual solvent and improve adhesion of the photoresist to the wafer. The photoresist was exposed to UV light for 10 s through a patterned photomask fabricated on chrome-coated glass in the Integrated Microfabrication Lab at Brigham Young University (BYU). After UV exposure, the wafer was submerged in Shipley MF-26A developer for 30 s to remove the exposed photoresist. The substrate was rinsed with water and postbaked in a preheated oven for 15 min at 120 °C to remove any remaining water and promote the adhesion of the remaining photoresist.[26] After postbaking, the wafer was immersed in 10% buffered HF for 7 min to remove the unprotected silicon dioxide. Finally, the pattern was wet etched to a ~20 μm depth in 40% aqueous KOH solution for 20 min at 70 °C. The etched silicon wafer served as a hot embossing template.

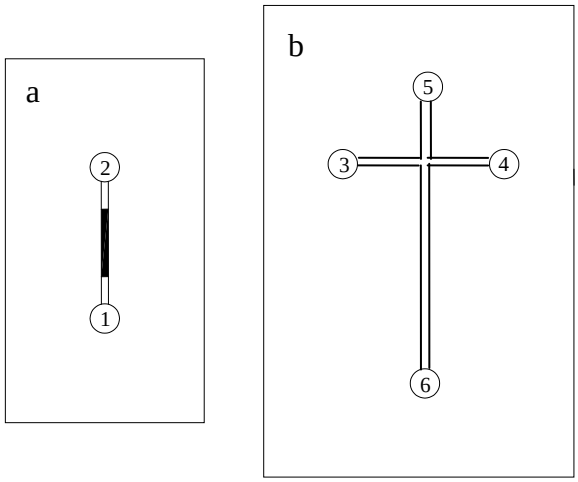

Figure 2.1. Schematic diagram of microchips; (a) an extractor chip and (b) a separation chip. In (a) the 0.5-cm-long monolith is formed between reservoirs 1 and 2. In (b) reservoir 3 is for sample and reservoir 4 is for injection waste. The separation channel connects reservoirs 5 and 6. The distance from the intersection to reservoirs 3-5 is 0.5 cm, and the distance to reservoir 6 is 3.5 cm.

PMMA substrates were imprinted by hot embossing at 140 °C for 30 min using etched Si templates. The patterned PMMA was then thermally bonded at 110 °C for 30 min to an unimprinted PMMA substrate with drilled holes for reservoirs. Channel widths at half height were 50 μm, and channel depths were 20 μm.

Porous polymer monoliths (0.5-cm long) were prepared in the extraction microchip (**Figure 2.1a**) by photoinitiated *in situ* polymerization. Monoliths were made from GMA and EDMA monomers with DMPA as the photoinitiator. Cyclohexanol and 1-dodecanol were used as the porogen. The monolith preparation followed published procedures.[27-29] Briefly, 0.005 g DMPA, 0.4 g GMA and 0.6 g EDMA were mixed in a 4-mL glass vial. Porogen (0.3 g cyclohexanol and 0.7 g 1-dodecanol) was added slowly to the mixture. Before polymerization, the solution was sonicated in a water bath for 3 min followed by nitrogen purging for 3 min to remove dissolved oxygen. The degassed mixture was aspirated into the microchannels by vacuum, and excess monomer in the reservoir was removed by pipet to minimize siphoning during polymerization.[30] Next, the microchip was partially covered with electrical tape or aluminum foil to provide spatial control over polymerization. The microchip was then put on a cooled aluminum plate and exposed to UV light (200 mW/cm^2) in the wavelength range of 320–390 nm for 10 min. Cooling the device helped eliminate undesired thermal polymerization.[30] Finally, unreacted monomer and porogen were removed by flushing 2-propanol through the microchannels using a syringe pump.

2.2.3 Tris-reacted monoliths

For general analyte preconcentration, the reactive GMA epoxy groups were blocked using Tris buffer (100 mM, pH 8.4) pumped through the monolith and incubated for 24 h at room temperature.[31] This protocol is based on the chemical reaction between GMA epoxy groups and Tris amine groups. The monolith was then rinsed with water using a syringe pump. The reservoirs were filled with deionized water, and the device was stored in a humidified Petri dish until use.

2.2.4 Immobilization of antibodies on monoliths

To provide analyte specificity, monolithic columns were functionalized with immobilized antibodies, as illustrated in **Figure 2.2.**[32] Briefly, amine groups were first introduced on the monolith surface by EDA reaction with the GMA epoxy groups; neat EDA was flowed into the monolith with a syringe pump (Harvard Apparatus, Holliston, MA) and incubated at room temperature for 24 h. The monolith was next washed with 100 mM PBS-EDTA buffer at 10 µL/min for 30 min to remove any remaining EDA. Pendant amines were reacted subsequently with a heterobifunctional crosslinker, sulfo-SMCC, which contains an amine-reactive N-hydroxysuccinimide ester and a maleimide group to react with thiols. Consequently, the sulfo-SMCC can link reduced antibodies to the amine-modified monolith. The crosslinker was prepared at 2 mg/mL in PBS-EDTA and was pumped through the monolith at 1 µL/min for 2 h. Then, 1 mg of anti-FITC was mixed with 200 µL of 6 mg/mL MEA and incubated for 2 h at 37 ºC. MEA preferentially reduces disulfide bonds in the antibody hinge region, largely leaving the remainder of the antibody intact (see **Figure 2.2**).[33, 34] The partially reduced antibody was purified using a desalting column (Pierce) equilibrated with PBS-EDTA. The fractions were monitored by measuring UV absorbance at 280 nm with a Nanodrop ND-1000 spectrophotometer (Nanodrop Inc., Wilmington, DE). Once the protein concentration was >10 µg/mL, the solution was pumped into the monolith and incubated for 4 h at room temperature to attach the antibodies. Unbound antibodies were washed out using PBS-EDTA, and the devices were stored in PBS-EDTA buffer containing 0.02% sodium azide until use.

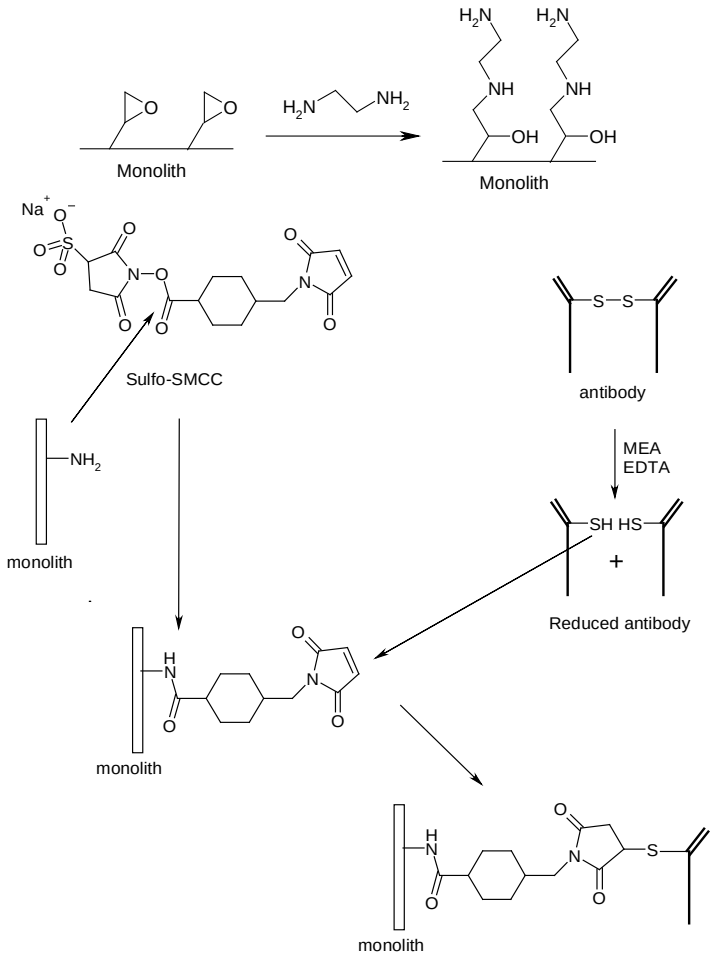

Figure 2.2. Protocol for attaching antibodies onto a monolith.

2.2.5 Electrophoresis experiments

FITC labeling of amino acids followed a literature procedure.[35] Operation of the separation chip (**Figure 2.1b**) has been described previously.[25, 36] Briefly, microchannels were filled with 10 mM carbonate buffer (pH 9.1) containing 0.5% (w/v) HPC using a syringe pump. The solution in reservoir 3 was removed by pipet and replaced with 15 μL of sample in running buffer. A platinum electrode was placed in each reservoir to provide voltage, and all electrodes were interfaced with a custom-built switch which connected to PS310 (providing 0.6 kV) and PS350 (providing 1.6

kV) high-voltage power supplies (Stanford Research Systems, Sunnyvale, CA). For injection, reservoirs 3, 5 and 6 were grounded while reservoir 4 was at 0.6 kV. For separation, reservoirs 3 and 4 were at 0.6 kV, reservoir 5 was grounded, and reservoir 6 was raised to 1.6 kV. Laser-induced fluorescence was used to detect FITC-tagged analytes and GFP. The detection system and data collection setup have been reported before,[25] and the sampling rate for data acquisition was 10 Hz; higher sampling rates may be desirable for quantitative work. Peaks in the electropherograms were identified by spiking 3 μL of 10-fold more concentrated analyte into reservoir 3 and repeating the separation under the same conditions.

2.2.6 Characterization and use of Tris-reacted monoliths

To quantitatively monitor sample loading and elution, I used 0.1 mM Trp in Tris buffer (pH 8.4). Because Trp absorbs at 280 nm, the UV absorbance (Nanodrop ND-1000) of the solution eluted from the monolith in reservoir 2 (**Figure 2.1a**) was measured. A UV absorbance calibration curve of Trp in Tris buffer (R^2=0.991) was generated to allow quantitation of the Trp eluted from the column. Tris buffer was first pumped through the monolith to reduce surface wetting losses. Trp solution was pumped through the monolith, and 50-μL fractions in reservoir 2 were collected in a 0.5-mL microcentrifuge tube. A 2-μL aliquot from each fraction was pipeted onto the Nanodrop system to probe UV absorbance at 280 nm. Once the UV absorbance reached a plateau (indicating column saturation), the monolith was rinsed with deionized water, and 50 μL fractions were collected. To elute Trp from the column, 10 mM phosphate buffer (pH 2.1) was pumped through the monolith, and 20 μL fractions were collected. The pump rate was 2 μL/min for all steps. The elution efficiency was calculated by dividing the amount of Trp collected in the elution step

by the total retained amount of Trp. The quantity of retained Trp was determined by subtracting the amount of Trp eluted in the loading step from the total amount of Trp pumped into the monolith.

To evaluate the enrichment achieved with Tris-reacted monoliths, electropherograms of 200 nM FITC-Asp were obtained before and after monolith extraction. Briefly, a 200-μL sample was separated into two parts. A 100-μL aliquot was pumped through the Tris-reacted monolith at 2 μL/min and rinsed with 10 μL deionized water. The retained analyte was then eluted with 20 μL of 10 mM phosphate buffer (pH 2.1). The pH of the eluted sample was adjusted to ~9 by mixing with 0.4 μL of 1 M NaOH solution. The monolith-enriched and control samples were subsequently analyzed by microchip CE as described in section 2.2.5.

2.2.7 Characterization and use of affinity monoliths

The amount of anti-FITC affixed on the monolith was determined by the 280 nm UV absorbance difference of the antibody solution before and after immobilization.[37] Briefly, 500 μL of 10 μg/mL partially reduced antibody solution was separated into two parts; 250 μL of the solution was used for immobilization and the other 250 μL were retained as a control. After derivatization, the affinity column was flushed with 10 μL PBS buffer. All solution removed from the column was combined, and the volume was determined by micropipette. The control antibody solution was diluted to the same volume with PBS, and the UV absorbance of both solutions was analyzed by the Nanodrop system.

Because nonspecific adsorption can cause carryover contamination and decrease sample loading capacity due to competitive effects, column performance can be improved if nonspecific adsorption sites are removed. To do so, 40 mg/mL lysozyme in PBS buffer[38] was flushed through the affinity monolith at 2 μL/min for 20 min after antibody immobilization. Then the affinity column was rinsed with deionized water at 5 μL/min for 10 min to wash out any unbound lysozyme. To examine the effectiveness of lysozyme treatment for blocking nonspecific adsorption, 50 μg/mL GFP solutions were used as a fluorescence probe and pumped through both control and lysozyme-blocked affinity columns. The monoliths were next rinsed with 10 mM Tris buffer (pH 8.4) at 10 μL/min for 3 min. A ~300-μm-long segment of the affinity column was illuminated with a laser at 488 nm, and fluorescence images were taken with a Nikon digital camera (Coolpix 995, Tokyo, Japan).[39] Quantitative fluorescence intensities were monitored by a cooled CCD camera (Coolsnap HQ, Roper Scientific, Tucson, AZ); the signal was determined from the average intensity on the monolith for each CCD image. Data processing and CCD parameter adjustments were carried out using V++ Precision Digital Imaging Software (Version 4.0, Auckland, New Zealand), and the CCD exposure time was 300 ms.

The extraction efficiency of lysozyme-treated affinity columns was measured somewhat differently from the Tris-reacted monoliths. FITC-Gly (1 mM) was used as the indicator, and the concentration of eluted analyte was monitored by CCD. To quantitatively determine the amount of FITC-Gly, a calibration curve was generated from the average fluorescence signal of standard FITC-Gly solutions in reservoir 2 (concentration range 0.01-10 mM, R^2=0.996).

To evaluate the selectivity of affinity monoliths, electropherograms of a FITC-amino acid/GFP mixture were obtained before and after monolith extraction. The procedures were similar to those described earlier for Tris-reacted monoliths. The mixture consisted of FITC-Gly, FITC-Phe, FITC-Arg and GFP. All amino acid concentrations were 10 nM while the concentration of GFP was 50 μg/mL. A 500-μL solution was separated into two parts: a 50-μL control and a 450-μL monolith-extracted sample. The 450-μL aliquot was pumped through the affinity monolith at 2 μL/min. The fractions in reservoir 2 (**Figure 2.1a**) were collected by micropipette, transferred to reservoir 3 (**Figure 2.1b**), and separated by microchip CE. The rinsing, elution, and pH adjustment were the same as described in section 2.2.6. The monolith-extracted and control samples were subsequently analyzed by microchip CE as outlined in section 2.2.5.

2.3 RESULTS AND DISCUSSION

2.3.1 Monolith characterization by SEM

SEM images of a typical monolith in a microdevice and more detailed monolith features are shown in **Figure 2.3**. Under my synthesis conditions, the monolith (see **Figure 2.3b**) has good porosity, which provides low backpressure and a large surface area to enhance loading capacity.

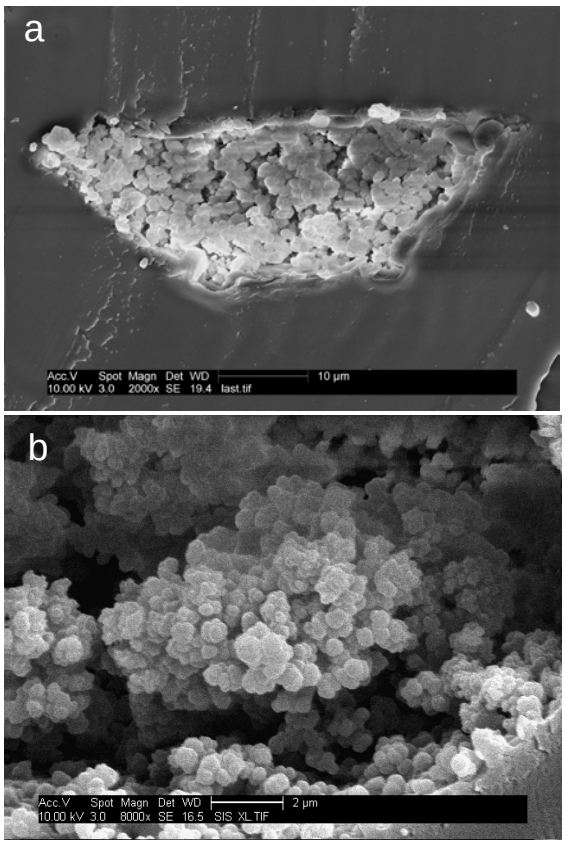

Figure 2.3. SEM images of (a) a typical monolith in the microchannel and (b) detailed monolith features.

2.3.2 Preconcentration of amino acids on Tris-reacted monoliths

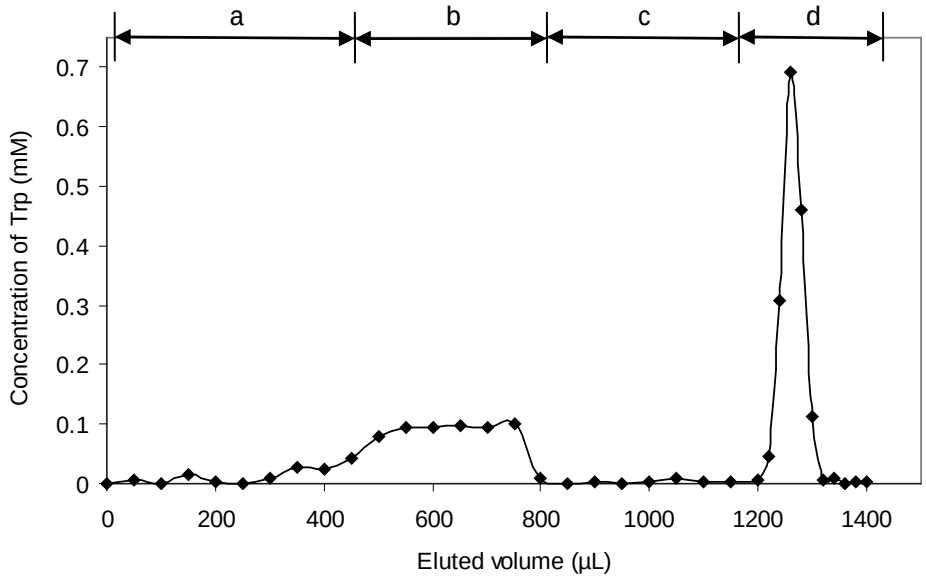

Figure 2.4. Concentration of Trp collected in reservoir 2 (**Figure 2.1a**) as a function of volume flowed through a Tris-reacted monolith at 2 µL/min. Intervals: (a) loading, (b) monolith saturation, (c) washing, and (d) elution. Fractions in reservoir 2 were collected at increments of 50 µL in (a-c), and 20 µL in (d). Fractions were quantified by UV-Vis detection.

A typical concentration profile for Trp over the course of loading, rinsing and elution from a Tris-reacted monolith is presented in **Figure 2.4**. Mean recovery volumes were 46 µL for the 50-µL fractions, indicating collection losses of <10%. During the loading step (**Figure 2.4a-b**), the Trp concentration in the reservoir after the monolith was near zero until after 350 µL of flow, and then increased with the flow volume until the maximum loading of 0.1 mM Trp was reached at around 500 µL (**Figure 2.4b**). During washing (**Figure 2.4c**), a small amount of Trp was removed from the column (<5%), indicating strong Trp retention on the monolith. Over 70% of the retained Trp was collected in 60 µL of elution buffer (**Figure 2.4d**). I define the elution efficiency as the moles of analyte eluted divided by the moles retained. The average elution efficiency was 82%, the run-to-run variability was 6.1% (n=3), and

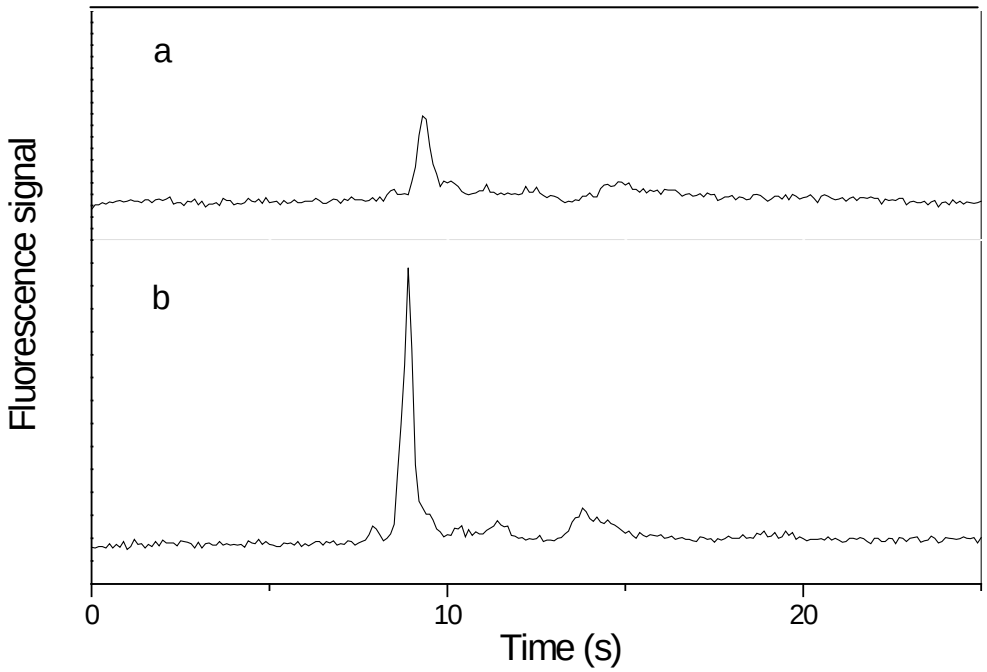

Figure 2.5. Microchip CE of FITC-Asp (a) before and (b) after native monolith extraction. CE conditions are described in section 2.2.5.

the chip-to-chip variability was 1.2% (n=3). These results demonstrate that monoliths can be integrated reproducibly in microdevices and have good SPE functionality.

To evaluate the feasibility of combining a monolith column with microchip CE separation, 200 nM FITC-Asp was loaded onto a Tris-reacted column, eluted and subsequently separated by microchip CE (**Figure 2.5**). In comparing the control (**Figure 2.5a**) and extracted sample (**Figure 2.5b**), the retention time of Asp was about the same, but the peak height of the extracted solution was threefold higher. Since a 100-μL sample was loaded and elution occurred in a fivefold smaller volume (20 μL), the threefold signal increase corresponds to ~60% recovery of FITC-Asp. This type of Tris-reacted column is useful for preconcentration and can be combined readily with microchip CE, but the extraction and preconcentration is not selective.

2.3.3 Characterization of affinity monoliths

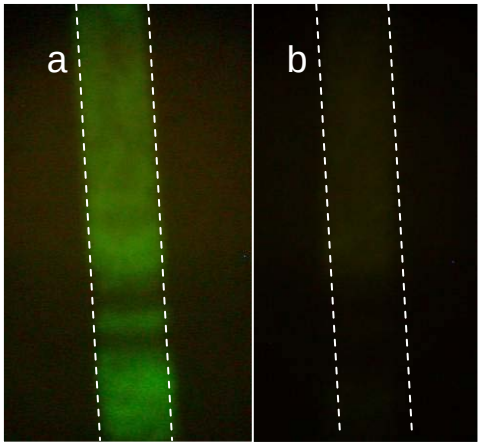

Figure 2.6. Fluorescence images of retained GFP on monoliths (a) without and (b) with lysozyme blocking.

Under my reaction conditions, the amount of anti-FITC immobilized on the 0.5-cm-long monolith column was 250±70 mg/g (n=3). This result is similar to published data on immobilized trypsin on a GMA-co-EDMA monolith (~320 mg/g),[37] and is somewhat higher than what was reported using the 1,1'-carbonyldiimidazole (CDI) method for immobilizing anti-FITC on the same monolith (61 mg/g).[31] Thus, my protocol yields comparable results to other methods and has several advantages. Unlike direct reaction with epoxy groups,[40] my technique works with tenfold lower antibody concentrations (~10 µg/mL) and sixfold shorter reaction times (~4 h). Furthermore, compared to my approach, the CDI method needs water-free conditions;[40] while the Schiff base and hydrazide techniques involve hydrolysis of the epoxy ring, which requires catalyst optimization.[41]

Fluorescence images comparing lysozyme-treated and unblocked monoliths are shown in **Figure 2.6**. Considerable GFP was adsorbed on the surface of monoliths not treated with lysozyme, and bright fluorescence was observed throughout the column. On the other hand, after lysozyme blocking, very low fluorescence (near background) was found on the monolith. The ratio of background-subtracted GFP signals in unblocked and blocked monoliths was 16, indicating that lysozyme passivation significantly reduces nonspecific protein adsorption on my affinity monoliths.

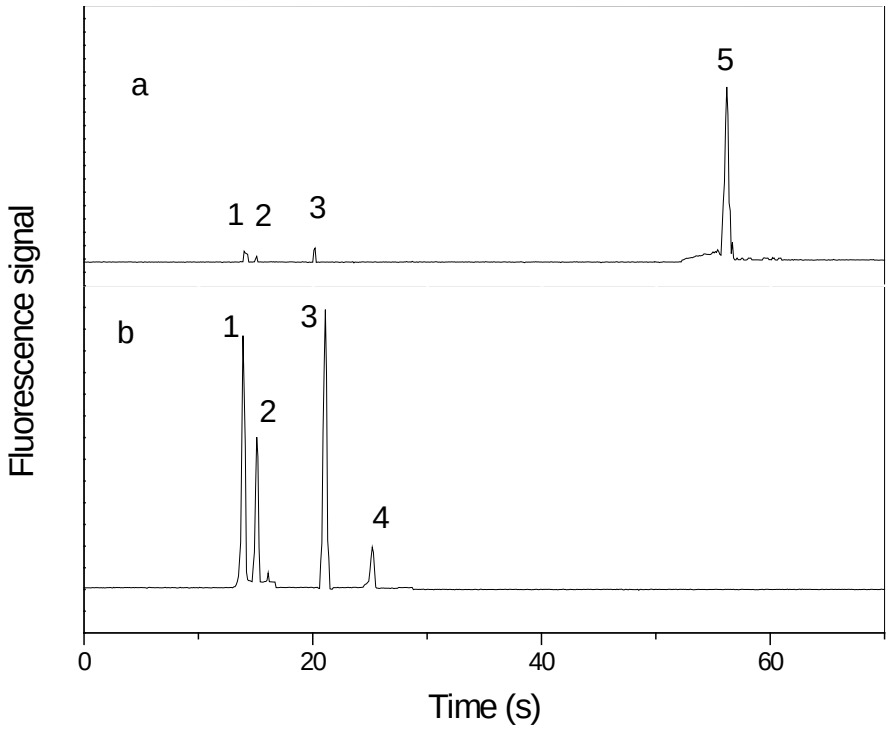

Figure 2.7. Microchip CE of amino acids and GFP (a) before and (b) after affinity column extraction. Peaks 1-5 are Gly, Phe, Arg, FITC, and GFP, respectively. CE conditions are described in section 2.2.5.

Based on the FITC-Gly CCD signal in reservoir 2 generated as described in section 2.2.7, the average elution efficiency of the lysozyme-treated affinity columns was 86%, and the chip-to-chip variability was 3.1% (n=3). These results indicate that the elution efficiency of my affinity columns is comparable to that of Tris-reacted monoliths, and my column performance is reproducible. Importantly, affinity monoliths have analyte selectivity, as I show in the following section.

2.3.4 Selective extraction by affinity monoliths

To evaluate the selectivity of my affinity columns, a mixture of FITC-labeled amino acids and GFP was pumped through an affinity monolith and then analyzed by microchip CE. In **Figure 2.7a**, the amino acid peak heights were about tenfold smaller

than GFP. Contrastingly, in **Figure 2.7b** the GFP peak is reduced significantly after affinity purification, while the FITC-amino acid peak heights increased around 20-fold. Based on the 22-fold reduction in volume during extraction, I calculate a 91% recovery of FITC-tagged amino acids. The higher recovery in this experiment compared to Tris-reacted monoliths may be attributed to reduced nonspecific adsorption with the affinity monolith. After extraction, a FITC peak appeared in the electropherogram (**Figure 2.7b**). The FITC peak was identified by spiking 3 μL of 500 nM FITC into reservoir 3 **(Figure 2.1b**) and repeating the separation under the same conditions. Uncoupled FITC, which is retained by the affinity monolith, was not visible above noise in the raw sample (**Figure 2.7a**). Based on the signal ratio of Arg to GFP in **Figure 2.7a-b**, a 25,000-fold reduction in GFP concentration was achieved after immunoaffinity extraction. My results clearly demonstrate that microchip affinity monoliths can selectively concentrate and purify target analytes through specific antibody-antigen interactions.

Pretreatment and selective analyte enrichment are essential in many applications where the samples are complex, including trace protein analysis. In this chapter, photo-defined monoliths were applied as sample preconcentrators and affinity purification columns in polymer microfluidic devices. Successful antibody immobilization and nonspecific adsorption blocking have also been shown. These results demonstrate that microchip immunoaffinity monoliths can selectively enrich desired species in complex biological mixtures for subsequent CE analysis. The good reproducibility in the amino acid work indicates the excellent potential for use of these affinity monoliths in fully integrated on-chip sample preparation and separation. These systems offer the possibility of fast, simple and sensitive protein analysis.

2.4 REFERENCES

1. Huck, C. W.; Bakry, R.; Bonn, G. K., Progress in capillary electrophoresis of biomarkers and metabolites between 2002 and 2005. *Electrophoresis* **2006,** 27, (1), 111-125.
2. Merrell, K.; Southwick, K.; Graves, S. W.; Esplin, M. S.; Lewis, N. E.; Thulin, C. D., Analysis of low-abundance, low-molecular-weight serum proteins using mass spectrometry. *J Biomol Tech* **2004,** 15, (4), 238-248.
3. Dolnik, V.; Liu, S., Applications of capillary electrophoresis on microchip. *J Sep Sci* **2005,** 28, (15), 1994-2009.
4. Marko-Varga, G. A.; Nilsson, J.; Laurell, T., New directions of miniaturization within the biomarker research area. *Electrophoresis* **2004,** 25, (21-22), 3479-3491.
5. Roddy, E. S.; Xu, H.; Ewing, A. G., Sample introduction techniques for microfabricated separation devices. *Electrophoresis* **2004,** 25, (2), 229-242.
6. Yi, C.; Zhang, Q.; Li, C. W.; Yang, J.; Zhao, J.; Yang, M., Optical and electrochemical detection techniques for cell-based microfluidic systems. *Anal Bioanal Chem* **2006,** 384, (6), 1259-1268.
7. Bharadwaj, R.; Santiago, J. G.; Mohammadi, B., Design and optimization of on-chip capillary electrophoresis. *Electrophoresis* **2002,** 23, (16), 2729-2744.
8. Lin, C. H.; Kaneta, T., On-line sample concentration techniques in capillary electrophoresis: velocity gradient techniques and sample concentration techniques for biomolecules. *Electrophoresis* **2004,** 25, (23-24), 4058-4073.
9. Zhao, Y.; McLaughlin, K.; Lunte, C. E., On-column sample preconcentration using sample matrix switching and field amplification for increased sensitivity of capillary electrophoretic analysis of physiological samples. *Anal Chem* **1998,** 70, (21), 4578-4585.
10. Monton, M. R.; Imami, K.; Nakanishi, M.; Kim, J. B.; Terabe, S., Dynamic pH junction technique for on-line preconcentration of peptides in capillary electrophoresis. *J Chromatogr A* **2005,** 1079, (1-2), 266-273.
11. Gong, M.; Wehmeyer, K. R.; Limbach, P. A.; Arias, F.; Heineman, W. R., On-line sample preconcentration using field-amplified stacking injection in microchip capillary electrophoresis. *Anal Chem* **2006,** 78, (11), 3730-3737.
12. Huang, Y. F.; Huang, C. C.; Hu, C. C.; Chang, H. T., Capillary electrophoresis-based separation techniques for the analysis of proteins. *Electrophoresis* **2006,** 27, (18), 3503-3522.
13. Burgi, D. S.; Chien, R. L., Optimization in Sample Stacking for High-Performance Capillary Electrophoresis. *Analytical Chemistry* **1991,** 63, (18), 2042-2047.
14. Wu, X.-Z.; Hosaka, A.; Hobo, T., An On-Line Electrophoretic Concentration Method for Capillary Electrophoresis of Proteins. *Anal Chem* **1998,** 70, (10), 2081 - 2084.
15. Foote, R. S.; Khandurina, J.; Jacobson, S. C.; Ramsey, J. M., Preconcentration of proteins on microfluidic devices using porous silica membranes. *Anal Chem* **2005,** 77, (1), 57-63.
16. Wei, W.; Yeung, E. S., On-line concentration of proteins and peptides in capillary zone electrophoresis with an etched porous joint. *Anal Chem* **2002,** 74, (15), 3899-3905.
17. Berrueta, L. A.; Gallo, B.; Vicente, F., A Review of Solid-Phase Extraction - Basic Principles and New Developments. *Chromatographia* **1995,** 40, (7-8), 474-483.

18. Kutter, J. P.; Jacobson, S. C.; Ramsey, J. M., Solid phase extraction on microfluidic devices. *Journal of Microcolumn Separations* **2000,** 12, (2), 93-97.
19. Jemere, A. B.; Oleschuk, R. D.; Ouchen, F.; Fajuyigbe, F.; Harrison, D. J., An integrated solid-phase extraction system for sub-picomolar detection. *Electrophoresis* **2002,** 23, (20), 3537-3544.
20. Yu, C.; Davey, M. H.; Svec, F.; Frechet, J. M., Monolithic porous polymer for on-chip solid-phase extraction and preconcentration prepared by photoinitiated in situ polymerization within a microfluidic device. *Anal Chem* **2001,** 73, (21), 5088-5096.
21. Stachowiak, T. B.; Rohr, T.; Hilder, E. F.; Peterson, D. S.; Yi, M.; Svec, F.; Frechet, J. M., Fabrication of porous polymer monoliths covalently attached to the walls of channels in plastic microdevices. *Electrophoresis* **2003,** 24, (21), 3689-3693.
22. Svec, F.; Huber, C. G., Monolithic materials: Promises, challenges, achievements. *Anal Chem* **2006,** 78, (7), 2101-2107.
23. Wen, J.; Guillo, C.; Ferrance, J. P.; Landers, J. P., Microfluidic-Based DNA Purification in a Two-Stage, Dual-Phase Microchip Containing a Reversed-Phase and a Photopolymerized Monolith. *Anal Chem* **2007,** 79, (16), 6135-6142.
24. Benoit, M. R.; Kohler, J. T., An evaluation of a ceramic monolith as an enzyme support material. *Biotech Bioeng* **1975,** 17, (11), 1617-1626.
25. Kelly, R. T.; Woolley, A. T., Thermal bonding of polymeric capillary electrophoresis microdevices in water. *Anal Chem* **2003,** 75, (8), 1941-1945.
26. Madou, M. J., *Fundamentals of microfabrication: the science of miniaturization*. second ed.; CRC press: Boca Raton, 2001.
27. Yu, C.; Xu, M. C.; Svec, F.; Frechet, J. M. J., Preparation of monolithic polymers with controlled porous properties for microfluidic chip applications using photoinitiated free-radical polymerization. *J Poly Sci* **2002,** 40, (6), 755-769.
28. Hahn, R.; Podgomik, A.; Merhar, M.; Schallaun, E.; Jungbauer, A., Affinity monoliths generated by in situ polymerization of the ligand. *Anal Chem* **2001,** 73, (21), 5126-5132.
29. Gu, B.; Li, Y.; Lee, M. L., Polymer monoliths with low hydrophobicity for strong cation-exchange capillary liquid chromatography of peptides and proteins. *Anal Chem* **2007,** 79, (15), 5848-5855.
30. Ramsey, J. D.; Collins, G. E., Integrated microfluidic device for solid-phase extraction coupled to micellar electrokinetic chromatography separation. *Anal Chem* **2005,** 77, (20), 6664-6670.
31. Jiang, T.; Mallik, R.; Hage, D. S., Affinity monoliths for ultrafast immunoextraction. *Anal Chem* **2005,** 77, (8), 2362-2372.
32. Mallik, R.; Wa, C.; Hage, D. S., Development of sulfhydryl-reactive silica for protein immobilization in high-performance affinity chromatography. *Anal Chem* **2007,** 79, (4), 1411-1424.
33. Domen, P. L.; Nevens, J. R.; Mallia, A. K.; Hermanson, G. T.; Klenk, D. C., Site-directed immobilization of proteins. *J Chromatogr* **1990,** 510, 293-302.
34. Palmer, J. L.; Nisonoff, A., Reduction and reoxidation of a critical disulfide bond in rabbit antibody molecule. *J Biol Chem* **1963,** 238, (7), 2393-2398.
35. Kelly, R. T.; Pan, T.; Woolley, A. T., Phase-changing sacrificial materials for solvent bonding of high-performance polymeric capillary electrophoresis microchips. *Anal Chem* **2005,** 77, (11), 3536-3541.
36. Liu, J.; Pan, T.; Woolley, A. T.; Lee, M. L., Surface-modified poly(methyl methacrylate) capillary electrophoresis microchips for protein and peptide analysis. *Anal Chem* **2004,** 76, (23), 6948-6955.

37. Krenkova, J.; Bilkova, Z.; Foret, F., Characterization of a monolithic immobilized trypsin microreactor with on-line coupling to ESI-MS. *J Sep Sci* **2005,** 28, (14), 1675-1684.
38. Naruishi, N.; Tanaka, Y.; Higashi, T.; Wakida, S., Highly efficient dynamic modification of plastic microfluidic devices using proteins in microchip capillary electrophoresis. *J Chromatogr A* **2006,** 1130, (2), 169-174.
39. Kelly, R. T.; Li, Y.; Woolley, A. T., Phase-changing sacrificial materials for interfacing microfluidics with ion-permeable membranes to create on-chip preconcentrators and electric field gradient focusing microchips. *Anal Chem* **2006,** 78, (8), 2565-2570.
40. Mallik, R.; Jiang, T.; Hage, D. S., High-performance affinity monolith chromatography: development and evaluation of human serum albumin columns. *Anal Chem* **2004,** 76, (23), 7013-7022.
41. Luo, Q.; Mao, X.; Kong, L.; Huang, X.; Zou, H., High-performance affinity chromatography for characterization of human immunoglobulin G digestion with papain. *J Chromatogr B* **2002,** 776, (2), 139-147.

3. INTEGRATED MICROFLUIDIC DEVICE FOR SERUM BIOMARKER QUANTITATION USING EITHER STANDARD ADDITION OR A CALIBRATION CURVE*

3.1 INTRODUCTION

The two most widely used quantitation tools in traditional analytical chemistry are the calibration curve and the method of standard addition.[1] Micromachined devices for chemical analysis[2, 3] that integrate multiple processes,[4] reduce sample and reagent consumption,[5] and decrease analysis time[6, 7] and instrument footprint,[8, 9] are becoming an attractive alternative to the classical separation-based analysis approaches. Although calibration curves have been used in microchip-based chemical analysis,[10, 11] the method of standard addition, which is especially desirable for addressing matrix effects in complex samples such as blood,[1] has seen extremely limited use. Very recently, a serial dilution microfluidic device was applied in standard addition quantitation of mM concentrations of $Fe(CN)_6^{4-}$, a model analyte, although the aqueous KCl solution was not one for which matrix effects were anticipated.[12]

Alpha-fetoprotein (AFP) is a diagnostic biomarker for *Hepatocellular carcinoma* (HCC),[13] with a reported specificity of 65% to 94%.[14] In general, patients with an elevated serum AFP concentration have a higher risk for HCC. Currently, enzyme linked immunosorbent assay (ELISA) is used in the clinical analysis of AFP in human

* This chapter is reproduced with permission from *Anal. Chem.*, 2009, 81, 8230-8235. Copyright 2009 American Chemical Society.

serum.[15] With trained personnel, an ELISA can provide reliable results, although the microplate format makes ELISA best suited for clinical, rather than point-of-care (POC) diagnostics. In contrast, rapid analysis[6, 7] and the ability to combine multiple processing steps[4, 16] on a single device make a microfluidic-based approach very attractive for POC AFP analysis. In addition, miniaturized devices can significantly reduce antigen-antibody reaction time compared with conventional microplate ELISA.[10] The analysis and separation of AFP in spiked buffer solutions in a microdevice platform have been reported,[17-19] and chip-based microfluidic assay systems for other analytes have been developed for saliva[10] and blood samples.[11, 20, 21] However, only calibration curve quantitation has been explored.

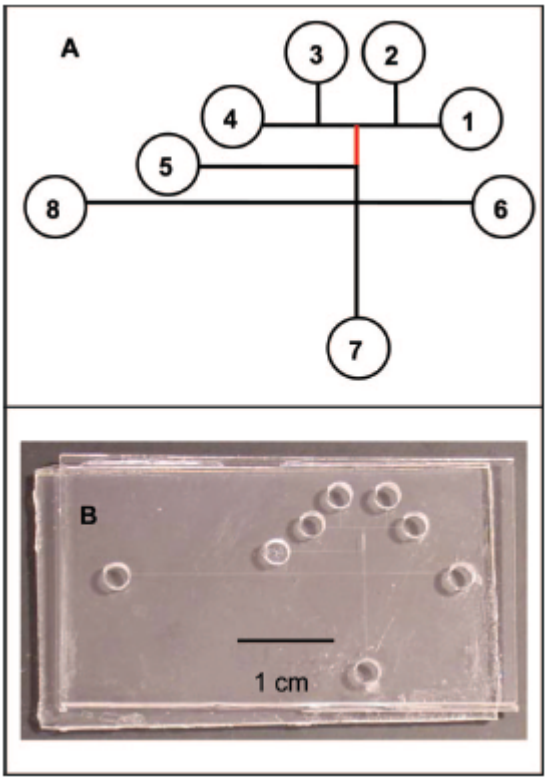

Figure 3.1. Microchip layout. (A) Design schematic; reservoirs are (1) rinse, (2) protein standard, (3) sample, (4) elute, (5) waste, (6) buffer, (7) inject waste, and (8) high voltage. The monolith location is indicated by the red line. (B) Photograph of a fabricated microchip.

Although previous antibody-based monolith work in Chapter 2 has shown promise in selective extraction for biological mixtures, off-chip extraction slows the overall analysis speed and efficiency. To solve this problem, an affinity column can be coupled with electrophoretic analysis in a single device. The new design with eight reservoirs is shown in **Figure 3.1**. Reservoirs 1-4 were the inlets for rinse solution, a

protein standard, sample, and elution buffer, respectively. Reservoir 5 served as the waste reservoir during sample preparation. Reservoir 6 contained separation buffer, reservoir 7 was for injection waste, and reservoir 8 was the separation high-voltage reservoir. A photograph of a completed microchip is shown in **Figure 3.1b**. The poly(methyl methacrylate) (PMMA) microchips were fabricated using a combination of photolithography, solvent imprinting, and thermal bonding methods described in Section 2.2.2. The monolith was also prepared in microchannel according to the protocol in Section 2.2.2.

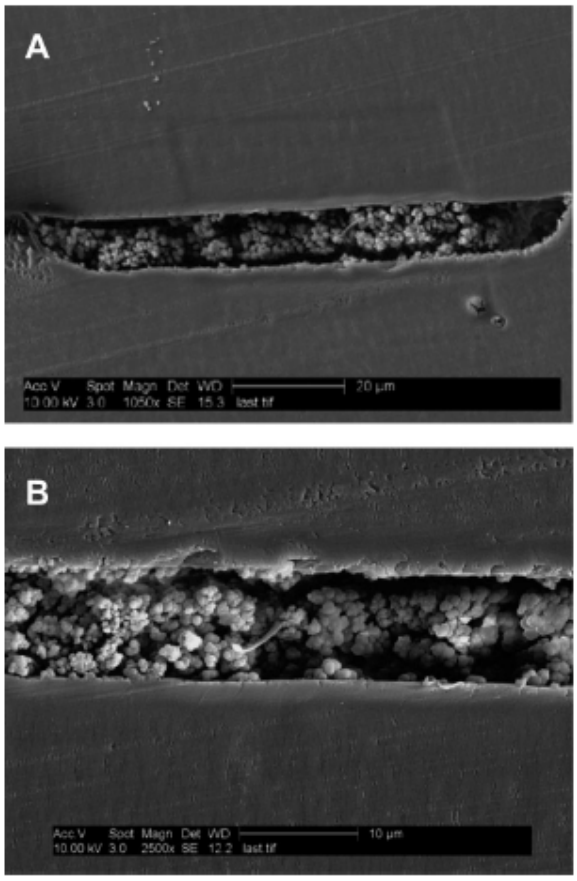

Figure 3.2. SEM images of monoliths inside a microfluidic channel. (A) Whole channel image; (B) magnified view.

Figure 3.2 shows scanning electron microscopy (SEM) images of a well-defined porous monolith inside a microfluidic channel. The polymer is cast uniformly over the cross section of the column. These images indicate that the fabricated monoliths have appropriate porosity for low back pressure and sufficient surface area for protein immobilization. Antibodies can be directly immobilized on the monolith surface via reaction between antibody amino groups and epoxy groups on the monolith surface. Although this protocol needs a higher antibody concentration, it is simpler and does not require additional reagents such as mercaptoethylamine that are

needed for the method described in Section 2.2.4. Briefly, the dry monoliths were sequentially wetted with 2-propanol and running buffer for 5 min each. One mg/mL anti-FITC in 0.05 M borate buffer (pH 8.0) was loaded into the monolith, and the microchip reservoirs were filled with buffer to avoid solution evaporation during reaction. Then, the whole chip was sealed with 3 M Scotch tape (St. Paul, MN) and put on a shaker at 37 °C for 24 h. Next, any remaining epoxy groups were blocked by flowing 100 mM Tris buffer (pH 8) through the monolith for 1 h. Finally, the entire chip was flushed with phosphate running buffer.

In this system, sample loading, rinsing, elution and separation were all performed in an automated manner by controlling the potentials applied to various reservoirs. FITC-tagged species were selectively retained by the anti-FITC column and separated from other contaminants. The retained proteins were then eluted from the monolith with 200 mM acetic acid.[22]

The monolith system worked well for simple systems such as buffered solution. However, when I applied real biological samples such as human serum, significant clogging was observed in many devices due to aggregation and non-specific adsorption of proteins. Thus, I also explored an open channel column where antibodies are immobilized on

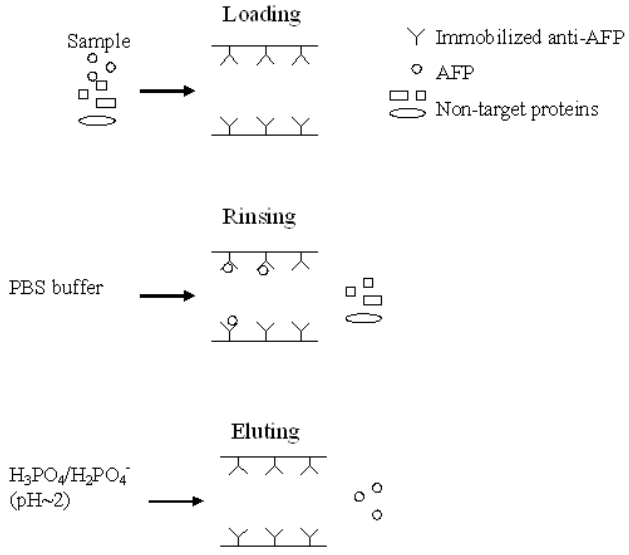

Figure 3.3. Immunoaffinity extraction overview.

a patterned section of a microchannel surface to form an affinity column. When a sample flows through the column, only antigen will be retained based on antibody-antigen interaction, while non-target material will pass through the column to waste (illustrated in **Figure 3.3**). This approach has been shown to capture target proteins from buffer solutions[23] in a microdevice, but the ability to work with complex specimens such as blood, and integrate capture with separation[22] has not been shown.

Here, I demonstrate an integrated microfluidic system capable of performing quantitative determination of AFP, a biomarker for liver cancer,[24] in human serum, using both the method of standard addition and a calibration curve. My approach utilizes an immunoaffinity purification step coupled with rapid microchip electrophoresis separation, all under voltage control, in a miniaturized polymer microchip. These systems with laser-induced fluorescence (LIF) detection can quantify AFP at ~1 ng/mL levels in ~10 μL of human serum in 30-50 minutes, offering exciting potential for POC applications.

3.2 MATERIALS AND METHODS

3.2.1 Reagents and materials

Monoclonal anti-AFP antibody, Fluorescein-5-isothiocyanate labeled bovine serum albumin (FITC-BSA), immunoglobulin G (IgG), dimethyl sulfoxide (DMSO, 99.7%), glycidyl methacrylate (GMA, 97%), poly(ethylene glycol) diacrylate (PEGDA, 575 Da average molecular weight), and 2,2'-dimethoxy-2-phenylacetophenone (DMPA, 99%) were purchased from Sigma-Aldrich (Milwaukee, WI). Human AFP (>95%) was from Lee Biosolutions (St. Louis, MO). Green fluorescent protein (GFP, 1.0 mg/mL) was from BD Biosciences (San Jose, CA). Glycine was obtained from ICN

Biomedicals (Aurora, OH). Sodium phosphate buffer (PBS, pH 7.2) was from Pierce (Rockford, IL). All solutions were prepared with deionized water (18.3 MΩ-cm) purified by a Barnstead EASYpure UV/UF system (Dubuque, IA). Poly(methyl methacrylate) (PMMA, Acrylite FF, 3-mm thickness) was from Cyro Industries (Rockaway, NJ) and was cut by a CO_2 laser cutter (VLS2.30, Universal Laser Systems, Scottsdale, AZ) before use.

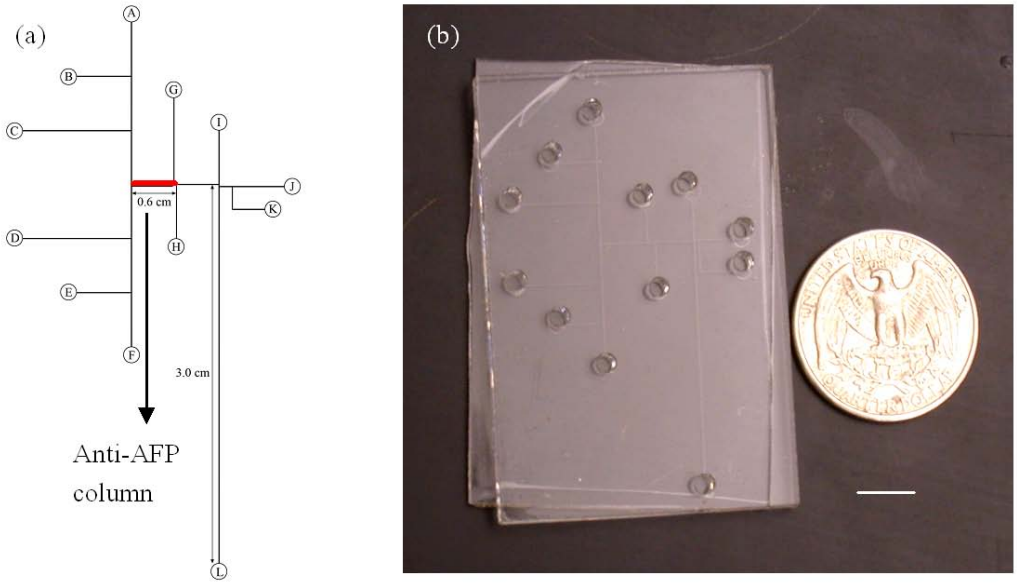

Figure 3.4. Layout of an integrated AFP analysis microchip. (a) Diagram and (b) photograph of a microfluidic device with integrated affinity column. Reservoir labels are A: sample, B: rinse buffer, C: elution solution, D: 5 ng/mL AFP standard solution, E: 10 ng/mL AFP standard solution, F: 20 ng/mL AFP standard solution, G: 5 mM NaOH (to neutralize the acidic elution solution during injection), H: waste, and I-L: electrophoresis buffer. Scale bar in (b) is 1 cm.

3.2.2 Affinity column formation

A prepolymer mixture containing GMA as the functional monomer, PEGDA (575 Da average molecular weight) as the crosslinker, and DMPA as the photoinitiator was prepared. Before polymerization, the mixture was sonicated in a water bath for 1 min,

followed by nitrogen purging for 3 min to remove dissolved oxygen. The degassed mixture (10 µL) was pipetted into reservoir G (**Figure 3.4a**), filling the microchannel via capillary action. Next, vacuum was applied to reservoir G to remove most of the monomer solution, leaving a coating of the prepolymer mixture on the channel walls (**Figure 3.5a-b**). The microchip was covered with an aluminum photomask with a 4×4 mm^2 opening to provide spatial control of polymerization. The microchip was then placed on a copper plate in an icebath, and exposed to UV light (200 mW/cm^2) in the wavelength range of 320–390 nm for 5 min (cooling helped minimize undesired thermal polymerization). Finally, any unpolymerized material was removed by flushing 2-propanol through the microchannels using a syringe pump. To provide analyte specificity, reactive polymer coated microchannels were derivatized with monoclonal anti-AFP according to the previously described procedure in Section 3.1.[22]

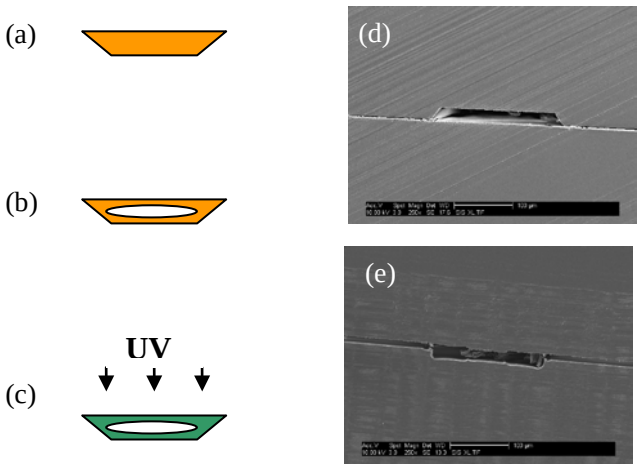

Figure 3.5. Schematic of preparing a reactive polymer coating inside a PMMA microchannel. (a) The microchannel is filled with monomer solution. (b) Bulk monomer is removed by vacuum. (c) UV initiated polymerization creates a functional thin-film polymer coating. (d) SEM image of a microchannel before coating. (e) SEM image of a microchannel after polymer coating.

3.2.3 Fluorescently tagged sample preparation

A 3-mL aliquot of fresh human blood was obtained from a healthy volunteer in a 4-mL Vacutainer tube (BD) at the Brigham Young University Student Health Center. The blood sample was centrifuged at 5,000 rpm (Eppendorf 5415C) for 10 min to

separate the serum from whole blood. FITC and Alexa Fluor 488 TFP Ester (Invitrogen) were used to label amino acids, proteins, and serum samples using protocols provided by Invitrogen (MP 00143). Briefly, 0.1 mg fluorescent dye was dissolved in 10 μL DMSO. For amino acid or protein standards, a 5-μL aliquot of this DMSO solution was immediately mixed with 0.2 mL of sample (1 mg/mL) in 10 mM carbonate buffer (pH 9.0). For serum samples, a 2-μL aliquot of DMSO solution with dissolved dye was mixed directly with 98 μL of human serum. The mixture was incubated in the dark at room temperature for 24 h (FITC) or 15 min (Alexa Fluor 488). In direct labeling of complex biological specimens, it is essential to have excess dye to ensure complete labeling.

3.2.4 Data analysis

The calculation of AFP concentration was based on the peak heights in the electropherograms both for calibration curve and standard addition methods. For the calibration curve, the AFP peak height from each standard electropherogram was plotted against the AFP standard concentration to generate a linear calibration curve by the method of least squares. The AFP concentration in the sample was obtained from the electropherogram peak height and the calibration curve. The standard addition method, which effectively eliminates matrix effects,[1] was also used to analyze the AFP samples. Indeed, my protocol of loading sample plus standard on the affinity column is microfluidically equivalent to spiking standards into a sample in a classical standard addition analysis. Peak heights from the electropherograms of the unknown sample, as well as those of the sample plus added standard, were plotted vs. concentration of added standard. The slope and intercept of this line were calculated by least squares analysis, and the unknown AFP concentration was given by the

intercept divided by the slope.[1] Standard deviations were calculated from the regression data.

3.3 RESULTS AND DISCUSSION

I used an acidic phosphate solution (pH ~2) to interrupt the antigen-antibody interaction and elute target components, which significantly decreased the fluorescence signal. To characterize this, I put fluorescein (10 μM) in Tris buffer (pH

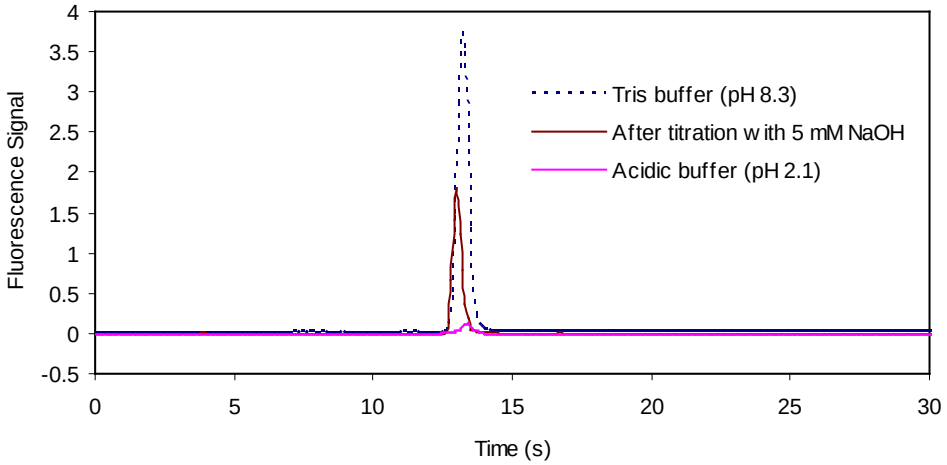

Figure 3.6. Electropherograms of fluorescein in different buffers.

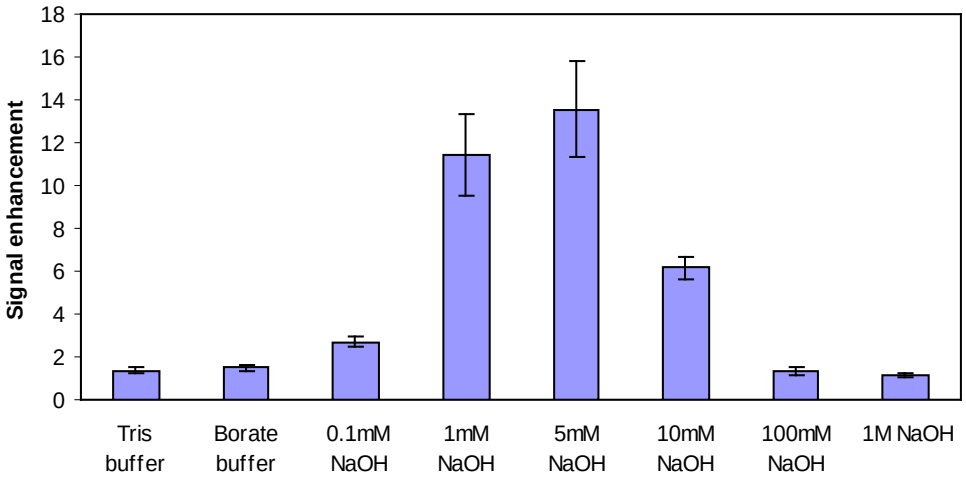

Figure 3.7. Signal enhancement for different titrants of phosphate buffer (pH 2.1).

8.3) and in phosphate buffer (pH 2.1) in reservoirs A and C, respectively (**Figure 3.4a**). In these experiments, affinity columns were not constructed inside the microchannel. During injection (by applying voltage at reservoir J in **Figure 3.4a**), the fluorescence signal was about 10 fold lower for fluorescein in the pH 2.1 solution, as shown in **Figure 3.6**. To overcome this issue, I introduced additional reservoir G (**Figure 3.4a**) into my microdevices to allow online titration. A 400 V potential was applied at reservoir J while reservoirs C and G were grounded causing the basic titrant in reservoir G to neutralize the acidic solution in reservoir C during injection. I used a CCD camera to monitor the fluorescence signal before and after titration with different solutions in reservoir G (**Figure 3.7**). My results indicated that 5 mM NaOH was the best titrant to enhance the signal from FITC-tagged analytes eluted in low-pH buffer.

I used a photo-defined immunoaffinity column in a polymeric microdevice to extract AFP from blood serum. Retained AFP was eluted through an injection cross and rapidly analyzed by microchip electrophoresis. To quantify the serum AFP concentration precisely, both standard addition and calibration curve functions were integrated into the chip. Importantly, all fluid control on-chip was carried out via voltages applied to reservoirs, facilitating automation. The fabrication protocol for poly(methyl methacrylate) (PMMA) microdevices was adapted from Section 2.2.2.[22, 25] The layout of my integrated AFP analysis microchip is shown in **Figure 3.4a**, and a device photograph can be seen in **Figure 3.4b**. PMMA itself is relatively inert toward direct chemical reaction, which necessitates making a photo-defined polymer on the microchannel surface to immobilize antibodies. The thickness of the reactive polymer formed on the channel surface was ~3 μm based on SEM images (**Figure 3.5d-e**).

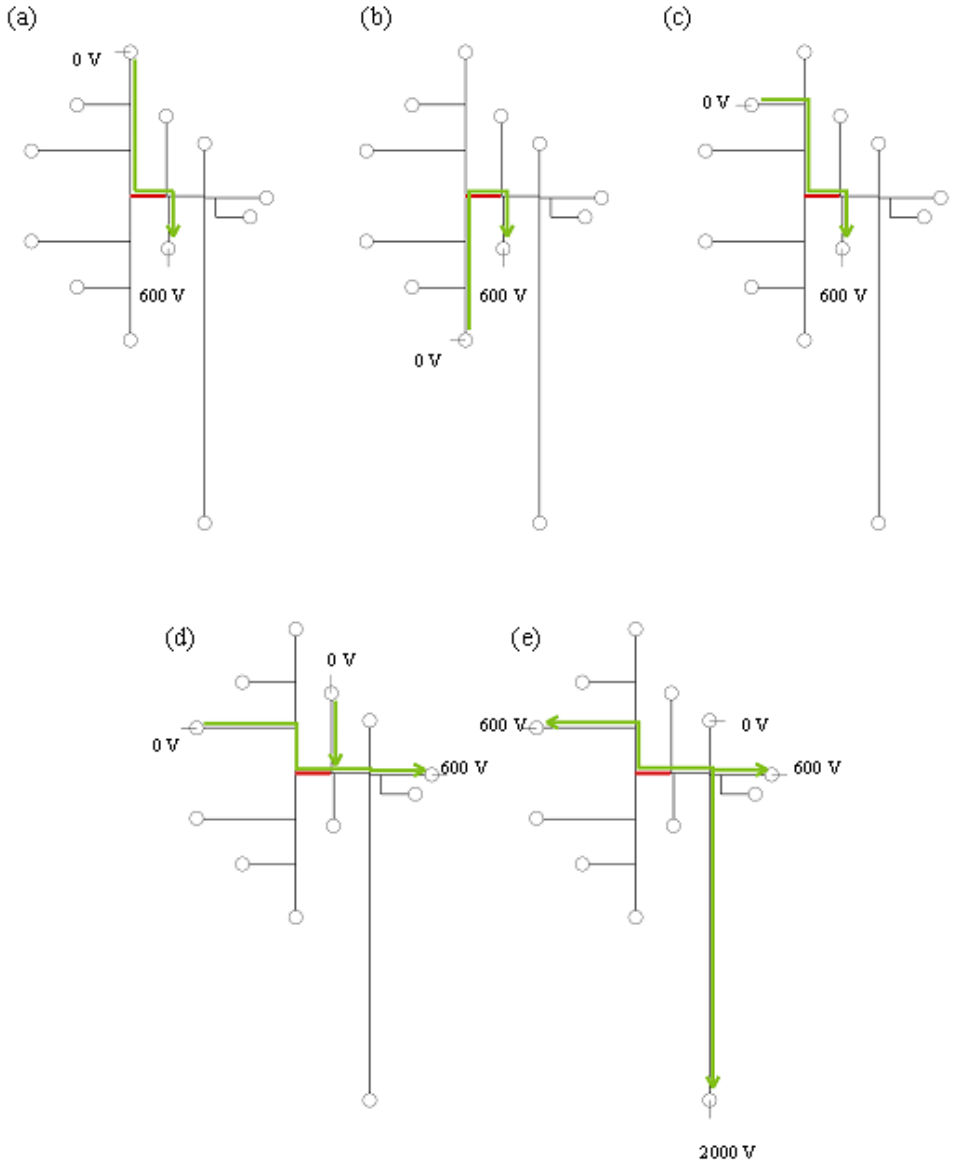

Figure 3.8. Schematic diagram of operation of the microchip with integrated affinity column. (a) Sample loading, (b) standard loading, (c) rinsing, (d) injection, and (e) separation.

To quantify the AFP concentration in serum samples, both calibration curve and standard addition methods were used to validate the accuracy and precision of microchip performance. The voltage configurations and flow paths during operation of the microchip (described below) are shown in **Figure 3.8**. For the calibration curve, each AFP standard solution was loaded on the affinity column for 5 min by applying

voltage between either reservoir D, E, or F and reservoir H; the column was rinsed with PBS buffer for 5 min by applying a potential between reservoirs B and H; analyte was eluted/injected with a voltage applied to reservoir J while grounding reservoirs C and G for 45 s using phosphoric acid/dihydrogen phosphate solution at pH 2.1; and then loaded material was separated by microchip electrophoresis using a potential between reservoirs I and L. The sample was analyzed by loading on the affinity column for 5 min with voltage applied between reservoirs A and H, and then rinsing, elution/injection and separation were done the same as with the standards. For the standard addition method, after loading sample on the affinity column for 5 min as above, one standard was loaded on the affinity column for 5 min as before, followed by rinsing, elution/injection and microchip electrophoresis separation, the same as for the calibration curve. This process was then repeated for each standard. LIF was used to detect the labeled AFP during microchip electrophoresis.[26] I note that miniaturized (shoebox size) LIF systems for microchip electrophoresis have been made,[27] indicating their suitability for POC assays.

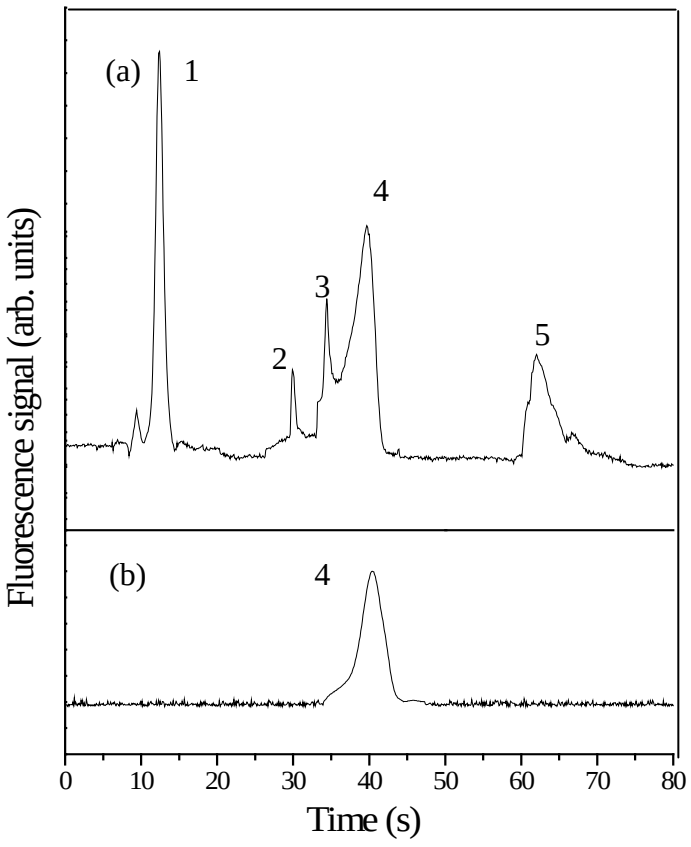

Figure 3.9. Microchip CE of a mixture (a) before and (b) after affinity column extraction. Peaks 1-5 are FITC-Gly, GFP, FITC-BSA, FITC-AFP, and FITC-IgG, respectively.

To demonstrate the integration of immunoaffinity extraction with microchip electrophoresis on a microdevice, a mixture of non-target fluorescent compounds along with FITC-AFP was loaded through an affinity column and then analyzed. Five peaks were observed before extraction, as shown in **Figure 3.9a**; I note that FITC-BSA and FITC-AFP have similar elution times, and are not baseline resolved in the electropherogram. Contrastingly, after on-chip affinity purification (**Figure 3.9b**), all non-target peaks are essentially eliminated, while only the AFP peak remains.

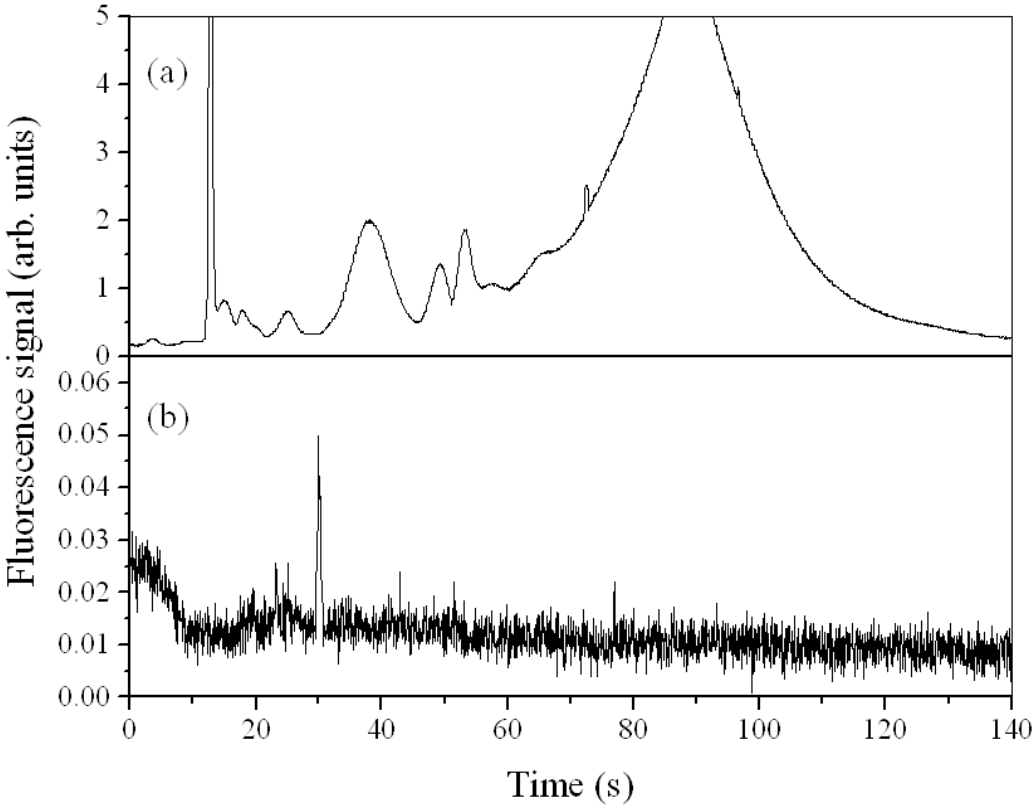

Figure 3.10. FITC-labeled human serum, run by microchip electrophoresis (a) before and (b) after integrated affinity column extraction.

Importantly, similar device performance was observed with a much more complex, fluorescently labeled human serum sample. Microchip electrophoresis of FITC-tagged human serum (**Figure 3.10a**) showed numerous overlapping peaks before extraction,

precluding facile AFP determination. On the other hand, after on-chip AFP extraction, a single, clear peak corresponding to AFP was observed in microchip electrophoresis (**Figure 3.10b**). The integrated immunoaffinity extraction step resulted in a ~5,000-fold reduction of non-target protein signal, and enabled detection of the AFP "needle" in the serum "haystack". I estimate that the AFP sample is >95% pure after immunoaffinity extraction, based on target to spurious peak ratios in the electropherograms in **Figure 3.10**. These results clearly indicate that my approach can selectively purify target analytes from very complex mixtures. A typical affinity column can perform well for at least a few tens of replicate runs.

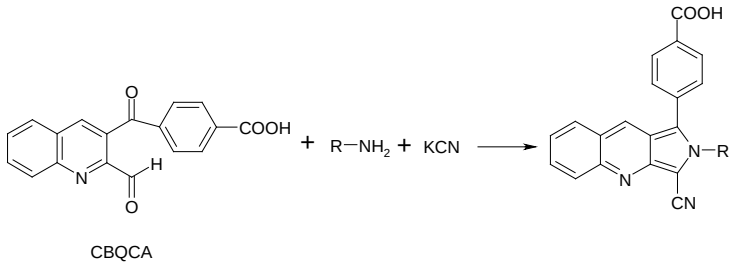

Figure 3.11. CBQCA labeling reaction.

FITC is a commonly used fluorescent dye for labeling amine-containing compounds such as proteins; however, the room-temperature reaction kinetics (~24 h), make this label less desirable for POC work. I tried two different fluorescent dyes to shorten the labeling process: 3-(4-carboxybenzoyl)quinoline-2-carboxaldehyde (CBQCA) and Alexa Fluor 488 TFP Ester (both from Invitrogen, Eugene, OR). Unconjugated CBQCA (**Figure 3.11**) doesn't fluoresce, and it can label proteins in several seconds, making this dye very well suited for POC work. However, CBQCA-labeled AFP generated relatively low fluorescence signal and a broad peak (**Figure 3.12**). In addition, potassium cyanide, a highly toxic substance, is used in the labeling process. The need for extreme care in handling is not ideal for clinical use.

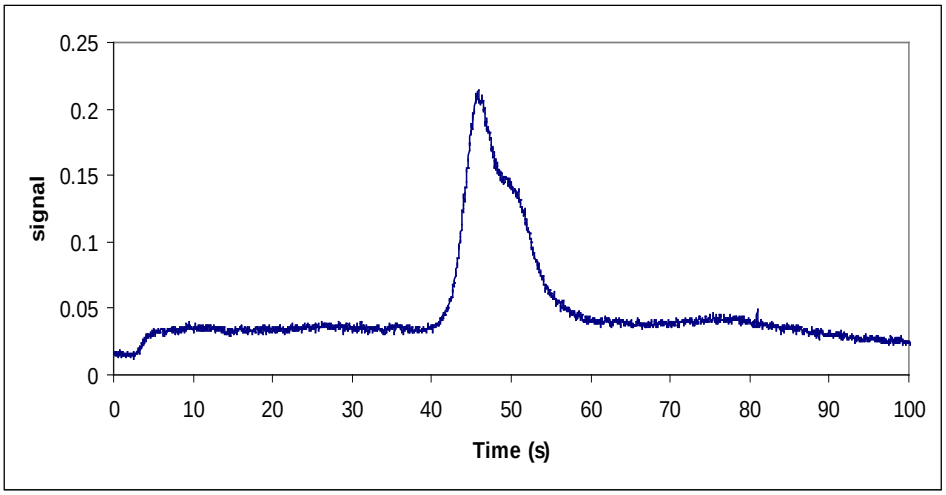

Figure 3.12. 1 μg/mL CBQCA-AFP run by microchip electrophoresis.

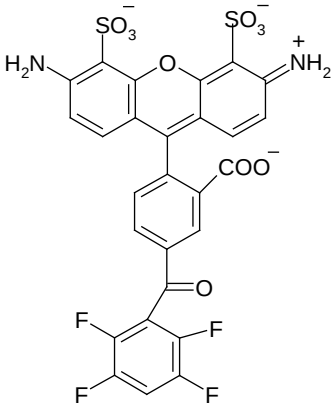

Figure 3.13. Structure of Alexa Fluor 488 TFP Ester.

On the other hand, I found that Alexa Fluor 488 TFP Ester (**Figure 3.13**) completely labeled AFP in ~30 min (**Figure 3.14** and **Table 3.1**), making this dye very attractive for a POC assay. The labeling process can be further sped up at 37 °C (**Figure 3.15**).

For some microchip bioassays, sample and standards share the same reservoir,[10, 28] requiring a cleaning step during analysis, which hampers the ability to automate for POC assays. In my design, sample and standard reservoirs are integrated on the microdevices. Finally, although previous systems have only used calibration curves to quantify biomarkers,[10, 11] my format enables both standard addition and calibration curve protocols to be performed on-chip.

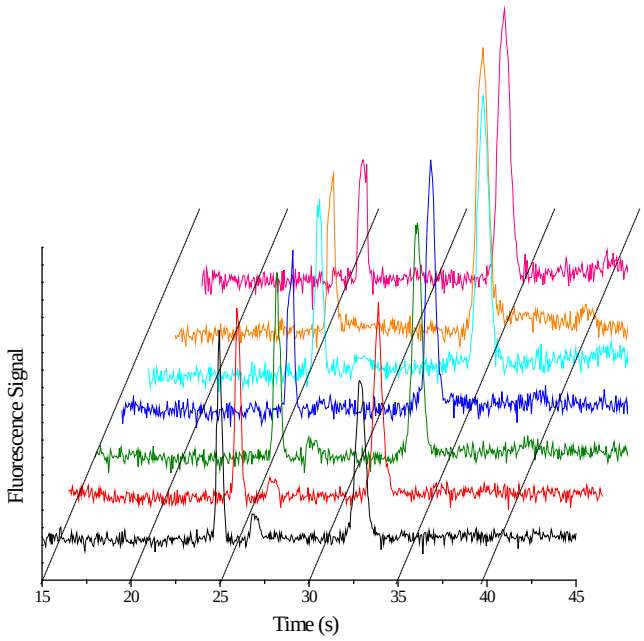

Figure 3.14. Dynamic labeling of AFP with Alexa Fluor 488 TFP Ester at room temperature. Traces are black: labeling 5 min, red: 10 min, green: 15 min, blue: 20 min, light blue: 30 min, orange: 60 min, and pink: 120 min. The unattached label migrates at ~23 s, and the AFP peak is at ~32 s.

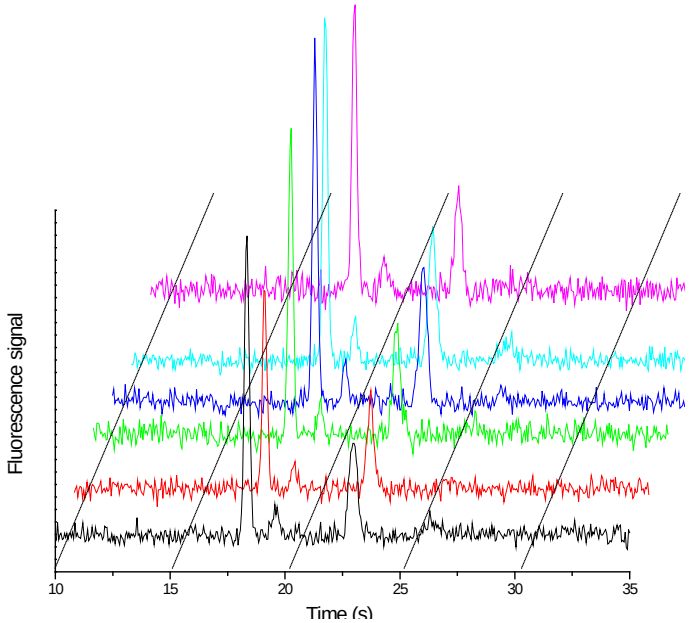

Figure 3.15. Dynamic labeling of AFP with Alexa Fluor 488 TFP Ester at 37 ^{o}C. Traces are black: 5 min red: 10 min, green: 15 min, blue: 20 min, light blue: 30 min, and pink: 60 min. The unattached label migrates at ~18 s, and the AFP peak is at ~23 s.

Table 3.1. Peak heights of AFP in dynamic labeling with Alexa Fluor 488 TFP Ester (*derived from **Figures 3.14** and **3.15***).

Labeling time (min)	AFP Peak Height (arb. units, 25 °C)	AFP Peak Height (arb. units, 37 °C)
5	0.0060	0.0041
10	0.0116	0.0085
15	0.0174	0.0185
20	0.0209	0.0238
30	0.0244	0.0235
60	0.0258	0.0209
120	0.0258	

I used my integrated microdevices to quantify AFP concentration in human serum using either a linear calibration curve (**Figure 3.16a, c**) or the standard addition method (**Figure 3.16b, d**). Both approaches yielded reproducible microchip electrophoresis data (**Figure 3.16a, b**) with concentration-dependent peak heights (**Figure 3.16c, d**). AFP concentrations and standard deviations determined both by calibration curve (4.1±0.9 ng/mL) and standard addition methods (4.6±0.9 ng/mL) were internally consistent. Calculation details can be found in Section 3.2.4. To further evaluate my approach, different amounts of AFP were spiked into human serum, and these samples were then labeled with Alexa Fluor 488 TFP Ester. In either calibration curve or standard addition protocols, the standard concentration should be close to the sample concentration for optimal accuracy and precision. However, in POC screening the AFP concentration is initially unknown.

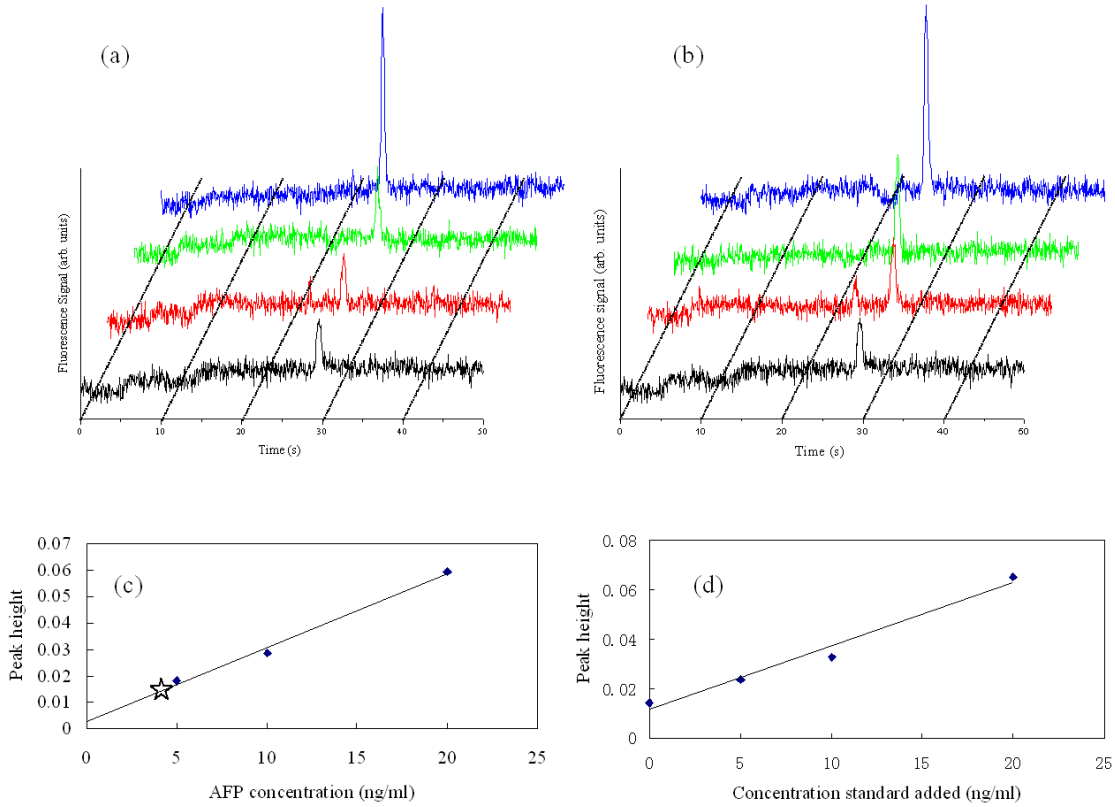

Figure 3.16. Integrated calibration curve and standard addition quantification of AFP in human serum. (a) Microchip CE of Alexa Fluor 488 labeled human serum and of AFP standard solutions after affinity column extraction. Curves are: black-unknown human serum sample, red-5 ng/mL standard AFP, green-10 ng/mL standard AFP, and blue-20 ng/mL standard AFP. (b) Microchip CE of Alexa Fluor 488 labeled human serum after standard addition and affinity column extraction. Traces are: black-sample, red-sample+5 ng/mL standard AFP, green-sample+10 ng/mL standard AFP, and blue-sample+20 ng/mL standard AFP. (c) Calibration curve generated from (a), with unknown sample data point indicated with a star. (d) Standard addition plot of concentration of standard added vs. peak height generated from (b).

Because the action threshold for serum AFP is 20 ng/mL,[15, 29] I set the standard concentrations to 5, 10 and 20 ng/mL in my protocol for optimal precision in the diagnostic range. The AFP concentrations measured in my microdevices using both calibration curve and standard addition methods were compared with values measured by a commercial ELISA kit (**Figure 3.17**). In general, both calibration curve and standard addition results matched ELISA results well (**Figure 3.17 and Table 3.2**). Because the AFP standard concentrations were optimized for the 20 ng/mL diagnostic

threshold, higher AFP concentrations (>50 ng/mL) had lower accuracy and precision; however, a POC assay that reports a concentration well above the action level would require more thorough subsequent clinical analysis.

Table 3.2. Results from the integrated microfluidic AFP assay.*

	Spiked AFP (ng/mL)	ELISA (ng/mL)	Calibration curve (ng/mL)	Standard addition (ng/mL)
unknown 1	250	110.4±2.7	126±6.8	198±41
unknown 2	100	55±2.1	52±1.1	64±8.8
unknown 3†	0	2.8±2.0	4.1±0.9	4.6±0.9
unknown 4	750	323.6±6.7	313±41	1050±520
unknown 5	50	49.3±2.0	29.4±0.1	33.2±2.7
unknown 6	300	205.1±4.3	165±25	169±82

**The number that follows the ± sign is the standard deviation.*

†*The blank concentration is ~4 ng/mL.*

Although my microdevices have been designed for AFP analysis, this approach is not limited to just AFP. These microchips could be easily adapted for detection of other biomarkers by simply immobilizing different antibodies in the affinity column. Moreover, it should be possible to attach multiple antibodies targeting different analytes to the same column, allowing multiplexed, simultaneous biomarker detection, which I next show in Chapter 4. My system shows great promise for rapid quantitation of biomarkers in a POC setting, which should be of considerable value in early stage disease diagnosis.

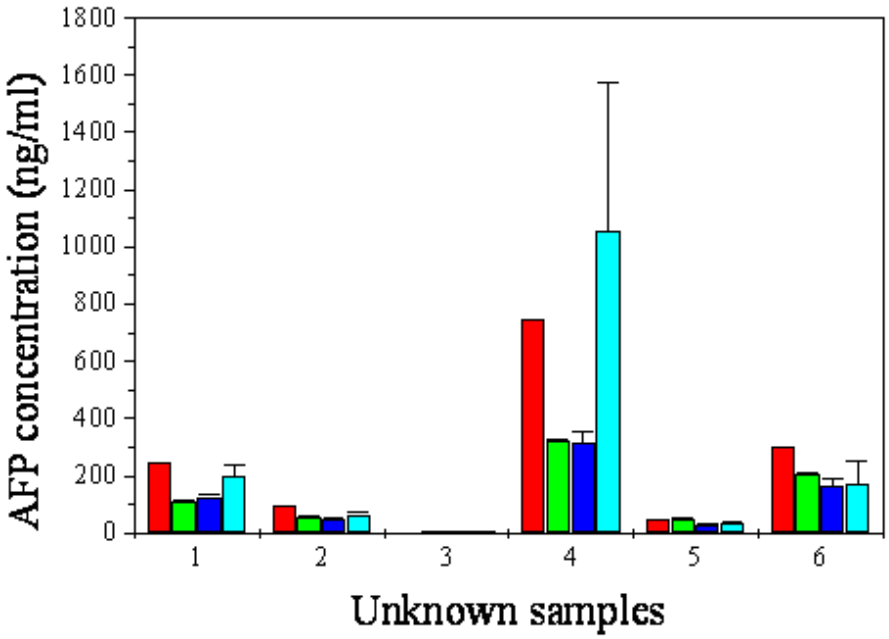

Figure 3.17. Accuracy and precision data for integrated microfluidic AFP assay. Red: spiked concentration, green: measured by ELISA, blue: measured by calibration curve, and light blue: measured by standard addition. Error bars indicate ± one standard deviation.

3.4 REFERENCES

1. Skoog, D. A.; Holler, F. J.; Nieman, T. A., *Principles of Instrumental Analysis* Brooks Cole: Philadelphia, 2006.
2. DeMello, A. J., Control and detection of chemical reactions in microfluidic systems. *Nature* **2006,** 442, (7101), 394-402.
3. Wheeler, A. R., Chemistry. Putting electrowetting to work. *Science* **2008,** 322, (5901), 539-40.
4. Toriello, N. M.; Liu, C. N.; Blazej, R. G.; Thaitrong, N.; Mathies, R. A., Integrated affinity capture, purification, and capillary electrophoresis microdevice for quantitative double-stranded DNA analysis. *Anal Chem* **2007,** 79, (22), 8549-56.
5. Murphy, B. M.; He, X.; Dandy, D.; Henry, C. S., Competitive immunoassays for simultaneous detection of metabolites and proteins using micromosaic patterning. *Anal Chem* **2008,** 80, (2), 444-50.
6. Jacobson, S. C.; Culbertson, C. T.; Daler, J. E.; Ramsey, J. M., Microchip structures for submillisecond electrophoresis. *Anal Chem* **1998,** 70, (16), 3476-3480.
7. McClain, M. A.; Culbertson, C. T.; Jacobson, S. C.; Allbritton, N. L.; Sims, C. E.; Ramsey, J. M., Microfluidic devices for the high-throughput chemical analysis of cells. *Anal Chem* **2003,** 75, (21), 5646-55.
8. Blazej, R. G.; Kumaresan, P.; Mathies, R. A., Microfabricated bioprocessor for integrated nanoliter-scale Sanger DNA sequencing. *Proc Natl Acad Sci U S A* **2006,** 103, (19), 7240-5.
9. Kumaresan, P.; Yang, C. J.; Cronier, S. A.; Blazej, R. G.; Mathies, R. A., High-throughput single copy DNA amplification and cell analysis in engineered nanoliter droplets. *Anal Chem* **2008,** 80, (10), 3522-9.
10. Herr, A. E.; Hatch, A. V.; Throckmorton, D. J.; Tran, H. M.; Brennan, J. S.; Giannobile, W. V.; Singh, A. K., Microfluidic immunoassays as rapid saliva-based clinical diagnostics. *Proc Natl Acad Sci U S A* **2007,** 104, (13), 5268-73.
11. Fan, R.; Vermesh, O.; Srivastava, A.; Yen, B. K.; Qin, L.; Ahmad, H.; Kwong, G. A.; Liu, C. C.; Gould, J.; Hood, L.; Heath, J. R., Integrated barcode chips for rapid, multiplexed analysis of proteins in microliter quantities of blood. *Nat Biotechnol* **2008,** 26, (12), 1373-8.
12. Stephan, K.; Pittet, P.; Sigaud, M.; Renaud, L.; Vittori, O.; Morin, P.; Ouaini, N.; Ferrigno, R., Amperometric quantification based on serial dilution microfluidic systems. *Analyst* **2009,** 134, (3), 472-7.
13. Wright, L. M.; Kreikemeier, J. T.; Fimmel, C. J., A concise review of serum markers for hepatocellular cancer. *Cancer Detect Prev* **2007,** 31, (1), 35-44.
14. Zinkin, N. T.; Grall, F.; Bhaskar, K.; Otu, H. H.; Spentzos, D.; Kalmowitz, B.; Wells, M.; Guerrero, M.; Asara, J. M.; Libermann, T. A.; Afdhal, N. H., Serum proteomics and biomarkers in hepatocellular carcinoma and chronic liver disease. *Clin Cancer Res* **2008,** 14, (2), 470-7.
15. Debruyne, E. N.; Delanghe, J. R., Diagnosing and monitoring hepatocellular carcinoma with alpha-fetoprotein: new aspects and applications. *Clin Chim Acta* **2008,** 395, (1-2), 19-26.
16. Wen, J.; Guillo, C.; Ferrance, J. P.; Landers, J. P., Microfluidic-based DNA purification in a two-stage, dual-phase microchip containing a reversed-phase and a photopolymerized monolith. *Anal Chem* **2007,** 79, (16), 6135-42.
17. Kawabata, T.; Watanabe, M.; Nakamura, K.; Satomura, S., Liquid-phase binding assay of alpha-fetoprotein using DNA-coupled antibody and capillary chip electrophoresis. *Anal Chem* **2005,** 77, (17), 5579-82.

18. Bharadwaj, R.; Park, C. C.; Kazakova, I.; Xu, H.; Paschkewitz, J. S., Analysis and optimization of nonequilibrium capillary electrophoresis of alpha-fetoprotein isoforms. *Anal Chem* **2008,** 80, (1), 129-34.
19. Kawabata, T.; Wada, H. G.; Watanabe, M.; Satomura, S., Electrokinetic analyte transport assay for alpha-fetoprotein immunoassay integrates mixing, reaction and separation on-chip. *Electrophoresis* **2008,** 29, (7), 1399-406.
20. Wen, J.; Guillo, C.; Ferrance, J. P.; Landers, J. P., Microfluidic chip-based protein capture from human whole blood using octadecyl (C18) silica beads for nucleic acid analysis from large volume samples. *J Chromatogr A* **2007,** 1171, (1-2), 29-36.
21. Peoples, M. C.; Karnes, H. T., Microfluidic capillary system for immunoaffinity separations of C-reactive protein in human serum and cerebrospinal fluid. *Anal Chem* **2008,** 80, (10), 3853-8.
22. Sun, X.; Yang, W.; Pan, T.; Woolley, A. T., Affinity monolith-integrated poly(methyl methacrylate) microchips for on-line protein extraction and capillary electrophoresis. *Anal Chem* **2008,** 80, (13), 5126-30.
23. Dodge, A.; Fluri, K.; Verpoorte, E.; de Rooij, N. F., Electrokinetically driven microfluidic chips with surface-modified chambers for heterogeneous immunoassays. *Anal Chem* **2001,** 73, (14), 3400-9.
24. Sterling, R. K.; Jeffers, L.; Gordon, F.; Sherman, M.; Venook, A. P.; Reddy, K. R.; Satomura, S.; Schwartz, M. E., Clinical utility of AFP-L3% measurement in North American patients with HCV-related cirrhosis. *Am J Gastroenterol* **2007,** 102, (10), 2196-205.
25. Yang, W.; Sun, X.; Pan, T.; Woolley, A. T., Affinity monolith preconcentrators for polymer microchip capillary electrophoresis. *Electrophoresis* **2008,** 29, (16), 3429-35.
26. Kelly, R. T.; Woolley, A. T., Thermal bonding of polymeric capillary electrophoresis microdevices in water. *Anal Chem* **2003,** 75, (8), 1941-5.
27. Lagally, E. T.; Scherer, J. R.; Blazej, R. G.; Toriello, N. M.; Diep, B. A.; Ramchandani, M.; Sensabaugh, G. F.; Riley, L. W.; Mathies, R. A., Integrated portable genetic analysis microsystem for pathogen/infectious disease detection. *Anal Chem* **2004,** 76, (11), 3162-70.
28. Tsukagoshi, K.; Jinno, N.; Nakajima, R., Development of a micro total analysis system incorporating chemiluminescence detection and application to detection of cancer markers. *Anal Chem* **2005,** 77, (6), 1684-8.
29. Trevisani, F.; D'Intino, P. E.; Morselli-Labate, A. M.; Mazzella, G.; Accogli, E.; Caraceni, P.; Domenicali, M.; De Notariis, S.; Roda, E.; Bernardi, M., Serum alpha-fetoprotein for diagnosis of hepatocellular carcinoma in patients with chronic liver disease: influence of HBsAg and anti-HCV status. *J Hepatol* **2001,** 34, (4), 570-5.

4. MICRODEVICES INTEGRATING AFFINITY COLUMNS AND CAPILLARY ELECTROPHORESIS FOR MULTI-BIOMARKER ANALYSIS IN HUMAN SERUM *

4.1 INTRODUCTION

Due to early stage diagnosis and advances in cancer treatment, the five-year relative survival rate (of patients compared with controls) for all cancers has improved from 50% in 1975-1977 to 66% in 1996-2004.[1] Presently, cancer diagnosis is based mainly on morphological examination of a tumor biopsy, which is expensive, time consuming, and, hence, low in throughput.[2] As an earlier stage tool, biomarkers can play an important role in cancer screening, diagnosis, and recurrence detection.[3, 4] For instance, prostate-specific antigen (PSA) is a widely used analyte for prostate cancer screening.[5] However, an abnormal level of a single biomarker alone is not generally sufficient to diagnose cancer.[6] Thus, many men with PSA levels less than the 4.0 ng/mL action threshold had prostate cancer detected by biopsy (i.e., false-negatives).[7] Furthermore, PSA levels above 4 ng/mL are associated with other conditions such as prostatitis, reducing the specificity (i.e., false-positives).[5] To overcome these shortcomings, simultaneous detection of multiple markers[8] would enable more sensitive and accurate cancer screening with higher throughput. For instance, Yang et al.[9] evaluated 12 biomarkers for gastrointestinal cancer diagnosis, and a combination of five markers significantly improved the diagnostic rate to ~40% relative to the

* This chapter is reproduced with permission from *Lab on a Chip*, 2010, DOI:10.1039/C005288D. Copyright 2010 Royal Society of Chemistry.

~27% rate achieved with just carcinoembryonic antigen (CEA).

Currently, most biomarkers are detected via immunoassays such as enzyme linked immunosorbent assay (ELISA).[10] Recently, Ladd et al.[11] developed a label-free detection protocol for cancer biomarker candidates using surface plasmon resonance imaging, with a limit of detection as low as a few ng/mL. Unfortunately, significant nonspecific adsorption was observed in diluted serum analysis, which led to a high background and much poorer detection limit. A recent review summarizes the advances and challenges of multiplexed immunoassay platforms.[12] However, these multimarker systems need further validation and quality control. Transferring these approaches to a microfluidic format could provide higher speed and lower reagent consumption.[13] Yet, analyzing real samples in complex matrices using microdevices is challenging because the small microchip platform reduces resolving power and peak capacity relative to full-size instruments.[14] Furthermore, due to small injected sample volumes and a short optical path, the concentration detection limit in microchips is often higher than in conventional techniques.[15] To overcome these shortcomings of microfluidic systems, multiple analysis functions can be integrated on a single device, enabling sample purification and preconcentration.[16] Many processing steps including sample desalting,[17] labeling,[18] and extraction[19] have been successfully performed in microchip systems. Because extraction can purify target components from complex matrices, it is an especially attractive technique for the pretreatment of real samples.

Solid phase extraction (SPE) is used heavily in sample purification. The principle of SPE is as follows: the targeted component (or components) is retained on a solid

medium to separate it from the matrix, and retained materials can then be eluted for analysis. SPE has been applied successfully in a microfluidic format;[20, 21] however, nonspecific interactions like hydrophobic absorption alone do not provide high selectivity. To circumvent this shortcoming, enzymes or antibodies can be immobilized on the solid surface.[21, 22] For instance, pisum sativum agglutinin has been immobilized on monolithic substrates to retain glycoproteins, which can be eluted in several fractions based on their affinities.[23] A recent review summarizes the application of immunoaffinity capillary electrophoresis (CE) for biomarker, drug and metabolite analysis in biological samples.[24] These studies indicate a promising future for immunoaffinity extraction as a pretreatment method for biological specimens in microdevices. In Chapter 3, I demonstrated an integrated microfluidic system that coupled immunoaffinity extraction with rapid microchip CE separation for quantitation of alpha-fetoprotein (AFP) in human blood serum, using either standard addition or a calibration curve for determining concentrations.[19] Although this method was effective at quantifying AFP, the affinity column properties were not fully characterized, and only one biomarker was detected.

Here I demonstrate an integrated microfluidic system that can simultaneously quantify multiple cancer biomarkers in human blood serum. I selected four commercially available biomarkers as test proteins (**Table 4.1**).[25-28] These four biomarkers were chosen more for their separation characteristics than their combined clinical relevance. Antibodies were attached to microchip columns, and the amounts of immobilized antibodies were characterized. I used my integrated microdevices to quantify these four proteins at low ng/mL levels, which are in the range of their action thresholds in human blood serum. These results demonstrate that my platform is

generalizable and applicable for the simultaneous quantification of multiple biomarkers in complex samples.

Table 4.1. Properties of the cancer biomarkers detected in this study.

Biomarker	Clinical use	Normal level (ng/mL)	Action threshold (ng/mL)
AFP[25]	liver cancer marker	<10	20
CEA[26]	colorectal cancer marker	<5	20
Cytochrome C (CytC)[27]	prognostic marker during cancer therapy	<0.5	25
Heat shock protein 90 (HSP90)[28]	many oncogenic proteins are HSP90 clients	n/a	Overexpression (no action threshold)

4.2 MATERIALS AND METHODS

4.2.1 Reagents and materials

CytC (from bovine heart), CEA (from human fluids), monoclonal anti-AFP antibody (produced in mouse), monoclonal anti-CEA antibody (produced in mouse), anti-CytC antibody (produced in sheep), glycidyl methacrylate (GMA, 97%), poly(ethylene glycol) diacrylate (PEGDA, 575 Da average molecular weight), and 2,2-dimethoxy-2-phenylacetophenone (DMPA, 99%) were purchased from Sigma-Aldrich (St. Louis, MO). HSP90 and monoclonal anti-HSP90 antibody (produced in mouse) were obtained from Stressgen (Ann Arbor, MI). AFP was from Lee Biosolutions (St. Louis, MO). Human blood serum from a healthy male (Sigma-Aldrich) was spiked with different concentrations of AFP, CytC, CEA, and HSP90 in the range of 20 to 250 ng/mL (all above normal clinical levels). These unknown serum samples were then labeled with Alexa Fluor 488 TFP Ester (Invitrogen, Eugene, OR) following an

Invitrogen protocol (MP 00143). Briefly, 0.1 mg fluorescent dye was dissolved in 10 μL dimethyl sulfoxide (DMSO), and a 2-μL aliquot of DMSO solution was mixed with 98 μL of spiked human serum. The mixture was left to react in the dark at room temperature for 15 min. For protein standards, a 5-μL aliquot of the DMSO solution containing the fluorescent label was mixed with 0.2 mL of 1 mg/mL protein in 10 mM carbonate buffer (pH 9.0). All solutions were prepared with deionized water (18.3 MΩ-cm) purified by a Barnstead EASYpure UV/UF system (Dubuque, IA). Poly(methyl methacrylate) (PMMA, Acrylite FF) was purchased from Cyro Industries (Rockaway, NJ) and was cut into 4.0 × 5.5 cm^2 blanks using a CO_2 laser cutter (VLS2.30, Universal Laser Systems, Scottsdale, AZ) before device fabrication.

4.2.2 Layout and fabrication of microfluidic devices

The device layout (**Figure 4.1**) and fabrication protocols were adapted from Chapters 2 and 3.[19, 29] Briefly, the microchips contained a sample reservoir (1), two SPE processing reservoirs (2-3) for wash buffer and elution solution, respectively; three reservoirs (4-6) having different standard concentrations for quantification; a waste reservoir (8) for the immunoaffinity extraction step; a reservoir (7) for basic solution (5 mM NaOH) to neutralize the acidic elution solution; and three reservoirs (9, 10 and 12) for standard microchip CE separation. The additional reservoir 11 was originally designed to facilitate the integration of a semi-permeable membrane near the injection intersection, but this capability was not utilized in the present experiments. The microchip pattern was transferred to silicon template wafers using photolithography and wet etching.[29] PMMA substrates (1.5-mm thick) were imprinted by hot embossing against the etched Si templates.[21] The patterned PMMA was thermally bonded to an unimprinted PMMA substrate (3.0-mm thick, to provide ~10 μL

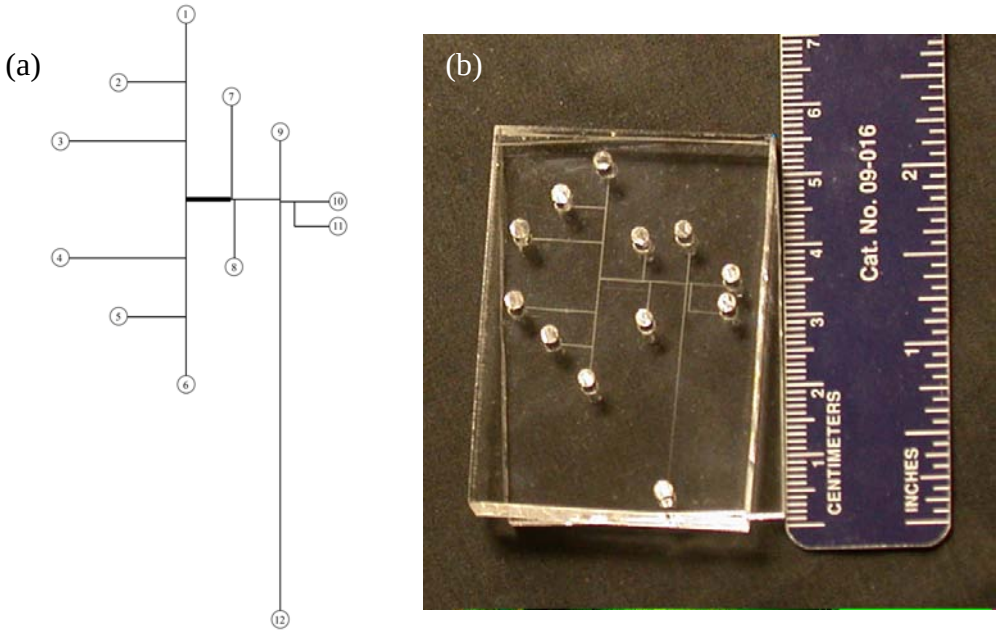

Figure 4.1. Layout of an integrated microdevice. (a) Schematic diagram and (b) photograph of a typical microchip with integrated affinity column. See the text for reservoir descriptions.

reservoir volume capacities) with laser-cut holes (2.0-mm diameter). Channel widths were ~50 µm, except the affinity column which was 100-µm wide, and channel depths were ~20 µm.

Since PMMA is inert to many chemical reactions, the microchannel surface was coated to form affinity columns. Briefly, a prepolymer mixture containing GMA (~60%), PEGDA (~40%), and DMPA (0.5%) was sonicated and then purged with nitrogen for 3 min to remove dissolved oxygen. The degassed mixture was introduced into the affinity microchannel region via reservoir 7, and a ~3 µm coating of the prepolymer mixture remained on the channel walls after applying vacuum to reservoir 7 and flowing nitrogen (~50 psi) from reservoir 1. The microchip was covered with an aluminum photomask, placed on a copper plate in an icebath, and exposed to UV light

(320–390 nm, 200 mW/cm^2) for 5 min. Finally, unpolymerized material was removed via flushing of 2-propanol through the microchip using a syringe pump.

For immobilization on the patterned affinity channel surface, the four antibodies (anti-AFP, anti-CEA, anti-CytC and anti-HSP90) were mixed at 0.5 mg/mL each in 50 mM borate buffer (pH 8.6). The antibody mixture was pipetted into reservoir 8 and the affinity column filled via capillary action. Borate buffer was placed into all other microchip reservoirs to avoid evaporation during reaction. The entire chip was sealed with 3M Scotch tape (St. Paul, MN), and the mixture was left to react at 37 °C for 24 h in the dark.[30] After reaction, the device was flushed using 100 mM Tris buffer (pH 8.3) for 0.5 h. This process also blocked any remaining epoxy groups on the column. Finally, the entire chip was rinsed with carbonate buffer (pH 9.1) before use.

4.2.3 Laser-induced fluorescence (LIF) detection setup

LIF detection was performed on a Nikon Eclipse TE300 inverted optical microscope equipped with a photomultiplier tube (PMT) detector (Hamamatsu, Bridgewater, NJ) and CCD camera (Coolsnap HQ, Roper Scientific, Sarasota, FL). The LIF detection system and data collection setup have been described in Section 2.2.5.[21, 29] CCD images were collected at 10 Hz and analyzed using V++ Precision Digital Imaging software (Auckland, New Zealand). The sampling rate for PMT detection was 20 Hz.

4.2.4 Characterization of affinity columns

To estimate the saturation point of affinity columns, different concentrations of fluorescently labeled AFP were loaded for 5 min by applying 400 V at reservoir 8 and 0 V at reservoir 1. Then, unbound AFP was rinsed off the affinity column with PBS

buffer for 3 min with 400 V applied to reservoir 8 while grounding reservoir 2. The fluorescence signal on the affinity column was monitored via CCD during the loading and rinsing processes (**Figure 4.2**).

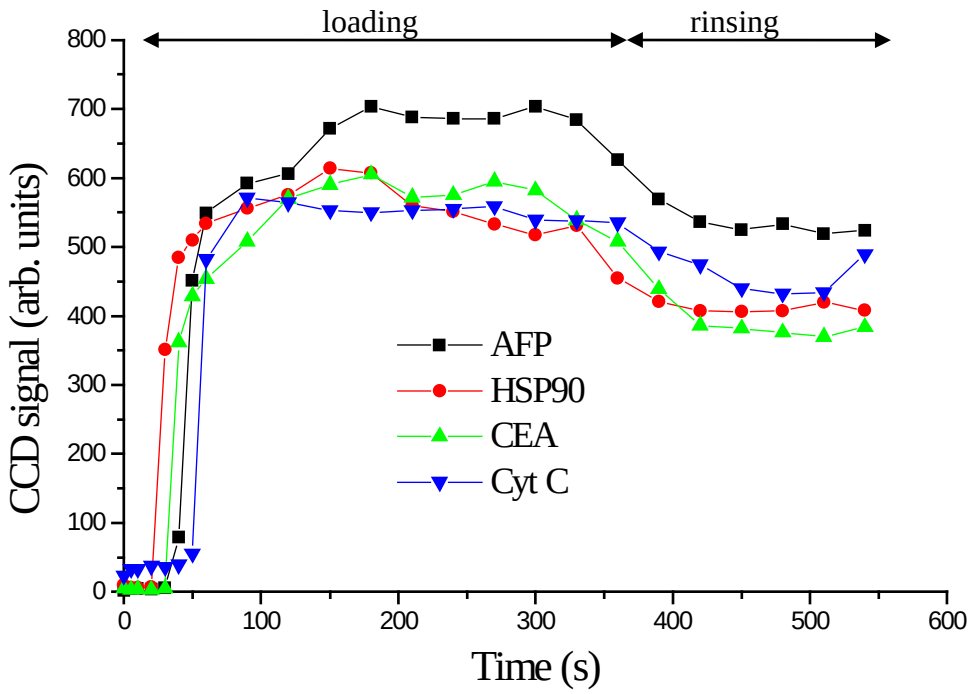

Figure 4.2. Fluorescence signal from the affinity column during loading and rinsing steps. All points are average values from CCD images, and standard deviations (not shown, ~200 units) were calculated from ~32,000 pixels in the CCD images. The relative standard deviation values reflect some heterogeneity in the density of immobilized antibodies on the column, as well as minor imperfections on the PMMA surfaces from device bonding.

For each analyte, standards of different concentrations were loaded into a microchannel, and fluorescence signal versus protein concentration plots were generated. These calibration curves provided the relationship between CCD signal and the concentration of fluorescently labeled protein in the column in **Figure 4.3**. To determine the amount of immobilized antibodies on the affinity column, 1 μg/mL biomarker standards were loaded on the column with 400 V between reservoirs 1 and 8 for 330 s to saturate all active antibody sites, and the column was washed with Tris

buffer using 400 V between reservoirs 2 and 8 for 210 s to remove unbound material. CCD images of the affinity column were recorded at 10 s intervals for the first 60 s, and then 30 s intervals for the remaining time during the loading and washing processes. The CCD signal after washing corresponded to column saturation with antigen; this signal was converted into the equivalent antigen concentration in the column based on the obtained calibration curves. From the column volume of 6 nL (length: 3 mm), I determined the mass of each protein bound on-chip at saturation. Then, assuming the antigen-antibody interaction occured with a 1:1 molar ratio, the quantity of immobilized antibodies on the column was determined.

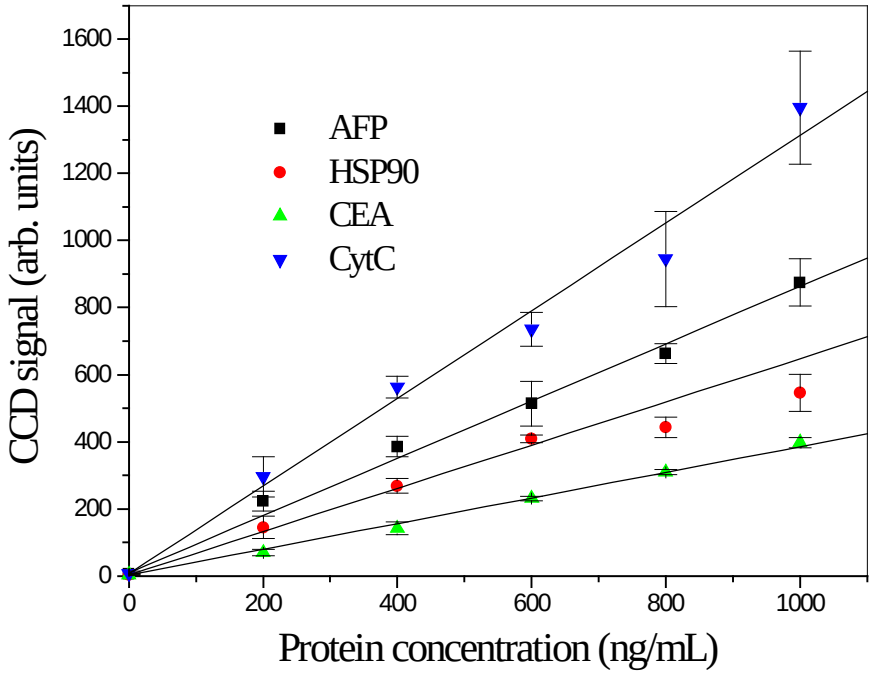

Figure 4.3. Relationship between background subtracted CCD signal and concentration of fluorescently labeled proteins. Error bars indicate standard deviations (n = 3).

4.2.5 Immunoaffinity extraction and electrophoretic separation

The operation of my integrated microchips and the data analysis were adapted from Section 3.2.4.[19] To demonstrate proof-of-principle of multiplexed operation, a mixture

of fluorescently labeled AFP, CytC, CEA and HSP90 in buffer was compared before and after microchip immunoaffinity extraction. A double-T microchip layout[29] was used to directly separate the mixture (without immunoaffinity extraction). The mixture was then pipetted onto an integrated microdevice, loaded for 5 min on the affinity column, rinsed for 5 min, eluted through the injection intersection for 45 s, and then separated by microchip CE.

For calibration curve quantitation, each standard solution containing all four proteins was loaded on the affinity column (5 min), rinsed with PBS buffer (5 min), eluted through the injection intersection for 1 min with phosphate buffer (pH 2.1), and separated by microchip CE, by applying a sequence of potentials to the various reservoirs for all steps as in Section 3.3.[19] The sample was analyzed by loading it on the affinity column, rinsing, eluting/injecting and separating the same as for the standards. The peak heights from each standard electropherogram were plotted against the series of known protein concentrations, and linear regression was used to fit a line to the data. The concentration of each component in the sample was calculated from its peak height in the electropherogram and the linear fit equation.

For standard addition quantification, sample was first analyzed the same way as for the calibration curve. Next, sample was loaded on the affinity column for 5 min, followed by loading of the first standard mixture for 5 min; the rinsing, elution/injection and microchip CE separation steps were then carried out as before. This same set of processes was repeated to spike the other two standards into the sample and analyze them as in Section 3.3.[19] A linear fit was generated from the peak heights in the electropherograms of the unknown sample and of the sample spiked

with standards, plotted against the standard concentrations spiked into the sample. The concentration of each protein was calculated from the intercept and slope of this line.

4.3 RESULTS AND DISCUSSION

4.3.1 Characterization of affinity columns

The fluorescence signal on affinity columns in my microdevices, as a function of AFP concentration is shown in **Figure 4.4**. The relationship between CCD signal and AFP concentration was linear up to ~500 ng/mL, and the signal approached a plateau at 1 µg/mL. Above ~1 µg/mL AFP, the antibody sites were all occupied with fluorescently labeled AFP (column saturation), such that the fluorescence signal did not change with further AFP concentration increases. Thus, after loading ~1 µg/mL of a target protein on the affinity column and washing off unbound material, the maximum amount of retained antigen can be monitored, as shown in **Figure 4.2**. During the rinsing step, the fluorescence signal decreased by ~15% due to the removal of some unbound protein. Importantly, the signal remained stable after this initial decline during rinsing, indicating strong interaction between antigens and antibodies. In addition, the fluorescence signals of all four proteins were in the same range after rinsing, indicating that the derivatization reaction had little bias toward any of the four antibodies I used.

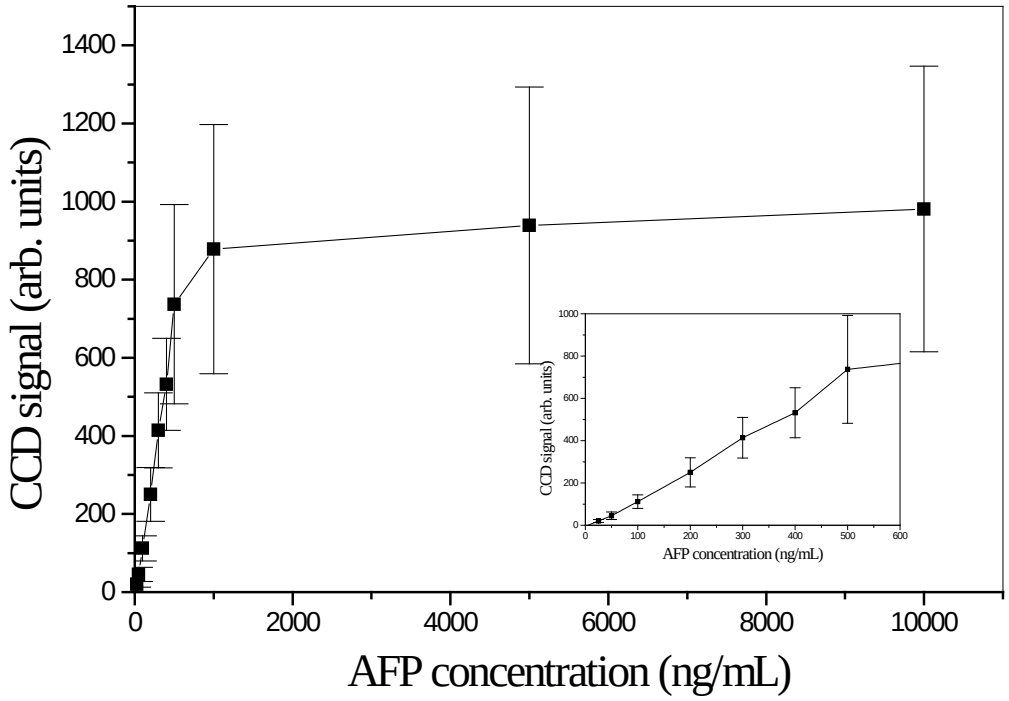

Figure 4.4. Background-subtracted fluorescence signal on a typical affinity column after washing, for multiple AFP concentrations. The lower concentration points are expanded in the inset.

Calibration curves relating fluorescence signal and standard protein concentration (**Figure 4.3)** converted the CCD signal into the effective concentration of fluorescently labeled protein attached to the column at saturation. For all four proteins, the CCD signal had a linear relationship with protein concentration ($R^2 > 0.95$). The difference in mass per volume sensitivity for the various analytes is due to molecular differences in terms of number of available fluorescent labeling sites and molecular weight. Based on the CCD signal during the rinsing step (**Figure 4.2**) and the 6-nL column volume, the amounts of retained proteins on the affinity column were determined (**Figure 4.5**). The retained protein amounts were all in the range of 2 to 7 pg, and were also consistent from chip to chip, indicating that immunoaffinity extraction is not affected adversely by multiplexing antibodies on the column. There was a 10–30% between-device variability in the amount of retained proteins, due to

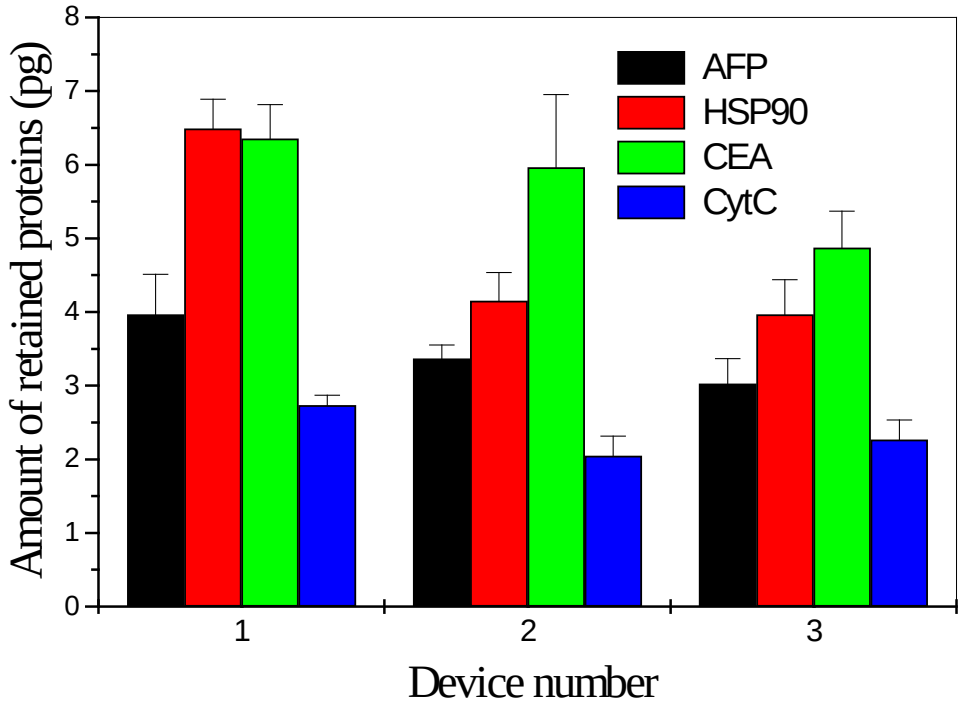

Figure 4.5. Amounts of retained proteins on the affinity columns in three different microdevices. Standard deviations were calculated from the regression data in **Figure 4.3**.

small differences in column surfaces and operation conditions. Importantly, since samples and standards are both analyzed on the same column, any minor between-device differences have no effect on quantitation. Assuming the antigen-antibody interaction occurs with a 1:1 molar ratio, the average amounts of immobilized anti-AFP, anti-CEA, anti-CytC, and anti-HSP90 were 60, 30, 190, and 45 amol, respectively (~0.1 nmol/m^2). My channel wall coated affinity columns have a lower density of immobilized antibodies than high surface area, porous beads (2–35 nmol/m^2).[31] Since submicroliter volumes of sample are loaded on my affinity columns, the present binding capacity is not a serious issue for trace (<μg/mL) biomarker analysis. In addition, the density of binding sites in my devices can be easily increased by using a porous material as the solid support. These results demonstrate that affinity columns with four antibodies can be integrated reproducibly in my microdevices with good functionality.

4.3.2 Separation of a model protein mixture

To demonstrate the feasibility of integrated microchip immunoaffinity extraction and CE for multiple biomarker analysis, a mixture of Alexa Fluor 488-labeled AFP, CytC,

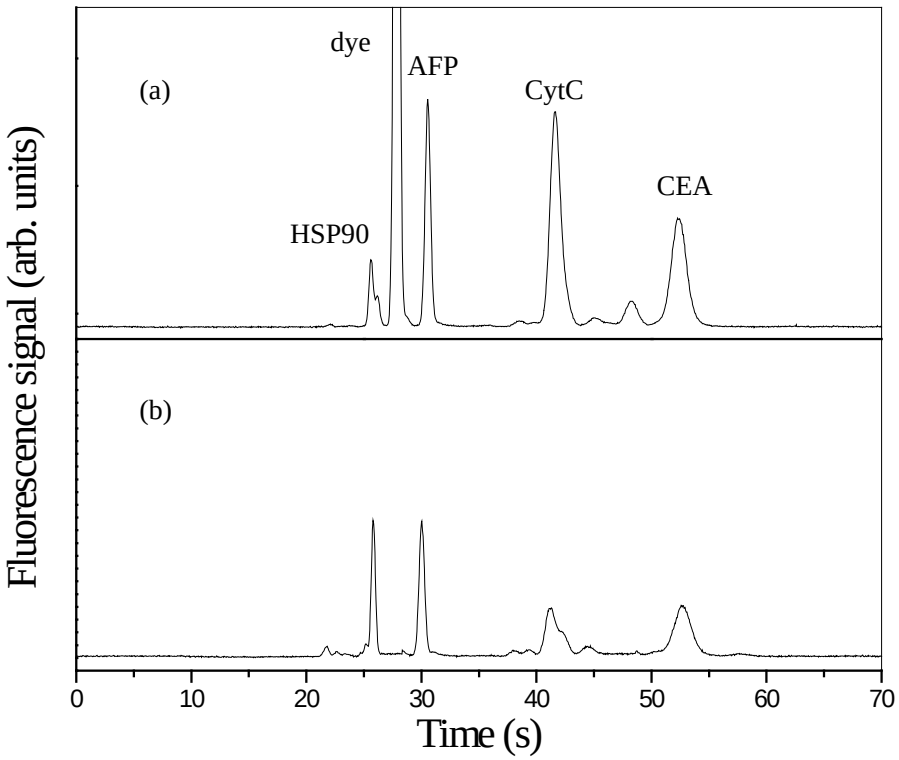

Figure 4.6. Alexa Flour 488-labeled biomarker mixture (1 μg/mL for each protein), run by microchip electrophoresis (a) before and (b) after integrated affinity column extraction.

HSP90 and CEA at 1 μg/mL each in carbonate buffer was analyzed. Five baseline-resolved peaks, including a significant fluorescent dye peak, were observed when this mixture was analyzed by standard microchip CE (without affinity extraction), as shown in **Figure 4.6a**. On the other hand, **Figure 4.6b** shows the electropherogram after this mixture was loaded on an affinity column having the requisite antibodies and then separated by microchip CE after rinsing and elution/injection. With on-chip affinity purification, the dye peak was essentially eliminated (over 10,000-fold

reduction), while the four biomarker peaks remained. In addition, the HSP peak was sharpened after extraction because of the removal of a co-eluting impurity from the sample. These results indicate that my integrated microdevices can selectively retain and analyze targeted compounds in samples.

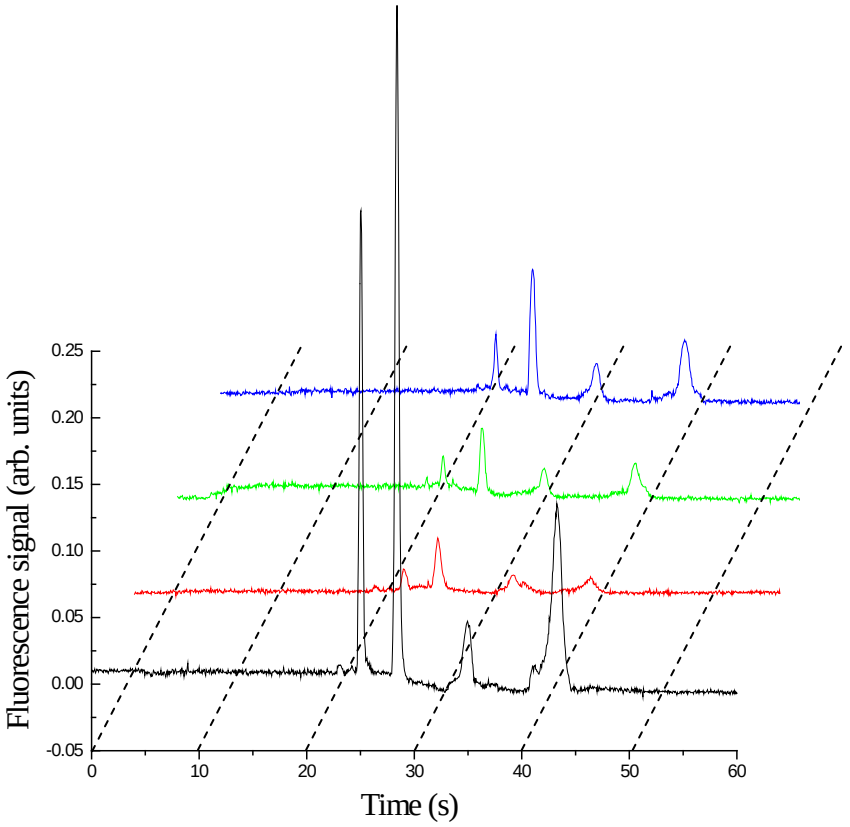

Figure 4.7. Microchip CE of Alexa Fluor 488-labeled human serum and of standard solutions after affinity column extraction. Curves are: black—unknown spiked human serum sample, red—5 ng/mL standard mixture, green—10 ng/mL standard mixture, and blue—20 ng/mL standard mixture.

4.3.3 Multiplexed biomarker quantitation in human serum

To assess the ability of my approach to quantify biomarkers in real samples, I analyzed a series of human blood serum specimens that had been spiked with four proteins and fluorescently tagged with Alexa Fluor 488 TFP Ester. Spiked biomarker concentrations in human serum were determined in the integrated affinity extraction and microchip CE devices using either a linear calibration curve (**Figure 4.7**) or the

standard addition method (**Figure 4.8**). In **Figure 4.7**, the peak heights of standards increased proportionally going from 5 ng/mL to 20 ng/mL, and the peak heights increased with spiked protein concentration in **Figure 4.8**. In all electropherograms after on-chip affinity purification, only four clean baseline-resolved protein peaks

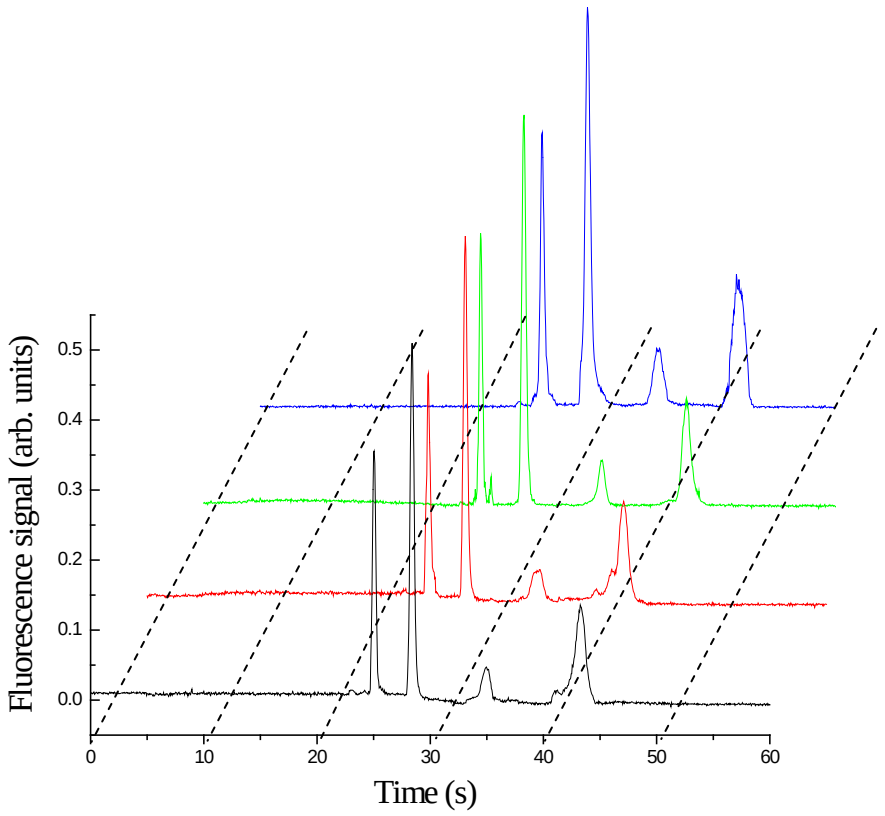

Figure 4.8. Microchip electrophoresis of Alexa Fluor 488-labeled human serum after standard addition and affinity column extraction. Curves are: black—unknown spiked human serum sample, red—serum sample + 5 ng/mL standard mixture, green—serum sample + 10 ng/mL standard mixture, and blue—serum sample + 20 ng/mL standard mixture.

were observed, indicating the efficacy of the multiplexed immunoaffinity extraction column. I tested four spiked human blood serum samples, and the calibration curve and standard addition results overall matched the known spiked concentrations well (**Table 4.2**). In general, the standard deviations for the calibration curve were smaller than those for standard addition; quantitation by standard addition involves extrapolation, which may partially explain the higher standard deviations. Because I

Table 4.2. Results from a blinded study with the integrated microfluidic biomarkers assay chip for spiked human serum samples (*all concentrations are ng/mL*)**.**

Analyte	Sample number	Concentration			Standard deviation	
		Spiked	Calibration curve	Standard addition	Calibration curve	Standard addition
HSP90	**1**	110	116	87	7	7
	2	183	200	140	13	94
	3	219	206	201	13	31
	4	58	73	60	4	12
AFP	**1**	116	106	128	7	5
	2	140	136	166	10	35
	3	37	27	50	2	13
	4	70	63	92	4	12
CytC	**1**	200	152	156	25	37
	2	53	38	22	5	3
	3	106	104	142	16	42
	4	160	118	128	19	27
CEA	**1**	27	38	42	2	8
	2	50	60	50	4	7
	3	83	95	131	6	21
	4	100	118	136	8	8

eliminated the serum matrix in the affinity purification step, the results were similar for the calibration curve compared to standard addition, which is most effective in complex mixtures. The total analysis time for these samples (including labeling) was <60 min; therefore, the integrated devices are well suited for point-of-care (POC) applications. To verify the ability of these microchips to quantify biomarkers at native levels, I also analyzed an unspiked serum sample (**Table 4.3**). The biomarker concentrations are all <6 ng/mL, indicating that this system works effectively with

naturally produced biomarkers at trace levels. The calibration curve method provided more reliable and precise results than standard addition in these analyses.

Table 4.3. Results for an unspiked human serum sample with the integrated microfluidic biomarkers assay chip (*all concentrations are ng/mL*)**.**

Analyte	Concentration		Standard deviation	
	Calibration curve	Standard addition	Calibration curve	Standard addition
HSP90	5.6	0.4	0.9	2.0
AFP	3.5	1.9	0.1	1.0
CytC	3.5	0.9	1.9	1.3
CEA	3.6	4.9	0.1	0.2

My approach could be easily extended up to ~10 biomarker detection by simply immobilizing more antibodies on the affinity column. The surface area of my open channel affinity column (i.e., column saturation) could be an obstacle to scaling to tens of biomarkers, although I note that the column saturation level is a factor of at least 25 above the diagnostic threshold for my markers. Furthermore, the binding capacity could be raised by increasing the surface area of columns (e.g., using a monolith material as the solid support). For more than ~10 components, the peak capacity in my present device design could be an issue, but a longer folded separation channel[32] (e.g., 8-cm length) could increase the peak capacity to ~30. Peak capacity could also be raised through spectral multiplexing, wherein several distinct fluorescent labels are used on different proteins. Thus, higher-level multiplexing should be able to significantly increase the number of biomarkers that can be quantified.

To make a real POC assay, the LIF system and power supplies would need to be miniaturized. A shoebox-size LIF package has been successfully demonstrated for microchip CE analysis of DNA, indicating strong potential to miniaturize the platform for POC applications.[33] In addition, post-column labeling could be used to decrease the labeling time and reduce operator intervention.[18] I further note that device throughput could be increased by performing separations in parallel,[15] with multiple extraction and separation units on a single chip. Such integrated capillary array devices would enable either replicate sample analysis or higher-level multiplexing.

4.4 CONCLUSIONS

Sample pretreatment, cleanup, and quantitation are essential in biomarker analysis in complex media. In this study, affinity purification columns with four different antibodies were prepared in polymer microfluidic devices. The amounts of antibodies immobilized on my columns were consistent from chip to chip, and comparable, mid-attomole amounts of each of the four antibodies were attached to the columns. Analysis of four proteins in buffer solution demonstrated that multiplexed immunoaffinity columns could selectively extract the desired species for subsequent CE analysis. With spiked human blood serum samples, four proteins in the ng/mL range were simultaneously quantified using both calibration curves and standard addition. In general, the calibration curve and standard addition results were close to the known spiked concentrations. These microdevices provide an excellent platform for fast, integrated and automated biomarker quantitation. I note that for clinical applications, the device-to-device and run-to-run variability should be further characterized. Furthermore, my system could be expanded to ~30 biomarker quantitation by immobilizing additional different antibodies on the affinity column, in

conjunction with using porous materials for the solid support to improve binding capacity, and longer separation channels as well as spectral multiplexing to raise the peak capacity. Importantly, with improvements in engineering and miniaturization, a straightforward POC instrument for multiple biomarker quantitation could result.

4.5 REFERENCES

1. American Cancer Society, Cancer Facts and Figures 2009. http://*www.cancer.org/downloads/STT/500809web.pdf (Access date: 3/23/2010*)
2. Nass, S. J.; Moses, H. L., *Cancer biomarkers: the promises and challenges of improving detection and treatment*. National Academies Press: Washington, D.C., 2007.
3. Kiviat, N. B.; Critchlow, C. W., Novel approaches to identification of biomarkers for detection of early stage cancer. *Dis Markers* **2002,** 18, (2), 73-81.
4. Verma, M.; Seminara, D.; Arena, F. J.; John, C.; Iwamoto, K.; Hartmuller, V., Genetic and epigenetic biomarkers in cancer : improving diagnosis, risk assessment, and disease stratification. *Mol Diagn Ther* **2006,** 10, (1), 1-15.
5. Makarov, D. V.; Loeb, S.; Getzenberg, R. H.; Partin, A. W., Biomarkers for prostate cancer. *Annu Rev Med* **2009,** 60, 139-151.
6. Sinise, G. A., *Tumor markers research perspectives*. Nova Science Publishers: New York, 2007.
7. Thompson, I. M.; Pauler, D. K.; Goodman, P. J.; Tangen, C. M.; Lucia, M. S.; Parnes, H. L.; Minasian, L. M.; Ford, L. G.; Lippman, S. M.; Crawford, E. D.; Crowley, J. J.; Coltman, C. A., Jr., Prevalence of prostate cancer among men with a prostate-specific antigen level < or =4.0 ng per milliliter. *N Engl J Med* **2004,** 350, (22), 2239-2246.
8. Sunami, E.; Shinozaki, M.; Higano, C. S.; Wollman, R.; Dorff, T. B.; Tucker, S. J.; Martinez, S. R.; Singer, F. R.; Hoon, D. S. B., Multimarker circulating DNA assay for assessing blood of prostate cancer patients. *Clin Chem* **2009,** 55, (3), 559-567.
9. Yang, X.-Q.; Yan, L.; Chen, C.; Hou, J.-X.; Li, Y., Application of C12 Multi-Tumor Marker Protein Chip in the Diagnosis of Gastrointestinal Cancer: Results of 329 Surgical Patients and Suggestions for Improvement. *Hepato-Gastroenterology* **2009,** 56, (94-95), 1388-1394.
10. Bronchud, M. H.; Foote, M.; Giaccone, G.; Olopade, O.; Workman, P., *Principles of molecular oncology*. 2nd ed.; Humana Press: Totowa, N.J., 2004.
11. Ladd, J.; Taylor, A. D.; Piliarik, M.; Homola, J.; Jiang, S., Label-free detection of cancer biomarker candidates using surface plasmon resonance imaging. *Anal Bioanal Chem* **2009,** 393, (4), 1157-1163.
12. Ellington, A. A.; Kullo, I. J.; Bailey, K. R.; Klee, G. G., Antibody-based protein multiplex platforms: technical and operational challenges. *Clin Chem* **2010**, 56, (2), 186-193.
13. Dittrich, P. S.; Tachikawa, K.; Manz, A., Micro total analysis systems. Latest advancements and trends. *Anal Chem* **2006,** 78, (12), 3887-3907.
14. Bharadwaj, R.; Santiago, J. G.; Mohammadi, B., Design and optimization of on-chip capillary electrophoresis. *Electrophoresis* **2002,** 23, (16), 2729-2744.
15. Yang, W.; Woolley, A. T., Integrated Multi-process Microfluidic Systems for Automating Analysis. *J Assoc Lab Autom,* **2010**, 15, (3), 198-209.
16. Lagally, E. T.; Emrich, C. A.; Mathies, R. A., Fully integrated PCR-capillary electrophoresis microsystem for DNA analysis. *Lab Chip* **2001,** 1, (2), 102-107.
17. Lion, N.; Gobry, V.; Jensen, H.; Rossier, J. S.; Girault, H., Integration of a membrane-based desalting step in a microfabricated disposable polymer injector for mass spectrometric protein analysis. *Electrophoresis* **2002,** 23, (20), 3583-3588.

18. Yu, M.; Wang, H.-Y.; Woolley, A. T., Polymer microchip CE of proteins either off- or on-chip labeled with chameleon dye for simplified analysis. *Electrophoresis* **2009,** 30, (24), 4230-4236.
19. Yang, W.; Sun, X.; Wang, H.-Y.; Woolley, A. T., Integrated microfluidic device for serum biomarker quantitation using either standard addition or a calibration curve. *Anal Chem* **2009,** 81, (19), 8230-8235.
20. Wen, J.; Guillo, C.; Ferrance, J. P.; Landers, J. P., Microfluidic-Based DNA Purification in a Two-Stage, Dual-Phase Microchip Containing a Reversed-Phase and a Photopolymerized Monolith. *Anal Chem* **2007,** 79, (16), 6135-6142.
21. Yang, W.; Sun, X.; Pan, T.; Woolley, A. T., Affinity monolith preconcentrators for polymer microchip capillary electrophoresis. *Electrophoresis* **2008,** 29, (16), 3429-3435.
22. Phillips, T. M.; Wellner, E. F., Chip-based immunoaffinity CE: application to the measurement of brain-derived neurotrophic factor in skin biopsies. *Electrophoresis* **2009,** 30, (13), 2307-2312.
23. Mao, X.; Luo, Y.; Dai, Z.; Wang, K.; Du, Y.; Lin, B., Integrated lectin affinity microfluidic chip for glycoform separation. *Anal Chem* **2004,** 76, (23), 6941-6947.
24. Guzman, N. A.; Blanc, T.; Phillips, T. M., Immunoaffinity capillary electrophoresis as a powerful strategy for the quantification of low-abundance biomarkers, drugs, and metabolites in biological matrices. *Electrophoresis* **2008,** 29, (16), 3259-3278.
25. Wright, L. M.; Kreikemeier, J. T.; Fimmel, C. J., A concise review of serum markers for hepatocellular cancer. *Cancer Detect Prev* **2007,** 31, (1), 35-44.
26. Park, Y. A.; Sohn, S. K.; Seong, J.; Baik, S. H.; Lee, K. Y.; Kim, N. K.; Cho, C. W., Serum CEA as a predictor for the response to preoperative chemoradiation in rectal cancer. *J Surg Oncol* **2006,** 93, (2), 145-150.
27. Barczyk, K.; Kreuter, M.; Pryjma, J.; Booy, E. P.; Maddika, S.; Ghavami, S.; Berdel, W. E.; Roth, J.; Los, M., Serum cytochrome c indicates in vivo apoptosis and can serve as a prognostic marker during cancer therapy. *Int J Cancer* **2005,** 116, (2), 167-173.
28. Mahalingam, D.; Swords, R.; Carew, J. S.; Nawrocki, S. T.; Bhalla, K.; Giles, F. J., Targeting HSP90 for cancer therapy. *Br J Cancer* **2009,** 100, (10), 1523-1529.
29. Kelly, R. T.; Woolley, A. T., Thermal bonding of polymeric capillary electrophoresis microdevices in water. *Anal Chem* **2003,** 75, (8), 1941-1945.
30. Sun, X.; Yang, W.; Pan, T.; Woolley, A. T., Affinity monolith-integrated poly(methyl methacrylate) microchips for on-line protein extraction and capillary electrophoresis. *Anal Chem* **2008,** 80, (13), 5126-5130.
31. Clarke, W.; Beckwith, J. D.; Jackson, A.; Reynolds, B.; Karle, E. M.; Hage, D. S., Antibody immobilization to high-performance liquid chromatography supports. Characterization of maximum loading capacity for intact immunoglobulin G and Fab fragments. *J Chromatogr A* **2000,** 888, (1-2), 13-22.
32. Paegel, B. M.; Hutt, L. D.; Simpson, P. C.; Mathies, R. A., Turn geometry for minimizing band broadening in microfabricated capillary electrophoresis channels. *Anal Chem* **2000,** 72, (14), 3030-3037.
33. Lagally, E. T.; Scherer, J. R.; Blazej, R. G.; Toriello, N. M.; Diep, B. A.; Ramchandani, M.; Sensabaugh, G. F.; Riley, L. W.; Mathies, R. A., Integrated portable genetic analysis microsystem for pathogen/infectious disease detection. *Anal Chem* **2004,** 76, (11), 3162-3170.

5. CONCLUSIONS AND FUTURE WORK

5.1. CONCLUSIONS

5.1.1 Affinity monolith preconcentrators for microchip capillary electrophoresis

The photo-defined monolith columns presented in Chapter 2 offer several advantages for sample preconcentration and pretreatment compared with packed columns. They have lower backpressure compared with packed columns, are easier to fabricate and can be integrated into polymeric microdevices. I successfully prepared these monolith columns in microfluidic devices via photopolymerization and demonstrated the preconcentration of amino acids on native monoliths to show the general nature of solid phase extraction. The concentrated eluent can be readily separated by microchip capillary electrophoresis, and threefold signal increase was achieved after extraction. However, due to the general column selectivity and some non-specific adsorption, the recovery of FITC-labeled amino acids on native monoliths was ~60%.

The selectivity of monolith columns can be improved by immobilizing antibodies on them. The amount of antibodies immobilized on the 0.5-cm-long monolith column was 250±70 mg/g (n=3) and was comparable with other methods. Moreover, unlike direct reaction between antibody amine groups and epoxy groups on monolith surfaces, my technique works with tenfold lower antibody concentrations (~10 µg/mL) and sixfold shorter reaction times (~4 h). In addition, coating with lysozyme solution can effectively remove the non-specific adsorption sites on the affinity columns. The average elution efficiency of the lysozyme-treated affinity columns was near 90%, and the chip-to-chip variability was 3.1% (n=3). These affinity columns can selectively enrich target analytes and reduce the signal of contaminant proteins up

to 25,000 fold after immunoaffinity extraction. These results clearly demonstrate that microchip affinity monoliths can selectively concentrate and purify target analytes through specific antibody-antigen interactions.

5.1.2 Integrated microfluidic device coupling affinity extraction with microchip capillary electrophoresis for AFP quantitation

Although the antibody-based monolith in Chapter 2 has shown promise in selective extraction, off-chip extraction slows the total analysis speed and efficiency. It would be beneficial to couple affinity columns with electrophoretic analysis in a single device. With a new design, both functions can be integrated into a micromachined system, and the monolith can be successfully prepared. However, such microdevices only run well for simple systems such as buffered solution. Once real biological samples such as human serum were applied, significant clogging was observed for many devices. Therefore, in Chapter 3, I developed new affinity columns using a wall coating protocol. To form the affinity columns, a thin film of a reactive polymer was UV polymerized in a microchannel, and scanning electron microscopy indicated that the channel walls were coated with ~3 μm of polymer. Antibodies were attached by reaction between the polymer epoxy groups and antibody amine groups. Only analytes of interest were retained on the affinity column, while non-target material was directed into the waste reservoir. Retention and enrichment of FITC-AFP in anti-AFP columns were shown through flow experiments, and negligible non-specific adsorption of proteins was found in these affinity columns. Retained proteins were eluted into the injection region of the capillary electrophoresis module for rapid separation. All assays, including loading, washing, and elution steps of the affinity extraction, as well as the capillary electrophoresis analysis, were achieved simply via

applying voltages to reservoirs on the microdevice. By adding reservoirs containing AFP standard into the same device, a quantitative method, either standard addition or a calibration curve, can be performed on chip. In conjunction with laser-induced fluorescence detection, my systems can quantify AFP at ~1 ng/mL levels in ~10 μL of human serum in a few tens of minutes. My polymer microdevices have been applied in determining AFP in spiked serum samples, and the results are comparable with the values measured from a commercial ELISA kit.

5.1.3 Integrated microfluidic device for multiple biomarker quantitation in human serum

Although the microdevices in Chapter 3 have been designed for AFP analysis, this approach is not limited to just AFP. These microchips can be easily adapted for detection of multiple biomarkers by simply immobilizing different antibodies in the affinity column. However, to make a multi-biomarker system, the affinity column properties needed be fully characterized and evaluated. In Chapter 4, I demonstrated an integrated microfluidic system that could simultaneously quantify multiple cancer biomarkers in human blood serum. I selected four commercially available biomarkers (AFP, CEA, CytC, and HSP90) as test proteins. Antibodies were attached to microchip columns, and the amounts of immobilized antibodies were characterized. The fluorescence signals of all four proteins were in the same range after rinsing, indicating that the derivatization reaction had little bias toward any of the four antibodies I used. For a buffer solution containing the four target proteins and fluorescent dye, after on-chip affinity purification, the dye peak was essentially eliminated, while the four biomarker peaks remained. I also tested four spiked human blood serum samples with my devices. With these samples, four proteins in the ng/mL

range were simultaneously quantified using both calibration curves and standard addition. In general, the calibration curve and standard addition results were close to the known spiked concentrations. These results indicate that my integrated microdevices can selectively retain and analyze targeted compounds in clinical samples. Moreover, my platform is generalizable and applicable for the simultaneous quantification of multiple biomarkers in complex samples.

5.2. FUTURE DIRECTIONS

5.2.1 Semi-permeable membrane preconcentrators

In my dissertation, I demonstrated integrated microdevices for analysis of biomarkers in human serum. The detection limit of current devices is in the low ng/mL level for biomarkers, which is comparable to commercial ELISA kits. A lower limit of detection would be beneficial for trace biomarker detection. More importantly, for each chip, the migration time of eluent to microchip CE injector needs to be fine tuned. Too long or too short of an injection time will result in peak loss and loading bias toward different proteins. To address these problems, I have done initial work toward integrating a semi-permeable polyacrylamide membrane in the microchip injector as a sample preconcentrator. This size-selective membrane, formed *in situ* by focused laser polymerization, allowed small molecules like fluorescein to pass through easily, but prevented protein transport.

Briefly, a freshly prepared acrylamide solution (total monomer concentration: 13% and weight percentage of crosslinker: 4 %) containing 12.5% acrylamide, 0.5% N,N'-methylene bisacrylamide (crosslinker), 0.1% tetramethylethylenediamine (provides radicals for polymerization), 0.05% riboflavin (initiator of photopolymerization),[1]

0.05% ammonium persulfate (provides initial radicals), and 0.1 μM fluorescein (for visualization) in water was degassed and introduced into the microchannel via capillary action. The monomer in the reservoirs was completely removed to reduce siphon effects. A 488-nm laser beam was focused 10~40 μm from the double T injection area with a 20× objective for 3 min. The unreacted monomer was flushed out by water and Tris buffer.

The apparent pore radius (R) of my 4 % crosslinker acrylamide gel can be estimated using the following equation where T is the total acrylamide percentage:[2]

$$R = 110\ T^{-0.5} = 30.5\ \text{nm} \qquad \textbf{(Eq. 5.1)}$$

Even though this dimension is larger than the molecular size of most proteins, as I summarized in Section 1.3.3, such a membrane can still enrich proteins because the negatively charged diffuse layer on the interior of the membrane repels anions. Consequently, protein ions should enrich at the junction of the membrane and injection area. As a result, the injection time of eluent from the affinity column should not change the amount of proteins injected into the separation channel.

I tested the integrated membrane preconcentration and microchip CE device with FITC-labeled bovine serum albumin (BSA). After a 10-min enrichment, the fluorescent signal for 100 ng/mL FITC-BSA increased ~140 fold (**Figure 5.1**). However, due to some penetration of proteins into the membrane, significant tailing was found after such a long injection time.

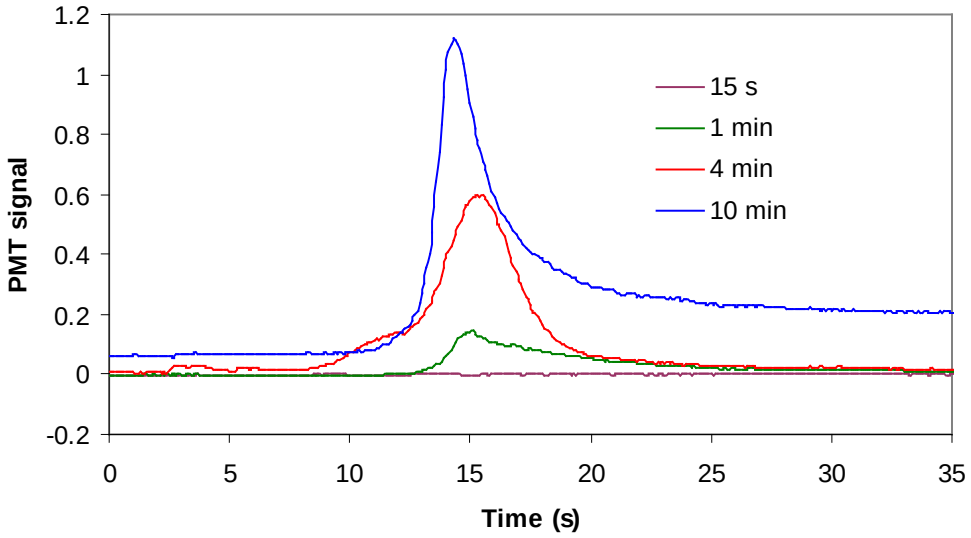

Figure 5.1. FITC-BSA enrichment with an integrated semi-permeable membrane.

In addition, microchip CE of a mixture with fluorescein and FITC-labeled IgG demonstrated selective enrichment of proteins at the injection preconcentrator (**Figure 5.2**). The on-chip enrichment factor for FITC-labeled IgG was ~80 fold after 4 min, while no significant enrichment (~1.3 fold higher signal) was found for

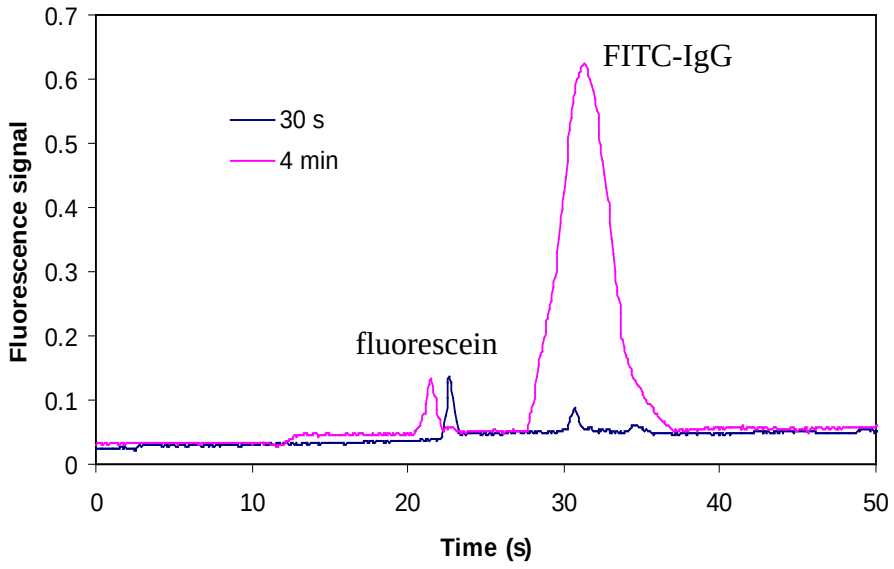

Figure 5.2. Selective preconcentration of FITC-IgG over fluorescein.

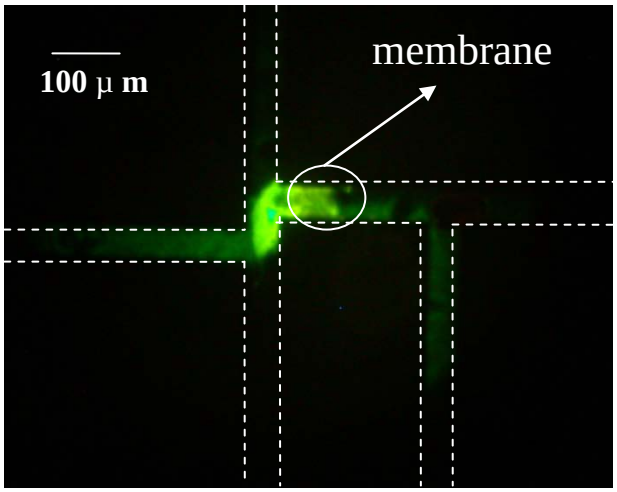

Figure 5.3. Microscope image of FITC-IgG enrichment with a membrane.

fluorescein after 4 min enrichment. From the microscope image (**Figure 5.3**), it is clear that some fluorescence (most likely a small molecule, fluorescein) passed through the membrane while the abundant fluorescence (most likely FITC-IgG) was accumulating next to the membrane.

5.2.2 Multiplexed immunoassays based on gel particles

I have successfully demonstrated quantification of multiple biomarkers in Chapter 4. However, such multiplexed analysis is still challenging, because of the limited number of immobilized antibodies on the affinity column. There are two common technologies used for multiplexing: planar arrays and suspension (particle-based) arrays.[3] Planar arrays, such as DNA and protein microarrays, are better suited for ultra-high-density analysis,[4] while suspension arrays offer ease of assay modification, higher sample throughput, and better quality control by batch synthesis.[5] To identify each protein in the mixture, it is important to differentiate proteins. Using multiple fluorescent signals as coding could solve this problem, but it brings higher cost with each fluorescent dye and its own exciter and detector, with potential interference. Therefore, a single-fluorescence method using graphical coding is more attractive. Recently, Doyle's group developed a simple technique to generate multifunctional particles with distinct regions for analyte coding and target capture in microfluidic formats.[6] Briefly, two monomer streams (one loaded with a fluorescent dye for coding

and the other with a probe) were adjacently flowed through a microfluidic channel, and continuous-flow lithography was used to polymerize particles across the streams (**Figure 5.4**). With dynamic focusing, 3-D gel particles with a sandwich shape can also be generated.[7] However, it is an on-going challenge to precisely read and decode barcoded gel particles.[8]

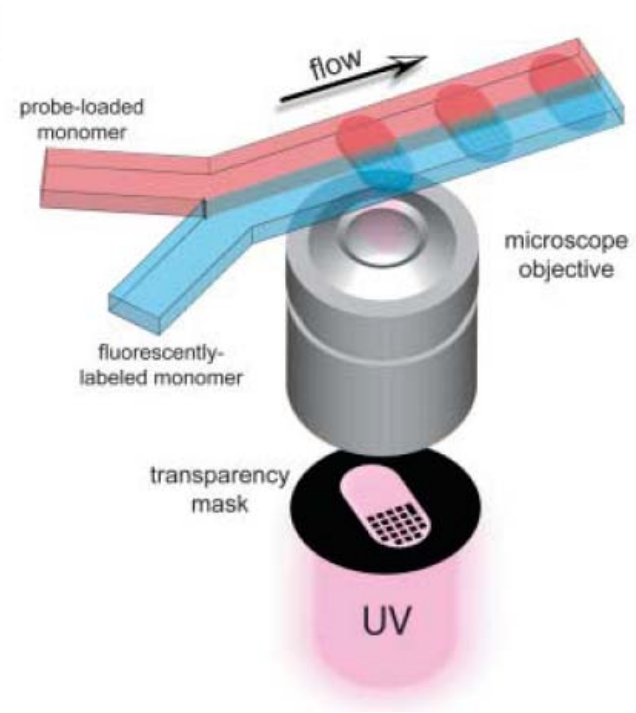

Figure 5.4. Schematic diagram of coded gel particle synthesis (reproduced with permission from ref. 6).

Thus, instead of using two streams of monomer, a prepolymer solution containing glycidyl methacrylate (GMA, monomer), poly(ethylene glycol) diacrylate (crosslinker, reduces non-specific adsorption of proteins), 2,2'-dimethoxy-2-phenylacetophenone (photoinitiator), and 2-acrylamido-2-methylpropane sulfonic acid (AMPS, provides negative charges)[1] will be pumped through a microchannel. Gel particles of different sizes (controlled by photomask) and charge (adjusted by AMPS percent) can be generated easily via lithography. Different antibodies can be anchored onto the gel particles based on the reaction between epoxy groups of GMA

and amine groups of antibodies. Because of the surface area of gel particles, more antibodies can be attached than with the wall coating protocol, which in turn increases the binding capacity for multiplex assays. To detect multiple biomarkers in human whole blood samples, the particles anchored with different antibodies can be immersed in fluorescently labeled sample, and then rinsed to remove any unbound material, separated via capillary electrophoresis (because of the unique mass/charge ratio for each particle), and decoded via CCD detector (**Figure 5.5**). The amount of antigen can be calculated from the fluorescence signal of the gel particles. These gel particles can be easily cleaned, packed, shipped, and used as part of a straightforward POC instrument for multiple biomarker quantitation.

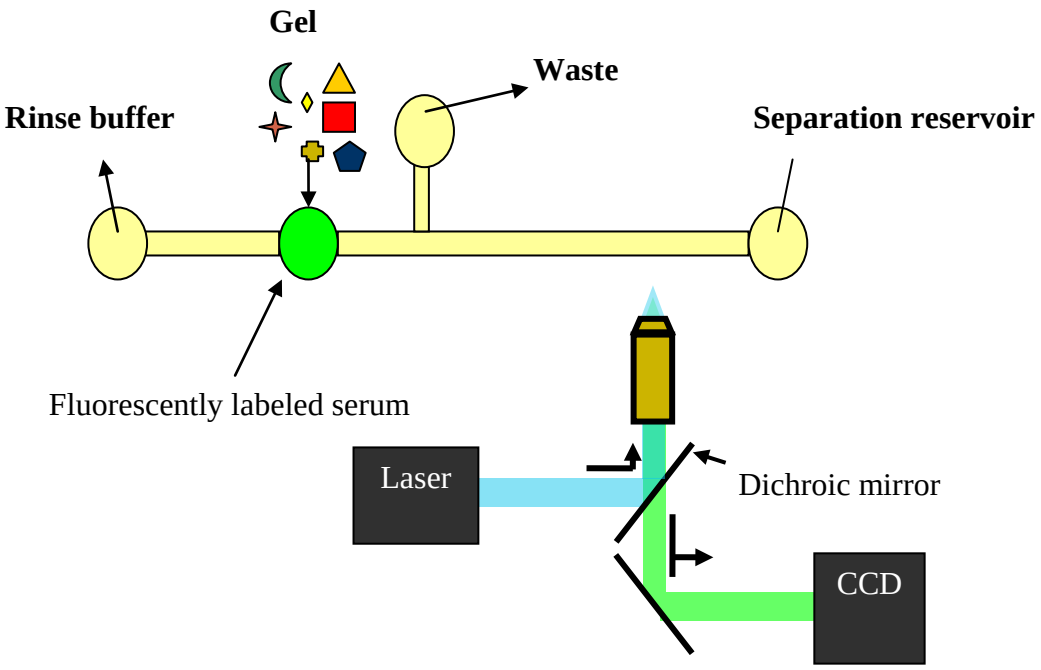

Figure 5.5. Schematic diagram of analysis using affinity gel particles.

In summary, in my dissertation I have developed a novel microfluidic system integrated with antibody-based sample purification and electrophoretic separation to

provide fast and accurate quantitation of multiple biomarkers in human serum. Further studies on engineering and miniaturization should enable fabrication of a POC instrument for cancer screening. Microfluidic separation was introduced over two decades ago and continues to grow. My work pushes the frontiers of this miniaturization technique and demonstrates strong potential for POC applications.

5.3 REFERENCES

1. Yamamoto, S.; Hirakawa, S.; Suzuki, S., In situ fabrication of ionic polyacrylamide-based preconcentrator on a simple poly(methyl methacrylate) microfluidic chip for capillary electrophoresis of anionic compounds. *Anal Chem* **2008,** 80, (21), 8224-8230.
2. Stellwagen, N. C., Apparent pore size of polyacrylamide gels: comparison of gels cast and run in Tris-acetate-EDTA and Tris-borate-EDTA buffers. *Electrophoresis* **1998,** 19, (10), 1542-1547.
3. Ellington, A. A.; Kullo, I. J.; Bailey, K. R.; Klee, G. G., Antibody-based protein multiplex platforms: technical and operational challenges. *Clin Chem* **2010,** 56, (2), 186-193.
4. Gershon, D., Microarray technology: an array of opportunities. *Nature* **2002,** 416, (6883), 885-891.
5. Zhi, Z. L.; Morita, Y.; Hasan, Q.; Tamiya, E., Micromachining microcarrier-based biomolecular encoding for miniaturized and multiplexed immunoassay. *Anal Chem* **2003,** 75, (16), 4125-4131.
6. Pregibon, D. C.; Toner, M.; Doyle, P. S., Multifunctional encoded particles for high-throughput biomolecule analysis. *Science* **2007,** 315, (5817), 1393-1396.
7. Bong, K. W.; Bong, K. T.; Pregibon, D. C.; Doyle, P. S., Hydrodynamic focusing lithography. *Angew Chem Int Ed Engl* **2010,** 49, (1), 87-90.
8. Chapin, S. C.; Pregibon, D. C.; Doyle, P. S., High-throughput flow alignment of barcoded hydrogel microparticles. *Lab Chip* **2009,** 9, (21), 3100-3109.